Higgs Dynamics during Inflation

Author:
Stephen Stopyra

Supervisor:
Professor Arttu Rajantie

Submitted in partial fulfilment of the requirements for the degree of Master of Science of Imperial College London.

Abstract

With the discovery of the Higgs boson, and recent measurements from the BICEP2 collaboration indicating a tensor-to-scalar ratio of $r = 0.20^{+0.07}_{-0.05}$[1], particle physics is now in an interesting position. The most precise measurements of the Higgs boson and top quark masses appear to show that the Electroweak vacuum is unstable under the fluctuations produced by inflation at the energy scale the BICEP results imply[2][3]. In this report we review the physics of electroweak vacuum stability, with particular emphasis on methods for solving the Fokker-Planck equation. We also present numerical results for a method of solving the Fokker-Planck eigenvalue problem, by means of a harmonic oscillator basis.

September 18, 2014

Acknowledgements

I would like to thank Professor Arttu Rajantie, who supervised my work on this project, for invaluable conversations, thoughtful suggestions, and insight. I would also like to thank Sofia Qvarfort for acting as a useful sounding board and for providing all round encouragement. Finally, I would like to thank my family, for supporting me through the many years it took to get here.

Contents

Chapter 1

Introduction

The aim of this report is to introduce some of the main tools and concepts needed to study the behaviour of the Higgs field during inflation, with an eye to understanding the implications of recent measurements of the Higgs mass for the stability of the Standard Model vacuum. This is a question of profound importance, since if the vacuum of the standard model is truly unstable or metastable, it raises questions as to why it has persisted for so long. Assuming that its survival is not just an extreme accident, then the instability hints at the existence of new physics, including the possibility of previously unseen particles that would be required to stabilise the vacuum. To summarise, the goals of the report are:

- To constitute a literature review for further research into the field of particle dynamics and their affect on cosmological models.
- To bring together a collection of tools and concepts useful to research in this field.
- To explore the question of vacuum stability, both for its own sake and for its potential consequences for particle physics and cosmology.
- To describe how to compute correlation functions in an inflationary (de-Sitter) background.
- To evaluate the usefulness of a numerical technique - namely the use of a harmonic oscillator basis - for solving the Fokker-Planck equation governing stochastic inflation.

Before beginning this, however, the introduction will provide a lay person's explanation of the concepts that the report explains in more technical detail. It is the duty of anyone engaged in scientific endeavours to try and explain their work to the general public. This is not only because the public supports scientific research, and thus has a right to know what scientists are doing: research, especially in theoretical physics, is not only done for the extensive technological benefits it provides, but also for the advancement of human knowledge as

a whole. Scientific research is rarely undertaken simply as a job, but because those who perform it genuinely enjoy the prospect of learning about the secrets of the universe. This excitement is not unique to scientists, however, for science is a human endeavour. Therefore, those with the privilege to spend their time uncovering the unknown are surely obliged to share their excitement with all those who wish to listen. I hope that this short introduction can at least begin to explain to non-physicists why it is so interesting to obtain increasingly precise measurements of, say, the top-quark mass, while at the same time remaining in the spirit of Einstein's words: "Everything should be made as simple as possible - but no simpler."

The report consists of six sections. The introduction is split into two parts - the first is a non-technical introduction to the subject of the report, aimed at non-physicists, while the second is a slightly more technical explanation, aimed at students of physics or physicists from other fields. Section 2 develops the technique of the effective potential formalism, originally devised by Coleman and Weinberg[4]. Section 3 uses this formalism to discuss the question of the stability of the electro-weak vacuum of the Standard Model, both against quantum tunnelling, and disturbances: especially those originating from inflationary fluctuations. Section 4 collates several tools for the computation of correlation functions - fundamental to any observation - in an inflationary background. It covers quantum field theory in de-Sitter space, the stochastic formulation of inflation, and the Fokker-Planck equation. Section 5 then details a numerical approach to solving the Fokker-Planck equation by using a harmonic oscillator basis to extract the eigenfunctions and eigenvalues of the ordinary differential equation appearing after separation of variables. It studies this method for a variety of potentials that occur in the study of scalar fields like the Higgs field. Finally, the conclusions of the report are discussed in section 6.

1.1 A lay person's introduction to inflation and the question of vacuum stability

> "*How wonderful that we have met with a paradox. Now we have some hope of making progress.*"
>
> - Niels Bohr

With the discovery of a particle which appears to be the Higgs boson, the Standard Model of particle physics is complete. However, no model in physics is ever expected to be the end of the story. There are several reasons that the Standard Model is less than ideal:

- It is not known why the parameters of the Standard Model - such as the masses of the various particles - take on the values they do.
- In some senses, the Standard Model seems to be a collection of theories stitched together and forced to meet observation. However, most physicists expect a more correct theory to be unified, with all the forces it describes turning out to be aspects of the same thing. This has both historical precedent in the form of electromagnetism (electric and magnetic forces turn out to be the same thing approached from a different perspective), and aesthetic appeal.
- Some parameters of the Standard Model require finely tuned values to describe anything like the universe we observe. Although there is no reason they cannot take on these values, this seems like an un-natural solution.

These reasons are somewhat heuristic, appealing mostly to aesthetics, rather than data. No experiment to date has contradicted the Standard Model. However, to properly understand the universe requires us to do better. The experience of scientists over centuries has taught that the best way to proceed is by attempting to find phenomena that do not match current theory. A great deal of effort has gone into doing this, all confirming the Standard Model, in some cases to very high degrees of precision. This tells us that if there is a better theory than the Standard Model, the new physics it describes only appears in exotic situations not yet studied by experiment. Searching for this new physics has two basic avenues:

- Re-creating these exotic physical scenarios in the laboratory, for example in particle accelerators such as the Large Hadron Collider (LHC).
- Searching for these exotic scenarios in nature.

The subject of this report is the latter. In the case of particle physics, we are searching for scenarios involving highly energetic particles, the likes of which are rarely seen in nature, outside of the occasional detection of cosmic rays from outside the solar system. However, cosmological theory tells us that the universe

was once much hotter - the so called 'Big Bang'. Thus, if we can observe signals from the time of the Big Bang, it is possible to gain some insight into the behaviour of physics at high temperatures, where energetic particles abound. Thus, we will be concerned in this report with what we can learn about high energy physics by studying the very early universe.

Most of our knowledge of the big bang theory comes from the study of the 'Cosmic Microwave Background' (or CMB). This is a microwave signal which appears to come from all directions of the sky, with very close to equal strength no matter what direction one chooses to look. It was first discovered (by accident) by Penzias and Wilson in 1964. The CMB is special partly because it possesses a *thermal distribution* (see figure 1.1), that is, the it emits microwaves in exactly the same pattern as a metal tool heated in a fire emits visible (red) light. This seems to imply that the entire universe has a temperature, albeit a very low one of $2.72548 \pm 0.00057\,\mathrm{K}$[5] (approximately -270°C). However, another feature revealed by cosmological theory is that light and microwaves lose energy over time: a process called *red-shift*. Because of this effect, extrapolating the CMB thermal distribution backwards in time seems to imply that approximately 13.8 billion years ago, the universe would have had an infinite temperature. This is clearly not a physically meaningful prediction and constitutes evidence that current cosmological theory ceases to be reliable at very high temperatures[1]. Thus, like the Standard Model, another theory must eventually replace it.
The conventional model of the early universe is known as the ΛCDM model[2]. The ΛCDM model states that the universe is expanding. This does not mean that everything in it is moving apart. The usual analogy is to picture space as a balloon, and draw dots on it. The dots (representing objects, such as galaxies) are fixed, but they still appear to move apart when the balloon (representing space) in blown up. This model is not without problems of its own, in addition to the aforementioned 'infinite temperature singularity'. Although it is very predictive, it requires two major components of the universe - so called dark energy and dark matter - that are essentially unknown material.

Another curious feature is that the CMB is the same in all directions. This is surprising, because the microwaves detected on opposite sides of the Earth must come from opposite sides of the universe. Since the signals are still arriving to this day, and we know that nothing can travel faster than light, then we know that the two regions on opposite sides of the universe cannot have been in contact with each other (as light from one has only now travelled half the distance between them, and nothing travels faster than light). It is a puzzle then why they should be the same. What process caused the universe in op-

[1] It is sometimes said that the Big Bang theory is a theory of how the universe began. This is misleading: it is a theory of what happened shortly afterwards. What happened before if the subject of much speculation.

[2] Λ represents the cosmological constant - a proposed explanation for the observed acceleration of the universe's expansion. CDM stands for cold dark matter, believed to be a major component of the matter making up the universe, but is poorly understood.

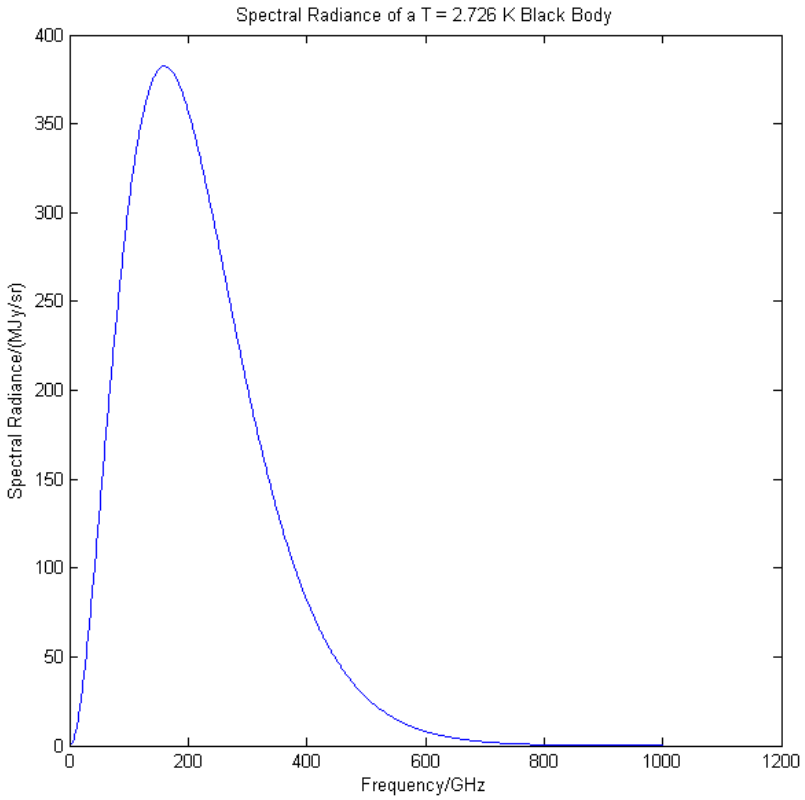

Figure 1.1: This plot shows the frequency of radiation emitted by the Cosmic Microwave Background (CMB). The peak, around 200 GHz, corresponds to microwave radiation (for comparison, visible light corresponds to $400,000 - 770,000$ GHz). Hotter objects emit increasingly higher frequency light: for example, human bodies emit mostly invisible infra-red light, but heated metal can emit visible red light.

posite directions to have the same temperature? To give an analogy - imagine putting a very precise thermometer into the sea and measuring the temperature to be 23.00001°C exactly, and then calling a friend on the other side of the world, who did the same and also found the sea there to be 23.00001°C. This would be an astounding coincidence, as you would expect the temperatures to be slightly different even if you knew in advance that they were similar. Not least because sea temperature usually fluctuates by much more than 0.00001°C. However, in the case of the CMB, the *entire universe* appears to be the same, to within about the same precision (one part in $100,000$). This apparent paradox is called the *horizon problem*, because opposite sides of the universe are beyond

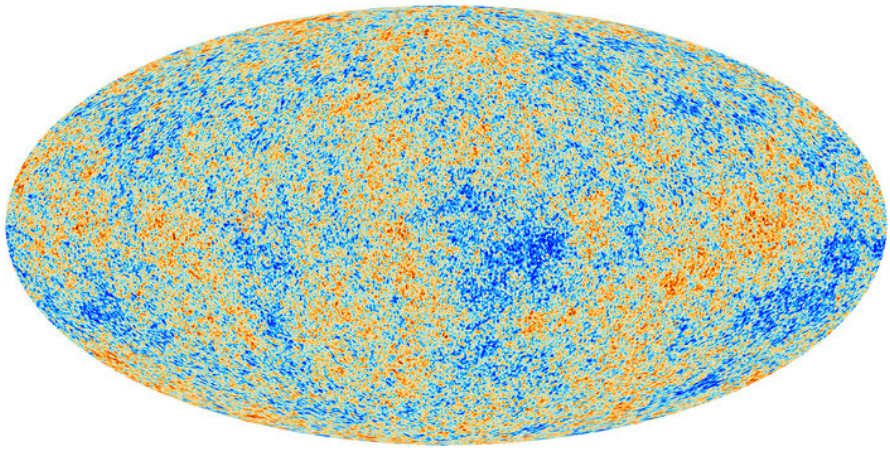

Figure 1.2: Temperature of the CMB, distributed over the sky. The red areas are slightly hotter than the average, while the blue areas are slightly cooler, but the temperature variation is only around a 10^{-5} fraction of the average temperature. These very slight variations from an otherwise uniform distribution reveal important properties of the early universe. In the context of inflationary cosmology, they are believed to be the result of quantum fluctuations amplified by the rapid expansion. Image credit: ESA and the Planck Collaboration[6].

each others 'horizons'[3]

One mechanism proposed to solve this, and other similar paradoxes, is called *inflation*. The basic idea of inflation is that the universe underwent a period of accelerated expansion very early on. However, we said earlier that the ΛCDM model also predicts expansion, so this difference demands some explanation. The key is to realise that cosmology is dominated by gravity, which is an attractive force. Thus, if the universe contains normal matter, then expansion should slow down because gravity pulls it together[4]. However, in the 1990s it was observed that the universe's expansion is actually *speeding up*. This is counter-intuitive, since it would be the everyday equivalent of objects *falling upwards*. The ΛCDM model posits the existence of a material - called 'dark energy' - that repels under gravity rather than attracts. In the ΛCDM model, this substance is proposed to originate from 'vacuum energy' - an energy associated to empty space. This is plausible, because particle physics has mechanisms for giving (seemingly) empty space an energy. We will discuss the technicalities of this in section 1.2. Now, if the energy is associated to empty space, then it follows that

[3] In this context, 'horizon' means the region of space-time with which something can interact

[4] If it isn't clear how a universe dominated by gravity can expand at all, think about a ball thrown in the air - it keeps moving upwards but gradually slows down and then falls back. The same happens with the universe - it keeps expanding, but the expansion slows and in theory the universe should eventually collapse again. The surprising thing is that this doesn't appear to be happening.

the more space there is, the more dark energy there will be. Thus, the total amount of dark energy should increase as the universe expands. This appears to fit what we see - for a long time, the universe's expansion was slowing down, but relatively recently (on the scale of billions of years), it began to accelerate again. This is consistent with what you would expect if the amount of dark energy was small when the universe was small (so attractive gravity dominated, and expansion slowed down) and increased as the universe increased in size.
However, the prospect of vacuum energy introduces a possible explanation for the paradox that different parts of the universe have the same temperature. If the vacuum energy dominates over matter in the universe then it promotes run-away expansion at an exponential rate (e.g, there is a time period T after which the universe doubles in size, at $2T$ it is 4 times larger, at $3T$ 8 times larger, etc...). This would allow the universe to grow to a very large size very quickly. If the vacuum energy were to be suddenly switched off, the universe would return to normal - it would keep expanding, but this expansion would gradually slow down due to gravity pulling everything together. Furthermore, in 'switching off' the vacuum energy would have to go somewhere. The most likely place for it to go is into the matter in the universe, which would then heat up tremendously as a result. This is the theory of inflation. It has the following attractive features:

- Switching off the vacuum places the universe at a high temperature, explaining the thermal distribution we observe in the CMB. This process is called 'Re-heating'.

- Because the universe only gained this temperature at the end of inflation (when the vacuum energy was switched off), the 'infinite temperature singularity' problem is avoided. This is because extrapolating back in time always assumes conditions did not change, which they clearly did if there was a large vacuum energy very early on which suddenly switched off.

- Inflation fixes the horizon problem, because widely separated parts of the universe were once very close together - and thus able to interact and share conditions that would give them the same temperature later on. They were then forced apart faster than the speed of light[5]

In this discussion, it may not be entirely clear how a vacuum can possess energy. The colloquial definition of a vacuum is empty space, with no air. If it is by definition empty, then how can it possess energy? To clear up this potential source of confusion, it is important to understand first how physicists describe matter. The basic building block of matter is a particle, and the study of these is particle physics. Particles are localised clumps of matter with specific properties. Now, Einstein's theory of relativity states that energy and mass are equivalent.

[5]Note that the speed of light restriction only prevents objects in space from moving faster than the speed of light. It does *not* prevent space itself from expanding faster than the speed of light, which is what happens in both inflation and the Big Bang theory.

So particles are also localised clumps of energy. We describe this in terms of *quantum field theory.*

A *field* is an abstract device, first introduced by Michael Faraday (who was a farmer). His analogy was that a farmer goes to a field and plants seeds at each point in the field. However, in physics, instead of planting seeds, numbers are planted. This gives a way of describing how something varies throughout space. For example, we might plot a temperature field on a weather map, indicating the temperature at different points across the country. In principle, we could do this for every point, even points infinitely close together. In the example of temperature, however, it doesn't make sense to talk about the temperature of individual atoms, because temperature is a measure of the average random motion of atoms in a substance, such as water or air. Thus, we naturally accept that the 'temperature field' is only an abstraction that applies on scales much larger than individual atoms.

The same is true with any other kind of field in physics. Fields are a way of describing the behaviour of some physical system. Fundamentally, a magnetic field, for example, is not some mysterious substance filling space, but the statement that objects placed near a magnet move in a certain way. The 'magnetic field' is really just a way of describing that motion in a manner independent of the object moving, and depending only on the properties of the object causing the motion (in this case, the magnet).

This, of course, means that we don't actually have to understand the mechanism behind the motion. We have always understood that things are hot and cold, and could have measured this with a thermometer, and plotted a temperature field, without ever needing to understand that temperature is due to the random motion of atoms. So it is with particle physics - although we do not really understand what particles *are*, we can represent their behaviour as a field throughout space-time. A 'quantum field' then, is just one of these fields obeying the laws of quantum mechanics[6].

Now, the intuitive definition of a vacuum is: that which we are left with if we take away all of the particles (matter). However, since particles are just clumps of matter described by the field, the vacuum is just what we get if the field lies in the state of minimum energy (if it were not the minimum, we could take particles away until it is, so it wouldn't be what we understand by 'vacuum'). However, what if there is energy present which isn't in the form of particles? That is, the field has a bulk energy associated to it which we can't remove. It is, after all, quite an assumption to think that all energy is found in the form of particles. In fact, one of the cornerstones of quantum theory is that quantities such as energy and position cannot be measured with infinite precision. All particles have a fundamental 'fuzziness' which cannot be removed. This is called the *uncertainty principle.* An object with no energy would violate this principle because it would not be moving, so its position could be known exactly. Quantum theory predicts, therefore, that if you remove everything possible, there should still be energy left. In a sense, this means the intuitive notion of a vac-

[6] A proper discussion of quantum mechanics is beyond the scope of this report, however.

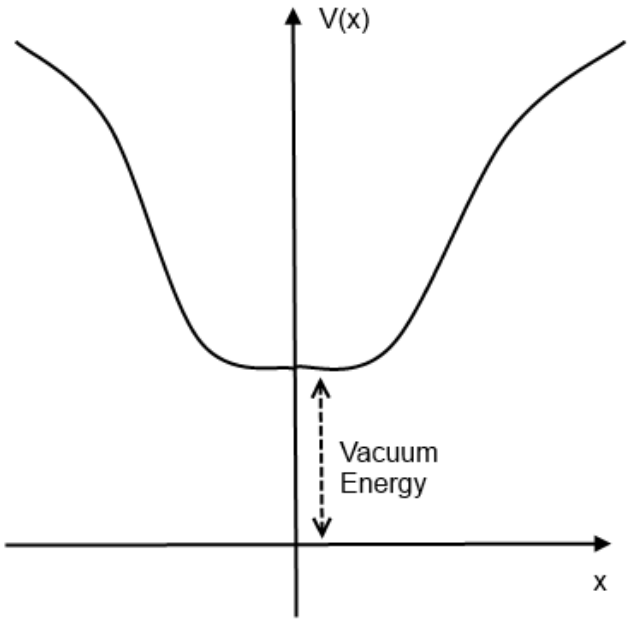

Figure 1.3: An example of an absolutely stable vacuum. The 'height' cannot be inferred from the shape of the potential. This is further complicated by quantum effects, since it isn't possible to have states of exactly zero energy.

uum does not exist. However the next best thing - a state of minimal, non-zero energy - does.

Figure 1.3 illustrates this. The 'potential' $V(\phi)$, is a function which describes how the field can interact. It is helpful to think of this as a valley. From our everyday experience of gravity, we know that objects will roll to the bottom of the valley and this is no different for fields. However, consider what happens in figure 1.4, where we now have two valleys. So long as a ball in the upper valley doesn't roll around too much, there is no way to tell the difference between the upper and lower valleys. However, if the ball is given sufficient energy, it will roll over the barrier into the lower potential, gaining a lot of energy as it does so.

If a valley floor is the lowest possible point, it is said to be an' absolutely stable vacuum', because given time, everything ends up there. Other valleys which are higher up, but still locally valleys, are called 'meta-stable vacua' because if the field is given enough energy, it will roll further down. Peaks (or actually, any point that isn't a valley) are called 'unstable vacua' because the slightest knock will send the field rolling to the nearest vacuum. Just as valleys and peaks exist for hills, so do they exist for particle fields, only this time the 'hill' is to be understood as an abstraction, describing the physics of the field.

Naturally then, it is reasonable to ask whether the vacuum state of the universe

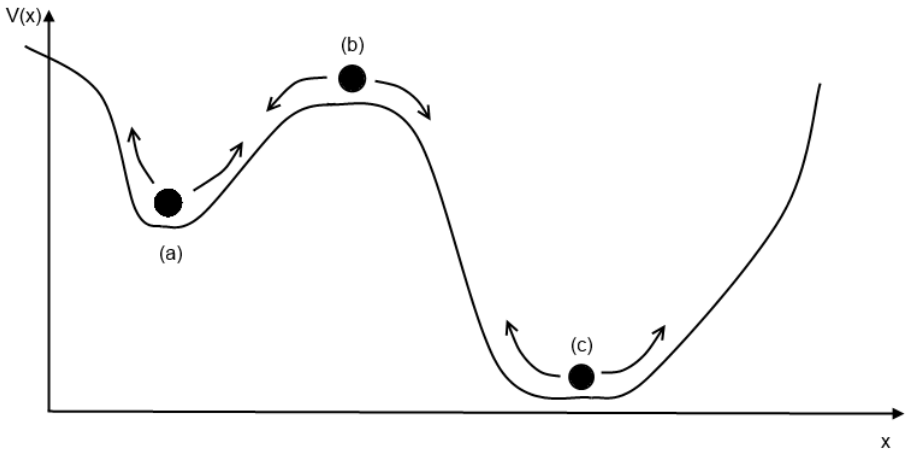

Figure 1.4: Three different types of vacua. (a) is metastable. Under small fluctuations, it behaves similarly to the true vacuum, (c), but large fluctuations can trigger a collapse to the true vacuum. (b) is said to be unstable, since even the smallest fluctuation will cause the system to collapse to (a) or (c).

is stable or only meta-stable. Answering this question requires a detailed understanding of the way matter in the universe interacts. This is described by the standard model, whose vacuum structure is controlled by the Higgs field[7]. It has been shown [7], that the stability of the Higgs vacuum depends strongly on the precise mass of two particles - the Higgs boson itself, and another particle called the top quark. The precision with which these masses are known, however, makes the status of the vacuum unclear, as the higgs boson and top quark masses are very close to the boundary between absolute stability and meta-stability.

The aim of this report then, is to first discuss how the stability of the Higgs vacuum is assessed. Secondly, it discusses what sort of phenomena can push the vacuum into a more stable state, should it be meta-stable. Particularly, we focus on inflation, since this run-away expansion tends to cause the Higgs field (actually any field) to fluctuate. These fluctuations could potentially destabilise the vacuum if it were only meta-stable. We devote a large section of the report to discussing how these fluctuations are generated (see section 4).

Although a collapse of the vacuum to a lower state would unquestionably be very bad for the universe, the real question here is not whether this would actually happen, but what the prediction would say about our current understanding of physics. The prediction rests entirely on the assumption that the Standard model is correct, however, this is not necessarily the case. The fact that the universe as we know it still exists, apparently in the same vacuum that it always has been, after billions of years, is good evidence that it is at least very long

[7]The Higgs boson is the particle - clump of matter - associated to the Higgs field

lived, if not absolutely stable. Thus, if our prediction contradicted this (by saying that it should have collapsed, when it clearly hasn't), then that would imply that the Standard model is not correct. From a scientific perspective, that is a good thing - because it means there is something left to learn.

1.2 Technical introduction

The main subject of this report is the behaviour of a scalar quantum field in an inflating universe. It is assumed that the reader is familiar with quantum field theory and general relativity. The simplest model of the universe starts from the assumption that it is flat and homogeneous. This leads to the FLRW metric:

$$\mathrm{d}s^2 = -\mathrm{d}t^2 + a^2(t)\left(\frac{\mathrm{d}r^2}{1-kr^2} + r^2\mathrm{d}\theta^2 + r^2\sin^2\theta\mathrm{d}\phi^2\right). \tag{1.1}$$

The scale factor, $a(t)$, carries dimensions of length, while r is a 'co-moving distance' and is dimensionless. In this co-ordinate system, 'stationary' objects, which remain at fixed co-moving distance from each other, appear to move apart, since the physical distance between them grows with the scale factor (such objects are called 'co-moving observers'). The scale factor is determined by requiring the metric to satisfy Einstein's Field equations. However, the subject of this report is an exponentially expanding universe:

$$a(t) = a(t_0)e^{H(t-t_0)}, \tag{1.2}$$

where H is a constant, the Hubble constant (for general $a(t)$, H is defined as $H \equiv \frac{\dot{a}}{a}$ and is not constant). Such a space-time is known as de Sitter space-time (though for reasons we will discuss in section 4.2, this co-ordinate system only covers half of the de Sitter manifold).
However, the universe cannot have been a pure de Sitter space, otherwise inflation would not have ended. To understand how it can be generated, we consider a scalar field, whose action in de Sitter space is:

$$S = \int \mathrm{d}^4x\sqrt{-\det(g)}\left[\frac{R}{16\pi G_N} - \frac{1}{2}\nabla_\mu\phi\nabla^\mu\phi - V(\phi)\right], \tag{1.3}$$

where G_N is Newton's gravitational constant. If it is assumed that the scalar field respects the homogeneity of the FLRW universe, then it can only be a function of time, $\phi = \phi(t)$. Variation with respect to the metric implies that the resulting stress-energy tensor is:

$$T_{\mu\nu} = \nabla_\mu\phi\nabla_\nu\phi - \frac{1}{2}g_{\mu\nu}\nabla_\rho\phi\nabla^\rho\phi - g_{\mu\nu}V(\phi). \tag{1.4}$$

This can be interpreted as the stress tensor of a perfect fluid:

$$T_{\mu\nu} = \begin{pmatrix} \rho & 0 & 0 & 0 \\ 0 & p & 0 & 0 \\ 0 & 0 & p & 0 \\ 0 & 0 & 0 & p \end{pmatrix}, \tag{1.5}$$

where $\rho = \frac{1}{2}\dot{\phi}^2 + V(\phi)$ is the energy density, and $p = \frac{1}{2}\dot{\phi}^2 - V(\phi)$ is the pressure. This has the interesting property that if the field varies slowly, $\dot{\phi} \sim 0$, then the pressure is negative. Thus, the fluid has the equation of state $p = -\rho$. This means that is behaves like a cosmological constant term in Einstein's field equations:

$$R_{\mu\nu} - \frac{1}{2}g_{\mu\nu}R + \Lambda g_{\mu\nu} = 0, \tag{1.6}$$

where $\Lambda = 8\pi G_N V(\phi)$. For a flat universe, Einstein's field equations reduce to the Friedmann equation:

$$H^2 = \frac{8\pi G_N}{3}\rho \implies \frac{\dot{a}}{a} = \sqrt{\frac{8\pi G_N V(\phi)}{3}}. \tag{1.7}$$

Thus, a slowly varying scalar field will cause space-time to behave approximately like de Sitter space.

One goal of this paper is to understand how fluctuations in the Higgs field during inflation can destabilise metastable vacua. First, this will require a discussion of how the vacuum of a quantum field theory is determined. Although the classical Higgs potential is well known, this determines only the equations of motion. Quantum theories, however, are concerned with the behaviour of observable quantities such as the vacuum expectation value of the field, $\langle\phi\rangle$. In particular, it is the behaviour of vacuum expectation value that determines the structure of the vacuum, not the classical potential. This will receive quantum corrections in the form of loop corrections which will modify the potential into an 'effective potential'. For example, the 1-loop correction to the potential for the scalar field in Yukawa theory is:

$$\begin{aligned} V(\phi_0) =& \frac{1}{2}m^2\phi_0^2 + \frac{\lambda}{4!}\phi_0^4 \\ &+ \frac{M^4}{64\pi^2}\left(\ln\left(\frac{M^2}{\mu^2}\right) - \frac{3}{2}\right) - \frac{\tilde{m}^4}{16\pi^2}\left(\ln\left(\frac{\tilde{m}^2}{\mu^2}\right) - \frac{3}{2}\right), \end{aligned} \tag{1.8}$$

where the first line gives the classical (0-loop) potential, and the second the 1-loop correction, at renormalisation scale μ. Here, $M^2 = m_\phi^2 + \frac{\lambda}{2}\phi_0^2$ and $\tilde{m} = m_\Psi + g\phi_0$. We will discuss the implications of this in the case of the Standard Model, where the vacuum structure is determined largely by the top quark and Higgs boson masses, (due to the strong quartic dependence on mass in the quantum corrections). We will discuss current data which appears to show that the electroweak vacuum is only meta-stable, and thus seemingly at risk of destabilisation by inflationarity fluctuations.

In section 4 we will discuss the quantisation of scalar fields in de Sitter space-time. We will find that the conventional perturbation theory approach encounters infra-red divergence problems, leading to a break-down of perturbation theory in cases where the mass, m, is light compared to the Hubble rate, H, or to be specific, when the condition:

$$m^2 \leq \left(\frac{27}{16} - 12\xi^2\right)H^2, \tag{1.9}$$

is satisfied, where ξ is a coupling describing a possible non-minimal coupling of the scalar field to gravity. This will lead on to the stochastic formulation of inflation, to which we will devote the latter half of the report. The basic idea is that the long wavelength part, $\bar{\phi}$, of a scalar field in de Sitter spacetime behaves classically and is governed by a stochastic differential equation known as a Langevin equation:

$$\frac{\mathrm{d}\bar{\phi}}{\mathrm{d}t} = -\frac{1}{3H}V'(\bar{\phi}) + f(\mathbf{x}, t), \tag{1.10}$$

where $f(\mathbf{x}, t)$ is a stochastic term resulting from the quantum behaviour of the short wavelength field. Thus, behaviour can only be characterised by a probability distribution, $\rho(\varphi, t)$ for the field to take on values between φ and $\varphi + \mathrm{d}\varphi$. This, as we will derive, is determined by a partial differential equation known as the Fokker-Planck equation, which for the field at a single point is given by:

$$\frac{\partial\rho(\varphi, t)}{\partial t} = \frac{1}{3H}\frac{\partial}{\partial\varphi}\left(V(\varphi)\rho(\varphi, t)\right) + \frac{H^3}{8\pi^2}\frac{\partial^2\rho(\varphi, t)}{\partial\varphi^2}. \tag{1.11}$$

Solving this by the method of separation of variables leads to a Sturm-Liouville eigenvalue problem. The final part of the report will discuss how this can be solved numerically: in particular, by means of a harmonic oscillator basis. That is, by treating the Sturm-Liouville equation as an effective Hamiltonian and expressing the position and derivative (momentum) operators in terms of the basis function of a harmonic potential. This can always be done (for arbitrary potentials) since the harmonic oscillator basis functions form a complete set. By truncating the (infinite) set of basis functions to some large value, N, we obtain a matrix form of the Sturm-Liouville equation, whose eigenvectors (in the harmonic oscillator basis) and eigenvalues approximately correspond to those of the Sturm Liouville problem. This provides an alternative to methods such as the Numerov method for discretising a differential operator, which has the advantage of being exact for harmonic potentials, and a good approximation for some non-harmonic potentials, in particular the quartic potential, $V(\phi) = \frac{\lambda}{4}\phi^4$. We will present our analysis of this method in section 5.

Chapter 2

The Effective Action and Effective Potential

The vacuum structure of the Standard model is determined by the Higgs field, since Lorentz invariance requires that only scalar fields can possess a vacuum expectation value. However, in a quantum theory the vacuum structure is determined not by the classical potential, but an effective potential which received quantum corrections. This section discusses the effective potential formalism.

2.1 Introduction to the Effective Action Formalism

The Higgs field in the standard model is a complex doublet, $\varphi = \begin{pmatrix} \varphi^+ \\ \varphi^0 \end{pmatrix}$, with Lagrangian terms (not including Yukawa interactions):

$$D_\mu \varphi^\dagger D^\mu \varphi - \lambda \left(\varphi^\dagger \varphi - \frac{\mu^2}{2\lambda} \right)^2 + \mathcal{L}_{\text{Yukawa}}, \tag{2.1}$$

where λ is the Higgs quartic coupling, $m_H^2 = 2\lambda v^2$ is the Higgs mass, defined in terms of the vacuum expectation value, v^2 of the electro-weak vacuum, and $\mu^2 = \lambda v^2$. The covariant derivative is:

$$D_\mu \varphi = \partial_\mu \varphi + i \frac{g_1}{2} B_\mu \varphi + i \frac{g_2}{2} \sigma^i W_\mu^i \varphi, \tag{2.2}$$

where g_1 and g_2 are gauge couplings for the weak hypercharge and weak isospin forces respectively, B_μ and W_μ^i their associated gauge bosons. σ^i are Pauli

matrices. After symmetry breaking, this can be written as:

$$\begin{aligned} S[H] =& \frac{1}{2}\partial_\mu H \partial^\mu H - \frac{1}{2}m_H^2 H^2 - \lambda v H^3 - \frac{\lambda}{4}H^4 + ... \\ &+ \text{ Gauge-Boson Higgs interactions } + \text{Fermion-Higgs interactions,} \end{aligned} \tag{2.3}$$

where H is a real scalar field. Note that this is the Lagrangian that is used to compute the quantum behaviour of the Higgs field. In classical field theory, the potential terms here would be sufficient, but if we wish to compute the bulk behaviour of the *quantum field*, H, we in fact have to ask how $\langle H \rangle$, the expectation value of the Higgs field, behaves, subject not only to the classical potential but also the net effect of quantum fluctuations.
In quantum field theory, this question can be answered using the *effective action*, $\Gamma[\phi]$. To understand how this comes about, consider that a generic quantum field theory for a scalar field can be expressed in terms of a generating functional, $Z[J]$:

$$Z[J] = \int \mathcal{D}\phi \exp\left[i \int \mathrm{d}^4x (\mathcal{L}[\phi] + J\phi) \right], \tag{2.4}$$

where $\mathcal{D}\phi$ indicates a path integral and J is an auxiliary 'external field'. In the path integral formulation, observables are computed in terms of correlation functions, which can be computed via the formula:

$$\langle 0| \phi(x_1)\phi(x_2)\dots\phi(x_N) |0\rangle = \frac{\int \mathcal{D}\phi \phi(x_1)\phi(x_2)\dots\phi(x_N) e^{i\int \mathrm{d}^4x \mathcal{L}[\phi]}}{\int \mathcal{D}\phi e^{i\int \mathrm{d}^4x \mathcal{L}[\phi]}} \tag{2.5}$$

$$= \frac{(-i)^N}{Z[0]} \frac{\delta}{\delta J(x_1)} \dots \frac{\delta}{\delta J(x_N)} Z[J]\Big|_{J=0} \tag{2.6}$$

$$\tag{2.7}$$

where $\frac{\delta}{\delta J(x_i)}$ are *functional derivatives*. The *classical field* is defined by:

$$\phi_{\mathrm{cl}}(x) \equiv \langle 0| \phi(x) |0\rangle_J, \tag{2.8}$$

where the subscript J indicates that this expectation value is to be computed in the presence of a non-zero external field, J. At $J = 0$, this is the quantity we are interested in (the expected value of the field).
Now, defining $\mathcal{L}_0$ to be the quadratic ('free') part of the Lagrangian, and $\mathcal{L}_I$ the interacting part, it is possible to re-write Z perturbatively as:

$$\begin{aligned} Z[J] &= \int \mathcal{D}\phi e^{i\int \mathrm{d}^4x \mathcal{L}_0[\phi]} \frac{\int \mathcal{D}\phi \exp\left[i\int \mathrm{d}^4x (\mathcal{L}_0[\phi] + \mathcal{L}_I[\phi] + J\phi)\right]}{\int \mathcal{D}\phi e^{i\int \mathrm{d}^4x \mathcal{L}_0[\phi]}} \\ &= \int \mathcal{D}\phi e^{i\int \mathrm{d}^4x \mathcal{L}_0[\phi]} \sum (\text{All diagrams including J as vertices}) \\ &= \int \mathcal{D}\phi e^{i\int \mathrm{d}^4x \mathcal{L}_0[\phi]} \exp\left(\sum [\text{All Connected diagrams}]\right), \end{aligned}$$

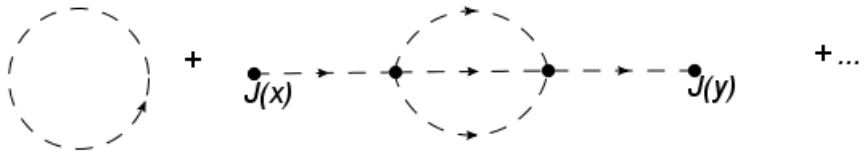

Figure 2.1: Example Feynman diagrams contributing to the generating functional. Notice that interacting theory also has one-point vertices giving a contribution $i \int \mathrm{d}^4 x J(x)$.

(for an example, see figure 2.1). The sum becomes an exponential over connected diagrams in the usual way, since products of n copies of some diagram are divided by appropriate symmetry factors ($n!$) and exponentiating a sum just gives a sum over all possible products of diagrams with precisely these symmetry factors. We can then define:

$$W[J] \equiv -i \ln Z[J], \tag{2.9}$$

as per Weinberg's convention [8]. Diagrammatically, this is:

$$W[J] = -i \ln \left(\int \mathcal{D}\phi e^{iS_0} \right) - i \sum (\text{All Connected Diagrams}) . \tag{2.10}$$

The classical field can then be expressed as:

$$\phi_{\mathrm{cl}}(x) = \frac{-i}{Z[J]} \frac{\delta}{\delta J(x)} Z[J] = \frac{\delta}{\delta J(x)} W[J]. \tag{2.11}$$

This relation implies that we can perform a Legendre transformation to eliminate J as the variable:

$$\Gamma[\phi_{\mathrm{cl}}] = W[J] - \int \mathrm{d}^4 x \phi_{\mathrm{cl}}(x) J(x). \tag{2.12}$$

Using the definition of ϕ_{cl}, it is clear that taking the functional derivative with respect to $J(x)$ will give zero. On the other hand, the functional derivative with respect to ϕ_{cl} gives:

$$\frac{\delta \Gamma[\phi_{\mathrm{cl}}]}{\delta \phi_{\mathrm{cl}}(x)} = -J(x). \tag{2.13}$$

It is interesting to note then, that if $J(x)$ is zero, the classical field satisfies:

$$\frac{\delta \Gamma[\phi_{\mathrm{cl}}]}{\delta \phi_{\mathrm{cl}}} = 0, \tag{2.14}$$

that is, the effective action is stationary with respect to variations in the classical field. This is why it is known as the 'effective action'. It plays the same role for

the expectation value of the field as the original action plays for a classical field. In this sense, we can treat the behaviour of the field ϕ_{cl} classically, so long as we use the effective action, Γ, rather than the original action, S.
To see how we should interpret Γ in terms of Feynman diagrams, consider the following argument based on S. Weinberg[8], though the use of the effective action in this way was first discussed in a PhD thesis by E. Weinberg [9]:
Any action, $S[\phi]$ can be expanded as a functional Taylor series:

$$S[\phi] = S[0] + \int \mathrm{d}^4x_1 \phi(x_1) \frac{\delta S[\phi]}{\delta\phi(x_1)} + \frac{1}{2}\int \mathrm{d}^4x_1 \mathrm{d}^4x_2 \phi(x_1) \frac{\delta^2 S[\phi]}{\delta\phi(x_1)\delta\phi(x_2)}\phi(x_2) + \dots \tag{2.15}$$

Counting the number of fields in each term, we see that the first term is a constant, the second is a one-point interaction, and the third gives the inverse of the propagator (since the propagator is by definition the inverse of the quadratic term, up to factors of i). Higher order terms give vertices. For example if:

$$S[\phi] = \int \mathrm{d}^4x \left[\frac{1}{2}\partial_\mu\phi\partial^\mu\phi - \frac{1}{2}m^2\phi^2\right], \tag{2.16}$$

then[1]:

$$\frac{\delta S[\phi]}{\delta\phi(x_1)} = -\partial_\mu\partial^\mu\phi(x_1) - m^2\phi(x_1) \tag{2.17}$$

$$\frac{\delta^2 S[\phi]}{\delta\phi(x_1)\delta\phi(x_2)} = -\delta(x_1 - x_2)(\partial_\mu\partial^\mu + m^2). \tag{2.18}$$

Weinberg argued that we can consider the quantum field theory associated to a new action:

$$Z[J,g] = e^{iW_S[J,g]} = \int \mathcal{D}\exp\left(ig^{-1}\left[S[\phi] + \int \mathrm{d}^4x J(x)\phi(x)\right]\right), \tag{2.19}$$

which reduces to the original theory if $g = 1$. Now, it is an important fact about Feynman diagrams that each independent[2] loop gives rise to an undetermined momentum. The independent loops in a Feynman diagram are in one-to-one correspondence with the number of faces of the diagram, interpreted in the graph theory sense (an empty region bounded by lines of the graph). Euler's formula for planar graphs states:

$$V - E + F = 2, \tag{2.20}$$

where V is the number of vertices of the graph, E the number of edges and F the number of faces. Note that in graph theory, the infinite exterior region of the graph counts as a face, but obviously this is not a loop, so $F = L + 1$ where L is the number of loops. See figure 2.2 for examples. Internal lines (I)

[1] Note - a function can be regarded as a functional since $f(x) = \int \mathrm{d}y\delta(x-y)f(y)$. That is, in the same sense that a constant can be regarded as a function for the purposes of differentiation.

[2] Independent in the sense that it cannot be decomposed into other loops already accounted for. E.g., we can devise three ways of going round the loops in the sunset diagram of figure 2.1 but the outer circle contains the two semi-circles, so is not independent of them. The sunset diagrams thus has two loops.

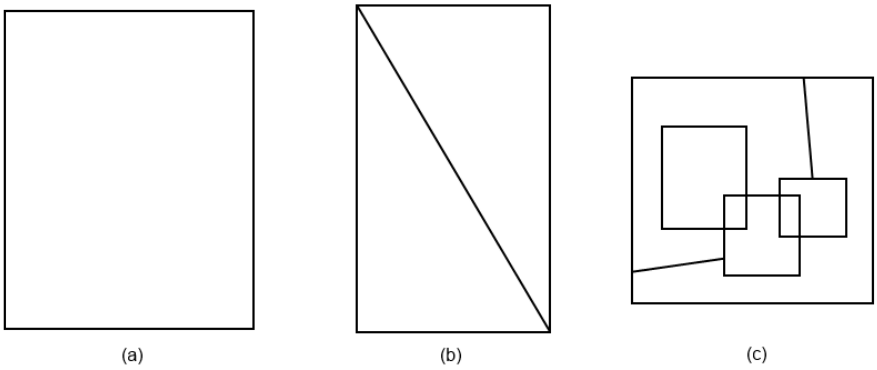

Figure 2.2: Three planar graphs. The rectangle, (a), has 4 vertices, 4 edges and 2 faces (including the infinite exterior region), where 4-4+2 = 2. The second shape, (b), is similar, with 4 vertices, 5 edges and 3 faces, giving 4 -5 + 3 = 2. Finally, the more complicated shape (c) has 24 vertices, 30 edges and 8 faces: 24-30+8 = 2. This result can be proven to hold for any planar graph, including Feynman diagrams.

correspond to edges and vertices to vertices, so this implies:

$$L = I - V + 1. \tag{2.21}$$

Now, the factor g^{-1} in the action will be included as a factor in every vertex. Also, every propagator will carry a factor of g (since propagators are the inverse of the quadratic term, so multiplying the quadratic term by g^{-1} multiplies the propagator by g). Thus, each diagram changes from the original by a factor g^{I-V}. But Euler's formula then implies this is just g^{L-1}, so diagrams are re-scaled depending on their number of loops. We can therefore choose to order the diagrams by their loop count, L:

$$W_S[J, g] = \sum_{L=0}^{\infty} g^{L-1} W_S^{(L)}[J]. \tag{2.22}$$

Now, take the limit as $g \to 0$. In this limit, the sum is dominated by the $L = 0$ contribution, going as g^{-1}. Because this ensures the action becomes large, it becomes possible to approximate the path integral by the method of stationary phase[8]:

$$e^{iW_S[J,g]} \to f(g, J, S) \exp\left(ig^{-1}\left[S[\phi] + \int \mathrm{d}^4x J(x)\phi(x)\right]\right), \tag{2.23}$$

where f is some proportionality function whose form is irrelevant here. The action, however, takes on its stationary value, and taking the logarithm of both

sides, one finds that:

$$W_S^{(0)}[J] = S[\phi_J] + \int \mathrm{d}^4x J(x)\phi_J(x), \tag{2.24}$$

by comparing the coefficients of g^{-1} on each side. Here, ϕ_J is the distribution of the field that makes the action $S[\phi_J] + \int \mathrm{d}^4x J(x)\phi_J(x)$ stationary. The original action, S, can then be represented diagrammatically by considering $J = 0$:

$$S[\phi] = W_S^{(0)}[0] = \sum (\text{All connected tree level diagrams, no external legs}), \tag{2.25}$$

since that is what is meant by $W_S^0[J = 0]$. In particular, we could choose $\Gamma[\phi]$ in place of S, in which case:

$$W_\Gamma^0[J] = \Gamma[\phi] + \int \mathrm{d}^4x J(x)\phi(x) = W[J]. \tag{2.26}$$

The significance of this is that it shows that the sum of tree level diagrams with Γ as the action is the same as the sum of all diagrams (to all orders) with S as the action. However, the inverse of the propagator, with Γ as the action, is given by:

$$-i\frac{\delta^2\Gamma}{\delta\phi(x)\delta\phi(y)} \tag{2.27}$$

and this must equal the full propagator with S as the action (see figure 2.3). Likewise, the n-leg vertices, and thus the sum of all n-leg 1PI diagrams[3], are given by the nth functional derivative of Γ. For this reason, Γ is sometimes referred to as the generating functional of 1PI diagrams. Using Eq. (2.15) then, the effective action can be written:

$$\Gamma[\phi] = \Gamma[0] + \sum(\text{All 1PI diagrams}). \tag{2.28}$$

This is represented diagrammatically in figure 2.4. To see how this expansion helps, consider terms order by order in the number of loops. For example, at zero loop order, there is only one diagram that contributes to the four external-field set (see figure 2.5).

2.2 Computing the Effective Action - Loop Expansion

The results of the previous section indicate that the effective action indeed includes the original action at lowest order, and higher loop terms are the quantum corrections. It is in fact much more convenient to compute the effective action

[3]This isn't so obvious for the two point diagram elements, where we compare inverses, but it is true there as well, since, for example, the full scalar field propagator is $\frac{i}{p^2 - m^2 - i\sum(1\text{PI})}$, the denominator of which is actually the sum of all 1PI diagrams, including the lowest order term $p^2 - m^2$.

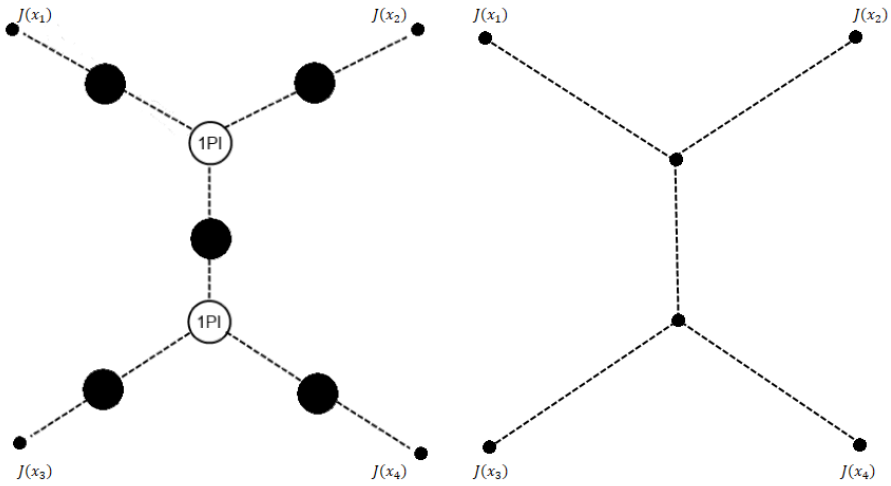

Figure 2.3: Comparison of a diagram calculated to all loop order with $W[J]$ and $S[\phi]$ as the action (left) and to zero loop order with $W_\Gamma^{(0)}[J]$ and $\Gamma[\phi]$ as the action (right). Since $W[J] = W_\Gamma^{(0)}[J]$, these must give the same result. We can always draw this one to one equivalence, since the sum of all loop diagrams can be re-written in terms of a tree level diagram with 1PI vertices (open circles) and full propagators (shaded circles).

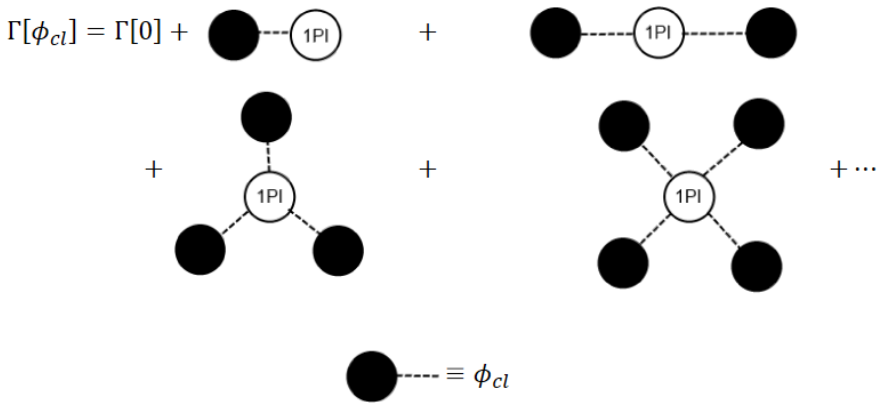

Figure 2.4: Feynman diagram representation of the effective action. The solid cicle represents the classical field (given by the sum of all connected tadpole diagrams plus a propagator). Note that this diagram excludes a factor of i, which is implied.

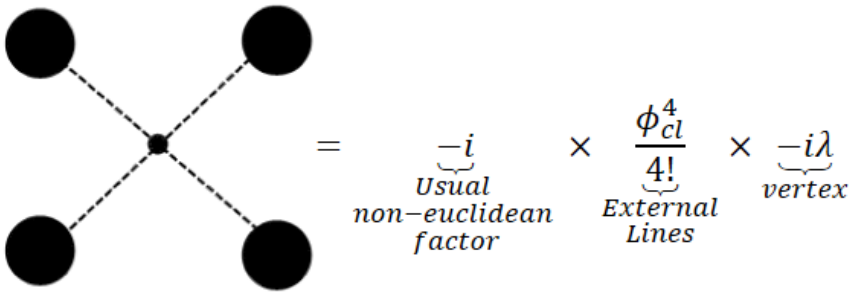

Figure 2.5: Four external field contribution to effective action at zero-loop order. Note that the external field constitutes a vertex, so there is a $\frac{1}{4!}$ symmetry factor included here. The factor of $-i$ at the front is the usual factor appearing in the path integral (ultimately a consequence of the Minkowski nature of space-time), and finally there is a contribution $-i\lambda$ from the vertex of $\frac{\lambda\phi^4}{4!}$ theory. The result is precisely that the effective action contains the $-\lambda\frac{\phi_{\rm cl}^4}{4!}$ term at lowest order.

by loop order. One way to do this was first derived by Jackiw[10] and involves simplifying the generating functional using functional analysis. We will follow a similar approach based on [8] and [11], and write the generating functional as:

$$Z[J_i] = \int \mathcal{D}\eta_i \exp\left(i\int \mathrm{d}^4x \left[\mathcal{L}_R[\phi_{\mathrm{cl}i}+\eta_i] + \delta\mathcal{L}[\phi_{\mathrm{cl}i}+\eta_i] + J_{\mathrm{cl}i}\phi_{\mathrm{cl}i} + J_{\mathrm{cl}i}\eta_i + \delta J\phi_{\mathrm{cl}i} + \delta J\eta_i\right]\right), \tag{2.29}$$

where $J_i = J_{\mathrm{cl}i}+\delta Ji$ and $\phi_i = \phi_{\mathrm{cl}i}+\eta_i$. For generality, we consider an unspecified number of fields, ϕ_i, which may be either bosonic or fermionic, or a mixture. We have also split the Lagrangian into the renormalised part, $\mathcal{L}$ and counter terms, $\delta\mathcal{L}$. $J_{\mathrm{cl}i}$ is chosen to satisfy:

$$\left.\frac{\delta\mathcal{L}_R}{\delta\phi_i}\right|_{\phi_i=\phi_{\mathrm{cl}i}} + J_{\mathrm{cl}i} = 0. \tag{2.30}$$

This is just the renormalised equation of motion. In other words, $J_{\mathrm{cl}i}$ fulfils the same roll for $\mathcal{L}_R$ as J_i did for $\mathcal{L}$. Thus, we can interpret $J_{\mathrm{cl}i}$ as a 'renormalised' J_i, with δJ_i the associated counter term.
We now expand in powers of η. Notice that this is exactly the process involved in computing the fluctuations of the Higgs field, H, about the vacuum expectation

value. $Z[J_i]$ becomes:

$$\begin{aligned} Z[J] = \int \mathcal{D}\eta_i \exp\Bigg(& i \int \mathrm{d}^4x \left[\mathcal{L}_R[\phi_{\mathrm{cl}i}] + \delta\mathcal{L}[\phi_{\mathrm{cl}i}] + J_{\mathrm{cl}i}\phi_{\mathrm{cl}i} + \delta J\phi_{\mathrm{cl}i}\right] \\ & + i \int \mathrm{d}^4x \left[\left.\frac{\delta(\delta\mathcal{L})}{\delta\phi_i}\right|_{\phi_{\mathrm{cl}i}} \eta_i(x) + \delta J_i \eta_i(x) \right] \\ & + \frac{i}{2!} \int \mathrm{d}^4x \mathrm{d}^4y \eta_i(x) \left[\left.\frac{\delta^2\delta\mathcal{L}}{\delta\phi_i(x)\delta\phi_j(y)}\right|_{\phi_{\mathrm{cl}i}} + \left.\frac{\delta^2\mathcal{L}_R}{\delta\phi_i(x)\delta\phi_j(y)}\right|_{\phi_{\mathrm{cl}i}} \right] \eta_j(y) + \dots \Bigg). \end{aligned} \tag{2.31}$$

Note that here we have used Eq. (2.30) to simplify the terms first order in η_i. The remaining two terms first order in η_i (second row) might be a problem, however, since they will correspond to non-zero tadpole interactions, which shift the vacuum expectation value of η_i. This is not what we want. However, we are free to choose δJ_i such that this term always vanishes. This is essentially imposing a renormalisation condition that $\phi_{\mathrm{cl}i}$ is the expectation value of the field to all orders[4]. Thus, we can ignore the second row here completely.
The higher order terms in η_i correspond to loop corrections, while the zeroth order terms have been extracted as the renormalised Lagrangian. We can compute the energy functional:

$$\begin{aligned} W[J_i] = & \int \mathrm{d}^4x \left[\mathcal{L}_R[\phi_{\mathrm{cl}i}] + \delta\mathcal{L}[\phi_{\mathrm{cl}i}] + J\phi_{\mathrm{cl}i}\right] \\ & - i \ln \Bigg(\int \mathcal{D}\eta_i \exp\Bigg(\frac{i}{2!} \int \mathrm{d}^4x \mathrm{d}^4y \eta_i(x) \left[\left.\frac{\delta^2\delta\mathcal{L}}{\delta\phi_(x)\delta\phi_j(y)}\right|_{\phi_{\mathrm{cl}i}} \right. \\ & \left. + \left.\frac{\delta^2\mathcal{L}_R}{\delta\phi_i(x)\delta\phi_j(y)}\right|_{\phi_{\mathrm{cl}i}} \right] \eta_j(y) \\ & + \frac{i}{3!} \int \mathrm{d}^4x \mathrm{d}^4y \mathrm{d}^4z \eta_i(x)\eta_j(y)\eta_k(z) \left[\left.\frac{\delta^3\delta\mathcal{L}}{\delta\phi_i(x)\delta\phi_j(y)\delta\phi_k(z)}\right|_{\phi_{\mathrm{cl}i}} + \right. \\ & \left. + \left.\frac{\delta^3\mathcal{L}_R}{\delta\phi_i(x)\delta\phi_j(y)\delta\phi_k(z)}\right|_{\phi_{\mathrm{cl}i}} \right] + \dots \Bigg) \Bigg). \end{aligned} \tag{2.32}$$

[4] As with most renormalisation conditions, we don't have to choose this particular condition, but it will simplify matters considerably.

Moving to $\Gamma[\phi_{\mathrm{cl}i}]$, by subtracting: $-\int \mathrm{d}^4x J_i\phi_{\mathrm{cl}i}$ gives:

$$\begin{aligned}\Gamma[\phi_{\mathrm{cl}i}] = &\int \mathrm{d}^4x\left[\mathcal{L}_R[\phi_{\mathrm{cl}i}] + \delta\mathcal{L}[\phi_{\mathrm{cl}i}]\right] \\ &- i\ln\left(\int \mathcal{D}\eta \exp\left(\frac{i}{2!}\int \mathrm{d}^4x\mathrm{d}^4y\eta_i(x)\left[\left.\frac{\delta^2\delta\mathcal{L}}{\delta\phi_i(x)\delta\phi_j(y)}\right|_{\phi_{\mathrm{cl}i}}\right.\right.\right. \\ &\left.\left.\left. + \left.\frac{\delta^2\mathcal{L}_R}{\delta\phi_i(x)\delta\phi_j(y)}\right|_{\phi_{\mathrm{cl}i}}\right]\eta_j(y)\right)\right) - i\ln\left(\frac{\int \mathcal{D}\eta\exp\left(iI_0[\eta_i] + I_{\mathrm{int}}[\eta_i]\right)}{\int \mathcal{D}\eta\exp\left(iI_0[\eta_i]\right)}\right),\end{aligned} \tag{2.33}$$

where:

$$I_0[\eta_i] = \frac{i}{2!}\int \mathrm{d}^4x\mathrm{d}^4y\eta_i(x)\left[\left.\frac{\delta^2\delta\mathcal{L}}{\delta\phi_i(x)\delta\phi_j(y)}\right|_{\phi_{\mathrm{cl}i}} + \left.\frac{\delta^2\mathcal{L}_R}{\delta\phi_i(x)\delta\phi_j(y)}\right|_{\phi_{\mathrm{cl}i}}\right]\eta_j(y) \tag{2.34}$$

$$\begin{aligned}I_{\mathrm{int}}[\eta_i] = &\frac{i}{3!}\int \mathrm{d}^4x\mathrm{d}^4y\mathrm{d}^4z\eta_i(x)\eta_j(y)\eta_k(z)\left[\left.\frac{\delta^3\delta\mathcal{L}}{\delta\phi_i(x)\delta\phi_j(y)\delta\phi_k(z)}\right|_{\phi_{\mathrm{cl}i}}\right. \\ &\left. + \left.\frac{\delta^3\mathcal{L}_R}{\delta\phi_i(x)\delta\phi_j(y)\delta\phi_k(z)}\right|_{\phi_{\mathrm{cl}i}}\right] + \ldots\end{aligned} \tag{2.35}$$

That is, we have multiplied by $\frac{\int \mathcal{D}\eta_i \exp(iI_0[\eta_i])}{\int \mathcal{D}\eta_i \exp(iI_0[\eta_i])}$ in order to write the third order and higher terms as a fraction which can be evaluated using Feynman diagrams, interpreting I_0 as a 'free' action. In reality, I_0 is a quantum correction, but it is a Gaussian one so we can compute it exactly. The logarithm only serves to ensure we sum over connected diagrams, so this becomes:

$$\begin{aligned}\Gamma[\phi_{\mathrm{cl}i}] = &S[\phi_{\mathrm{cl}i}] - i\sum(\text{Connected third order } \eta \text{ diagrams and higher}) \\ &- i\ln\left(\int \mathcal{D}\eta_i \exp\left(\frac{i}{2!}\int \mathrm{d}^4x\mathrm{d}^4y\eta_i(x)\left[\left.\frac{\delta^2\delta\mathcal{L}}{\delta\phi_i(x)\delta\phi_j(y)}\right|_{\phi_{\mathrm{cl}i}}\right.\right.\right. \\ &\left.\left.\left. + \left.\frac{\delta^2\mathcal{L}_R}{\delta\phi_i(x)\delta\phi_j(y)}\right|_{\phi_{\mathrm{cl}i}}\right]\eta_j(y)\right)\right).\end{aligned} \tag{2.36}$$

Now, the second line here involves a Gaussian integral which we can perform by a discrete analogue:

$$\int \mathrm{d}^N\mathbf{x}\exp\left(-\frac{1}{2}x_iM_{ij}x_j\right) = \left(\frac{(2\pi)^N}{\det M}\right)^{\frac{1}{2}} = \left(\det\frac{M}{2\pi}\right)^{-\frac{1}{2}}, \tag{2.37}$$

since $\det(\lambda M) = \lambda^N \det M$. Thus:

$$-i\ln\left(\int \mathrm{d}^N\mathbf{x}\exp\left(-\frac{1}{2}x_iM_{ij}x_j\right)\right) = +\frac{i}{2}\ln\left(\det\frac{M}{2\pi}\right). \tag{2.38}$$

However, $\det M = \prod_i m_i$ where m_i are the eigenvalues of M. Thus, the logarithm gives:

$$\ln\left(\det\frac{M}{2\pi}\right) = \ln\left(\prod_i \frac{m_i}{2\pi}\right) = \sum_i \ln\left(\frac{m_i}{2\pi}\right) = \mathrm{Tr}\left(\ln\left(\frac{M}{2\pi}\right)\right), \tag{2.39}$$

since the trace is the sum of the eigenvalues, and if M is a matrix with eigenvalues m_i, $f(M)$ has eigenvalues $f(m_i)$. Generically, we can write the second order terms as:

$$M_{ij}(x,y) = -i\left[\left.\frac{\delta^2\delta\mathcal{L}}{\delta\phi_i(x)\delta\phi_j(y)}\right|_{\phi_{\mathrm{cl}i}} + \left.\frac{\delta^2\mathcal{L}_R}{\delta\phi_i(x)\delta\phi_j(y)}\right|_{\phi_{\mathrm{cl}i}}\right]. \tag{2.40}$$

It is convenient to change the basis by means of a similarity transform, in this case a Fourier transform[5]:

$$M_{ij}(k,q) = \int \mathrm{d}^4x \int \mathrm{d}^4y e^{-ip\cdot x} M_{ij}(x,y) e^{iq\cdot y}. \tag{2.41}$$

$M_{ij}(x,y)e^{iq\cdot y}$ will generically be of the form $M_{qij}\delta^{(4)}(x-y)e^{iq\cdot y}$ (in the similarity transform analogy, $e^{iq\cdot y}$ is an eigenvector of this operator), in which case this Fourier transform gives:

$$M_{ij}(k,q) = \int \mathrm{d}^4x e^{-ip\cdot x} M_{qij} e^{iq\cdot x} = (2\pi)^4 M_{qij}\delta^{(4)}(p-q). \tag{2.42}$$

This is why the momentum space basis is useful - it diagonalises differential operators. Because it is (block) diagonal in this basis, we can take the logarithm easily since it is found by taking the logarithm of each diagonal element:

$$\ln\left(\frac{M}{2\pi}\right)_{p,q,ij} = \ln((2\pi)^4 M_q)_{ij}\delta^{(4)}(p-q). \tag{2.43}$$

The trace comes from summing over all diagonal elements:[6]

$$\begin{aligned}\mathrm{Tr}\left(\ln\left(\frac{M}{2\pi}\right)\right) =& \int \frac{\mathrm{d}^4k}{(2\pi)^4} \ln\left((2\pi)^4 M_k\right)_{ii} \delta^{(4)}(k-k) \\ =& \frac{V_4}{(2\pi)^4}\int \frac{\mathrm{d}^4k}{(2\pi)^4} \ln\left((2\pi)^4 M_k\right)_{ii},\end{aligned} \tag{2.44}$$

where $V_4 = \int \mathrm{d}^4x$ is the volume of Minkowski space-time. Leaving aside the infinite volume, the integral part will usually diverge. However, that can be

[5] We choose different signs for $e^{-ip\cdot x}$ and $e^{iq\cdot y}$ in order to make the analogy with a similarity transform clearer, as the change of basis goes like $SMS^\dagger$ in this case.

[6] Note that if the trace is obtained by a sum $\int \mathrm{d}^4x M(x,x)$ in position space then the momentum space sum must include a factor $\frac{1}{(2\pi)^4}$ in order to give the right result (this is to be consistent with the usual properties of a Fourier transform - essentially it is just a scale factor).

dealt with by the renormalisation terms.
Note, the logarithm of M_k may not be trivial, especially if there are numerous fields. Diagonalising M_{kij} will not really help, because this may mix fermion and boson fields, which is undesirable as their Gaussian integrals are different. In fact, it is convenient to simply evaluate the Gaussian integrals for each field one at a time, each time using the fact that we have a linear term:

$$\int \mathrm{d}^N \mathbf{x} \exp\left(-\frac{1}{2}x_i M_{ij} x_j + J_i x_i\right) = \left(\det\left(\frac{M}{2\pi}\right)\right)^{-\frac{1}{2}} \exp\left(\frac{1}{2}J_i {M^{-1}}_{ij} J_j\right). \tag{2.45}$$

We can then perform the Gaussian path integrals one at a time:

$$\begin{aligned}
I &= \int \prod_{i=1}^{N} (\mathcal{D}\eta_i) \exp\left(-\frac{1}{2}\sum_{i,j=1}^{N} \int \mathrm{d}^4x \mathrm{d}^4y \eta_i(x) M_{ij}(x,y) \eta_j(y)\right) \\
&= \int \mathcal{D}\eta_1 \int \prod_{i=2}^{N} (\mathcal{D}\eta_i) \exp\Bigg(-\frac{1}{2}\int \mathrm{d}^4x \mathrm{d}^4y \eta_1(x) M_{11}(x,y)\eta_1(y) \\
&\quad -\frac{1}{2}\int \mathrm{d}^4x \mathrm{d}^4y \eta_1(x) \sum_{i=2}^{N} M_{1i}(x,y)\eta_i(y) - \frac{1}{2}\mathrm{d}^4x \mathrm{d}^4y \sum_{i=2}^{N} \eta_i(x) M_{i1}(x,y)\eta_1(y) \\
&\quad -\frac{1}{2}\int \mathrm{d}^4x \mathrm{d}^4y \sum_{i,j=2}^{N} \eta_i(x) M_{ij}(x,y)\eta_j(y)\Bigg) \\
&= \det\left(\frac{M_{11}}{2\pi}\right)^{-\frac{1}{2}} \int \prod_{i=2}^{N} (\mathcal{D}\eta_i) \exp\left(-\frac{1}{2}\int \mathrm{d}^4x \mathrm{d}^4y \sum_{i,j=2}^{N} [\eta_i(x) M_{ij}(x,y)\eta_j(y)]\right) \\
&\quad \times \exp\left(\frac{1}{2}\int \mathrm{d}^4x \mathrm{d}^4y N_1(x) M_{11}^{-1}(x,y) N_1(y)\right),
\end{aligned} \tag{2.46}$$

where $N_1(x) \equiv -\frac{1}{2}\int \mathrm{d}^4y \sum_{i=2}^{N} M_{1i}(x,y)\eta_i(y)$. Thus, the entire integral can be computed iteratively and the logarithm also computed. In practice, however, we can generally arrange for $N_i = 0$ to hold at one the loop level, since for this not to be the case, we would require a term in the Lagrangian corresponding to one particle propagating, then turning into another type at a 2-point vertex. This can happen, but in gauge theories it can usually be avoided by an appropriate choice of gauge.
An important point, however, is that if we have any Grassman variables, then the Gaussian integrals must be evaluated as:

$$\int \prod_{i=1}^{N} (\mathrm{d}\eta_i^* \mathrm{d}\eta_i) \exp\left(-\eta_i^* M_{ij} \eta_j + \eta_i^* J_i + J_i^* \eta_i\right) = \det(M) \exp\left(J_i^* {M^{-1}}_{ij} J_j\right). \tag{2.47}$$

The differing position of the determinant makes an important difference. When we compute the logarithm, instead of a factor of $-\frac{1}{2}$ we obtain a factor of 1.

Thus, *fermions give the opposite contribution to the effective potential.* In terms of perturbation theory, this can be understood to be a consequence of the fact that fermion loops always give an extra minus sign.
It is not entirely obvious that this approach does in fact split terms order by order in loops. In fact, the Gaussian integral we have just computed is equivalent to summing all of the 1-loop diagrams that would contribute to the effective action. To see this, note that we can regard it as a sum of two-point interactions, since it only involves powers of η up to second order. However, it is topologically impossible to construct diagrams with more than one loop using only two point interactions (see figure 2.6), and since the only end points of propagators are the classical field vertices (Which are strictly speaking not external lines, but vertices), all the diagrams contributing to this Gaussian integral must have at least one loop.

Once we start computing the third order and higher terms in η, however, the

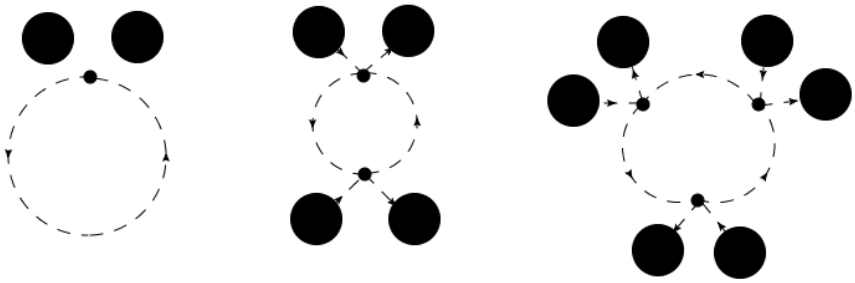

Figure 2.6: Some possible 1 loop corrections to the effective action. Note that to have more than one loop would require higher order interaction vertices, which don't appear in the computation of the Gaussian integral.

third line of Eq. (2.33) shows that we can easily compute these terms via Feynman diagrams, where we are allowed 3rd and higher order vertices, which can mix in the same diagram. Note that we couldn't mix higher order vertices into the computation of the second line of Eq. (2.33) since as a perturbation series, that would be performed using the $S[\phi_{\text{cl}}]$ as the action in the denominator, while the third line is performed using $I_0[\eta]$ as the action in the denominator (so they are technically different sorts of perturbation series). Since I_{int} contains all the higher order terms, however, then we are allowed to mix them for higher loops. Furthermore, it is also impossible to construct 1-loop diagrams if we have any third order or higher vertices and no external legs. This is illustrated in figure 2.7

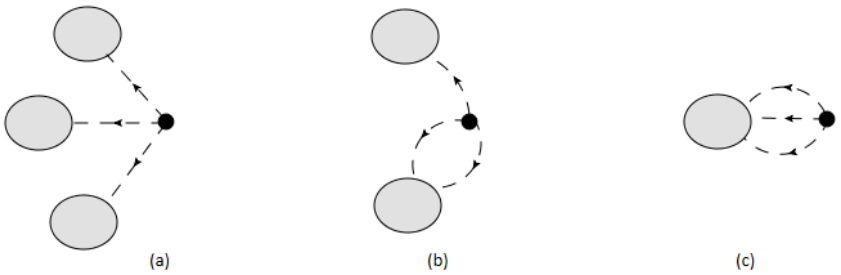

Figure 2.7: All possible diagrams with no external legs, involving a three point vertex. Each grey ellipse in (a) must contain at least one loop because no external legs or one-point vertices are allowed (excluding the classical field, which is suppressed here for simplicity, but is attached to the three point vertex). In (b), one loop is visible, and the upper grey ellipse must contain at least one loop. In (c), the ellipse need not contain a loop, but two loops are already visible.

2.2.1 Example: Scalar Field Effective Potential

To see how this works in practice, it is useful to consider an example. Consider a scalar field with the action:

$$S[\phi] = \int \mathrm{d}^4x \left[\frac{1}{2}\partial_\mu\phi\partial^\mu\phi - \frac{1}{2}m^2\phi^2 - \frac{\lambda}{4!}\phi^4\right]. \tag{2.48}$$

Expanding as $\phi = \phi_0 + \eta$ gives:

$$\begin{aligned} S[\phi_0+\eta] = &\int \mathrm{d}^4x \left[\frac{1}{2}\partial_\mu\phi_0\partial^\mu\phi_0 - \frac{1}{2}m^2\phi_0^2 - \frac{\lambda}{4!}\phi_0^4\right] \\ &+ \int \mathrm{d}^4x \left[\partial_\mu\phi_0\partial^\mu\eta - m^2\phi_0\eta - \frac{\lambda}{6}\phi_0^3\eta\right] \\ &+ \int \mathrm{d}^4x \left[\frac{1}{2}\partial_\mu\eta\partial^\mu\eta - \frac{1}{2}m^2\eta^2 - \frac{\lambda}{4}\phi_0^2\eta^2\right] \\ &+ \int \mathrm{d}^4x \left[-\frac{\lambda}{6}\phi_0\eta^3\right] + \int \mathrm{d}^4x \left[-\frac{\lambda}{4!}\eta^4\right]. \end{aligned} \tag{2.49}$$

The first row gives the classical action, the second is the first order correction which we arrange to vanish, while the third is the second order correction. The

fourth row contains the higher order terms. Thus the effective action is:

$$\begin{aligned}\Gamma[\phi_0] =& \int \mathrm{d}^4x \left[\frac{1}{2}\partial_\mu\phi_0\partial^\mu\phi_0 - \frac{1}{2}m^2\phi_0^2 - \frac{\lambda}{4!}\phi_0^4\right] \\ & - i\ln\left(\int \mathcal{D}\eta \exp\left(i\int \mathrm{d}^4x \left[\frac{1}{2}\partial_\mu\eta\partial^\mu\eta - \frac{1}{2}m^2\eta^2 - \frac{\lambda}{4}\phi_0^2\eta^2\right]\right)\right) + \text{h.o.t.} \\ =& \int \mathrm{d}^4x \left[\frac{1}{2}\partial_\mu\phi_0\partial^\mu\phi_0 - \frac{1}{2}m^2\phi_0^2 - \frac{\lambda}{4!}\phi_0^4\right] \\ & - i\ln\left(\int \mathcal{D}\eta \exp\left(-\frac{1}{2}\int \mathrm{d}^4x \int \mathrm{d}^4y \eta(x) i\delta^{(4)}(x-y)\times\right.\right. \\ & \left.\left.\times \left[\partial_\mu\partial^\mu + m^2 + \frac{\lambda}{2}\phi_0^2\right]\eta(y)\right)\right) \\ & + \text{h.o.t.}\end{aligned} \tag{2.50}$$

Thus:

$$\begin{aligned}M(k,q) =& \int \mathrm{d}^4x \int \mathrm{d}^4y e^{-ik\cdot x} i\delta^{(4)}(x-y)[-q^2 + m^2 + \frac{\lambda}{2}\phi_0^2]e^{iq\cdot y} \\ =& i(2\pi)^4\delta^{(4)}(k-q)[-q^2 + m^2 + \frac{\lambda}{2}\phi_0^2].\end{aligned} \tag{2.51}$$

Hence:

$$\begin{aligned}\Gamma[\phi_0] =& \int \mathrm{d}^4x \left[\frac{1}{2}\partial_\mu\phi_0\partial^\mu\phi_0 - \frac{1}{2}m^2\phi_0^2 - \frac{\lambda}{4!}\phi_0^4\right] \\ & + \frac{i}{2}\int \frac{\mathrm{d}^4k}{(2\pi)^4} \ln\left((2\pi)^4 i[-k^2 + m^2 + \frac{\lambda}{2}\phi_0^2]\right) + \text{h.o.t.}\end{aligned} \tag{2.52}$$

Note that the integral over k actually diverges. However, writing $M^2 = m^2 + \frac{\lambda}{2}\phi_0^2$ we can differentiate to obtain a different integral:

$$\begin{aligned}I(M^2) =& \int \frac{\mathrm{d}^4k}{(2\pi)^4} \ln\left((2\pi)^4 i[-k^2 + M^2]\right), \\ I'(M^2) =& \int \frac{\mathrm{d}^4k}{(2\pi)^4} \frac{1}{-k^2 + M^2}.\end{aligned}$$

This is still divergent, but can be dealt with using the standard techniques of dimensional regularisation. In $d - \varepsilon$ dimensions, we can show that:

$$I_n(M) \equiv \int \frac{\mathrm{d}^dk}{(2\pi)^d} \frac{1}{(k^2 - M^2)^n} = \lim_{\varepsilon\to 0} \frac{(-1)^n i M^{d-\varepsilon-2n}}{(4\pi)^{\frac{d-\varepsilon}{2}}} \frac{\Gamma\left(n - \frac{d}{2} + \frac{\varepsilon}{2}\right)}{\Gamma(n)}, \tag{2.53}$$

where $d = 4$ here and $\Gamma(n)$ is the Gamma function. Consequently:

$$\begin{aligned} I'(M^2) =& \frac{i\mu^{-\varepsilon}M^2}{(4\pi)^2}\left(\frac{M^2}{4\pi\mu^2}\right)^{-\frac{\varepsilon}{2}}\Gamma\left(-1+\frac{\varepsilon}{2}\right) \\ =& \frac{i\mu^{-\varepsilon}M^2}{16\pi^2}e^{-\frac{\varepsilon}{2}\ln\left(\frac{M^2}{4\pi\mu^2}\right)}\Gamma(-1+\frac{\varepsilon}{2}) \\ =& -\frac{i\mu^{-\varepsilon}M^2}{16\pi^2}\left(\frac{2}{\varepsilon}-\gamma+1-\ln\left(\frac{M^2}{4\pi\mu^2}\right)+O(\varepsilon)\right). \end{aligned} \tag{2.54}$$

where γ is the Euler-Mascheroni constant, appearing from the Taylor expansion of $\Gamma(-l+\frac{\varepsilon}{2})$. Note that we were forced to introduce an arbitrary energy scale, μ, so that the exponential of a dimensional quantity like M^2 makes sense. In the $\overline{\text{MS}}$ renormalisation scheme, we introduce counter terms which subtract the $\frac{2}{\varepsilon}-\gamma+\ln 4\pi$ part. After renormalisation and taking $\varepsilon \to 0$ we have:

$$I'(M^2) = \frac{iM^2}{16\pi^2}\left(\ln\left(\frac{M^2}{\mu^2}\right)-1\right). \tag{2.55}$$

To integrate this, use the fact that $\int x\ln x \mathrm{d}x = \frac{x^2}{2}\ln x - \frac{x^2}{4}$, to give:

$$\begin{aligned} I(M^2) =& \frac{i}{16\pi^2}\left(\frac{M^4}{2}\ln M^2 - \frac{M^4}{4} - \frac{M^4}{2}\ln\mu^2 - \frac{M^4}{2}\right) + C \\ =& \frac{iM^4}{32\pi^2}\left(\ln\left(\frac{M^2}{\mu^2}\right)-\frac{3}{2}\right)+C. \end{aligned} \tag{2.56}$$

The integration constant only renormalises the vacuum energy, so we will neglect it here. Thus, the final contribution to the effective action is:

$$\begin{aligned} \Gamma[\phi_0] = \int \mathrm{d}^4x \Bigg[&\frac{1}{2}\partial_\mu\phi_0\partial^\mu\phi_0 - \frac{1}{2}m^2\phi_0^2 - \frac{\lambda}{4!}\phi_0^4 \\ &-\frac{1}{64\pi^2}(m^2+\frac{\lambda}{2}\phi_0^2)^2\left(\ln\left(\frac{m^2+\frac{\lambda}{2}\phi_0^2}{\mu^2}\right)-\frac{3}{2}\right)\Bigg] + \text{h.o.t.} \end{aligned} \tag{2.57}$$

However, the effective action will not actually depend on μ^2, due to the variation of the coupling constants. There is one problem with this, however. The diagrams at each loop order will give rise to terms of order $\lambda(\lambda\ln\left(\frac{m^2+\frac{\lambda}{2}\phi_0^2}{\mu^2}\right))^n$ for order n [4]. The perturbation series is valid only if these are small, which will fail to be the case when the logarithm becomes large, as it does for either small or large arguments. Thus, this formula can only be trusted for a limited range of ϕ_0.

However, it is possible to get around this problem by requiring that the effective action satisfy the Callan-Symanzik equation[4]:

$$\left[\mu\frac{\partial}{\partial\mu}+\beta_\lambda\frac{\partial}{\partial\lambda}+\beta_{m^2}\frac{\partial}{\partial m^2}+\gamma\int\mathrm{d}^4x\phi_0(x)\frac{\delta}{\delta\phi_0(x)}\right]\Gamma[\phi_0]=0 \tag{2.58}$$

After deducing the approximate form of the beta functions, solving this equation can give a potential valid for a much wider range of ϕ_0. Thus, all that is needed to compute the effective potential is an accurate computation of the beta functions of the theory.

2.3 Example: Yukawa Theory

For the standard model, the situation is more complicated, since there is more than one field. We can begin to understand this by considering Yukawa theory for a real scalar interacting with a fermion:

$$S_{\text{Yuk}} = \int \mathrm{d}^4x \left[\frac{1}{2}\partial_\mu\phi\partial^\mu\phi - \frac{1}{2}m_\phi^2\phi^2 - \frac{\lambda}{4!}\phi^4 + i\bar{\Psi}_a\gamma^\mu_{ab}\partial_\mu\Psi_b - m_\Psi\bar{\Psi}_a\Psi_a - g\bar{\Psi}_a\Psi_a\phi \right]. \tag{2.59}$$

We will choose to expand this around $\phi = \phi_0$ and $\Psi = 0$, since we are only interested in the contribution to the scalar potential, derived from the action where all fermions are set to zero. One finds by applying the Euler-Lagrange equations:

$$M_{\phi\phi}(x,y) = -i \left.\frac{\delta^2\mathcal{L}}{\delta\phi(x)\delta\phi(y)}\right|_{\phi=\phi_0,\Psi=0} = i\partial_\mu\partial^\mu\left(\delta^{(4)}(x-y)\right) + im_\phi^2\delta^{(4)}(x-y) + i\frac{\lambda}{2}\phi_0^2 \tag{2.60}$$

$$M_{\phi\Psi} = -i \left.\frac{\delta^2\mathcal{L}}{\delta\phi(x)\Psi_a(y)}\right|_{\phi=\phi_0,\Psi=0} = 0 \tag{2.61}$$

$$M_{\Psi\phi} = -i \left.\frac{\delta^2\mathcal{L}}{\delta\bar{\Psi}_a(x)\delta\phi(y)}\right|_{\phi=\phi_0,\Psi=0} = 0 \tag{2.62}$$

$$M_{\Psi\Psi} = -i \left.\frac{\delta^2\mathcal{L}}{\delta\bar{\Psi}_a(x)\delta\Psi_b(y)}\right|_{\phi=\phi_0,\Psi=0} = \gamma^\mu_{ab}\partial_\mu\left(\delta^{(4)}(x-y)\right) + i(m_\Psi + g\phi_0)\delta_{ab}\delta^{(4)}(x-y). \tag{2.63}$$

The mixed derivatives vanish because the only interaction is cubic, so there is always one Ψ or $\bar{\Psi}$ left over which is set to zero. Consequently, the second line of Eq. (2.36) factorises as:

$$\begin{aligned}\int \mathcal{D}\bar{\Psi}\mathcal{D}\Psi\mathcal{D}\phi \exp\Bigg(&-\frac{1}{2}\int \mathrm{d}^4x\mathrm{d}^4y\left[\phi(x)M_{\phi\phi}(x,y)\phi(y)\right] \\ &- \int \mathrm{d}^4x\mathrm{d}^4y\left[\bar{\Psi}(x)M_{\Psi\Psi}\Psi(y)\right]\Bigg) \\ &= \det\left(\frac{M_{\phi\phi}}{2\pi}\right)^{-\frac{1}{2}}\det\left(M_{\Psi\Psi}\right).\end{aligned} \tag{2.64}$$

We therefore conclude that the 1-loop contribution to the effective potential is:

$$\frac{i}{2}\ln\det\left(\frac{M_{\phi\phi}}{2\pi}\right)-i\ln\det\left(M_{\Psi\Psi}\right). \tag{2.65}$$

The first term is identical to Eq. (2.57), while the second can be computed in the following manner:

$$-i\ln\det\left(M_{\Psi\Psi}\right)=-i\mathrm{Tr}\ln\left(\gamma^{\mu}_{ab}\partial_{\mu}\left(\delta^{(4)}(x-y)\right)+i(m_{\Psi}+g\phi_0)\delta_{ab}\delta^{(4)}(x-y)\right). \tag{2.66}$$

In momentum space, we have:

$$\begin{aligned}M_{ab}(k,q)=&\int \mathrm{d}^4x\mathrm{d}^4y e^{ip\cdot x}\left(\gamma^{\mu}_{ab}\partial_{\mu}\left(\delta^{(4)}(x-y)\right)+i(m_{\Psi}+g\phi_0)\delta_{ab}\delta^{(4)}(x-y)\right)e^{-iq\cdot y}\\ =&\int \mathrm{d}^4x\mathrm{d}^4y\left(e^{ip\cdot x}\gamma^{\mu}_{ab}iq_{\mu}\delta^{(4)}(x-y)+i(m_{\Psi}+g\phi_0)\delta_{ab}\delta^{(4)}(x-y)\right)e^{-iq\cdot y}\\ =&\int \mathrm{d}^4x e^{ix\cdot(p-q)}i(\gamma^{\mu}_{ab}q_{\mu}+(m_{\Psi}+g\phi_0)\delta_{ab})\\ =&(2\pi)^4\delta^{(4)}(p-q)i(\gamma^{\mu}_{ab}q_{\mu}+(m_{\Psi}+g\phi_0)\delta_{ab}).\end{aligned} \tag{2.67}$$

Taking the momentum space trace then gives:

$$I\equiv-i\ln\det\left(M_{\Psi\Psi}\right)=-i\int\frac{\mathrm{d}^4k}{(2\pi)^4}\mathrm{Tr}\ln\left(i(2\pi)^4(\gamma^{\mu}k_{\mu}+(m_{\Psi}+g\phi_0))\,\mathbb{I}\right)\delta^{(4)}(k-k). \tag{2.68}$$

Let $\tilde{m}=m_{\Psi}+g\phi_0$ and differentiate:

$$\frac{\mathrm{d}I}{\mathrm{d}\tilde{m}}=-\frac{iV_4}{(2\pi)^4}\int\mathrm{d}^4k\mathrm{Tr}\left((\gamma^{\mu}k_{\mu}+\tilde{m}\mathbb{I})^{-1}\right). \tag{2.69}$$

Where V_4 is the volume of space-time. This last step is valid because[7]:

$$\begin{aligned}\frac{\mathrm{d}}{\mathrm{d}\tilde{m}}\ln(\gamma^{\mu}k_{\mu}+\tilde{m})=&\lim_{\delta\tilde{m}\to0}\frac{\ln(\gamma^{\mu}k_{\mu}+\tilde{m}+\delta\tilde{m})-\ln(\gamma^{\mu}k_{\mu}+\tilde{m})}{\delta\tilde{m}}\\ =&\lim_{\delta\tilde{m}\to0}\frac{\ln(\gamma^{\mu}k_{\mu}+\tilde{m})+\ln(\mathbb{I}+(\gamma^{\mu}k_{\mu}+\tilde{m})^{-1}\delta\tilde{m})-\ln(\gamma^{\mu}k_{\mu}+\tilde{m})}{\delta\tilde{m}}\\ =&(\gamma^{\mu}k_{\mu}+\tilde{m})^{-1}.\end{aligned} \tag{2.70}$$

This inverse is well known:

$$\begin{aligned}\frac{\mathrm{d}I}{\mathrm{d}\tilde{m}}=&-\frac{iV_4}{(2\pi)^4}\int\mathrm{d}^4k\mathrm{Tr}\left(\frac{\gamma^{\mu}k_{\mu}-\tilde{m}}{k^2-\tilde{m}^2}\right)\\ =&-\frac{iV_4}{(2\pi)^4}\int\mathrm{d}^4k\frac{-4\tilde{m}}{k^2-\tilde{m}^2}\\ =&4i\tilde{m}V_4I_1(\tilde{m}),\end{aligned} \tag{2.71}$$

[7]This derivation is not entirely trivial, because $\ln(AB)\neq\ln A+\ln B$ for generic non-commuting A,B, however in this case $(\gamma^{\mu}k_{\mu}-\tilde{m})$ commutes with $\mathbb{I}+\delta\tilde{m}(\gamma^{\mu}k_{\mu}+\tilde{m})^{-1}$, so this operation is valid. A generic function, $\ln f(\tilde{m})$ would not have this property.

since $\mathrm{Tr}\gamma^\mu = 0$ and $\mathrm{Tr}\mathbb{I} = 4$. The integral $I_1(\tilde{m})$ is divergent and can be computed using Eq. (2.53). The answer is:

$$I_1(\tilde{m}) = \frac{i\tilde{m}^2}{16\pi^2}\left(\frac{2}{\varepsilon} - \ln\left(\frac{\tilde{m}^2}{4\pi\mu^2}\right) + 1 - \gamma\right). \tag{2.72}$$

We renormalise this using $\overline{\mathrm{MS}}$ to give:

$$\begin{aligned}
\frac{\mathrm{d}I}{\mathrm{d}\tilde{m}} =& 4i\tilde{m}V_4\frac{i\tilde{m}^2}{16\pi^2}\left(1 - \ln\left(\frac{\tilde{m}^2}{\mu^2}\right)\right) \\
=& -\frac{4V_4}{16\pi^2}\left(\tilde{m}^3 - 2\tilde{m}^3\ln(\tilde{m}) + \tilde{m}^3\ln(\mu^2)\right) \\
\implies I(\tilde{m}) =& \frac{-4V_4}{16\pi^2}\left(\frac{\tilde{m}^4}{4} - 2\frac{\tilde{m}^4}{4}\ln(\tilde{m}) + 2\frac{\tilde{m}^2}{16} + \frac{\tilde{m}^4}{4}\ln(\mu^2)\right) + C \\
=& \frac{4V_4\tilde{m}^4}{64\pi^2}\left(\ln\left(\frac{\tilde{m}^2}{\mu^2}\right) - \frac{3}{2}\right) + C.
\end{aligned} \tag{2.73}$$

The constant C only serves to renormalise the vacuum. We conclude, therefore, that the one loop effective action is[8]:

$$\begin{aligned}
\Gamma[\phi_0, \Psi = 0] = \int \mathrm{d}^4x \Bigg[& -\frac{1}{2}m^2\phi_0^2 - \frac{\lambda}{4!}\phi_0^4 \\
& - \frac{M^4}{64\pi^2}\left(\ln\left(\frac{M^2}{\mu^2}\right) - \frac{3}{2}\right) + \frac{4\tilde{m}^4}{64\pi^2}\left(\ln\left(\frac{\tilde{m}^2}{\mu^2}\right) - \frac{3}{2}\right)\Bigg].
\end{aligned} \tag{2.74}$$

Where $M^2 = m_\phi^2 + \frac{\lambda}{2}\phi_0^2$ and $\tilde{m} = m_\Psi + g\phi_0$. Notice that the fermions contribute a term of opposite sign to the bosons (due to their anti-commuting nature and thus different determinant in the path integral), with a multiplicity of 4 which ultimately originates from the trace of the $\mathbb{I}$ matrix (and thus can be traced back to the fact that there are four fermionic degrees of freedom but only one bosonic degree of freedom). Furthermore, notice that the logarithm depends on the fourth power of the mass of the particle[9]. Consequently, only the very heaviest mass particles contribute significantly to the effective potential.

[8] The kinetic term is missing, because ϕ_0 is assumed to be constant in space-time.
[9] In the standard, model, $\tilde{m}$ *is* the mass, since all fermions have $m_\Psi = 0$

Chapter 3

Stability of the Electroweak Vacuum

3.1 The Standard Model Effective Potential

The classical Higgs potential is stable in the sense that once a system reaches the minimum, there is no other minimum into which it can decay, as the potential grows monotonically for large ϕ. From our discussion of the Yukawa theory, however, it can be seen that if the scalar field couples to fermions (as the Higgs field does, in order to give rise to fermion masses) then the potential receives negative contributions:

$$\begin{aligned} V(\phi_0) =& \frac{1}{2}m^2\phi_0^2 + \frac{\lambda}{4!}\phi_0^4 + \frac{\left(m_\phi^2 + \frac{\lambda}{2}\phi_0^2\right)^2}{64\pi^2}\left(\ln\left(\frac{m_\phi^2 + \frac{\lambda}{2}\phi_0^2}{\mu^2}\right) - \frac{3}{2}\right) \\ & - \frac{(m_\Psi + g\phi_0)^4}{16\pi^2}\left(\ln\left(\frac{(m_\Psi + g\phi_0)^2}{\mu^2}\right) - \frac{3}{2}\right). \end{aligned} \tag{3.1}$$

Consequently, if the theory contains sufficiently massive fermions, then for large values of ϕ_0 the potential can be forced downwards again. This results in the minimum being a 'false vacuum' - sufficiently large fluctuations in the field can push it over the potential barrier and into a region containing either another, lower energy, minimum, or potentially a region unbounded below. Equally, in quantum theories, it is possible for a system in the false vacuum to decay to a lower minimum via quantum tunnelling. This essentially gives the universe a half-life as such a decay occurs spontaneously.

In the standard model, the two most important parameters for determining the vacuum structure of the theory are the mass of the top quark and the mass of the Higgs field itself. The top quark contribution dominates over other fermions, because its mass ($\sim 173.1\,\text{GeV}$) is so much larger, and as we can see from Eq. (3.1), the negative contributions depend on the *fourth* power of the mass of the

fermion. In order to answer the question in the Standard model, it is necessary to perform very precise calculations of the Higgs effective potential, including higher loop order corrections.

To illustrate this, we used the beta-functions of the standard model to two

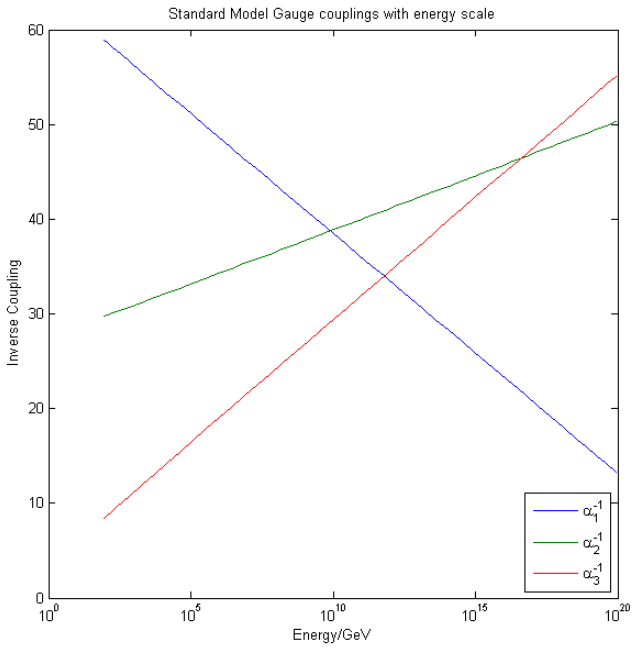

Figure 3.1: Standard model gauge couplings, $\alpha_i = \frac{g_i^2}{4\pi}$ running with the energy scale μ in $\overline{\text{MS}}$, to two loops. Note that these fail to meet, however, the energy scale where these cross is in reality higher than the diagram indicates, due to not taking into account quantum corrections to the relationship between the Yukawa coupling and the mass.

loops, which can be found in [7] and [12]. As an illustrative example, we use the initial conditions $\lambda = 0.13$ (for the $\frac{\lambda\phi^4}{4}$ normalisation), $g_1 = 0.4617$, $g_2 = 0.6502$, $g_3 = 1.2198$ and $h = 1.0017$ (these are taken from [13]), all in $\bar{\text{M}}\text{S}$ where g_1, g_2, g_3 are the gauge couplings for $U(1)_Y$, $SU(2)$ and $SU(3)_c$ respectively, λ is the Higgs quartic coupling, and h is the Yukawa coupling for the top quark to the Higgs field. We consider only the top quark as it has a mass significantly larger than the other quarks and leptons in the Standard model. The results for the gauge couplings are given in figure 3.1 and for the Higgs quartic coupling in figure 3.2. To one loop, the Higgs effective potential in $\overline{\text{MS}}$ can be written[14]:

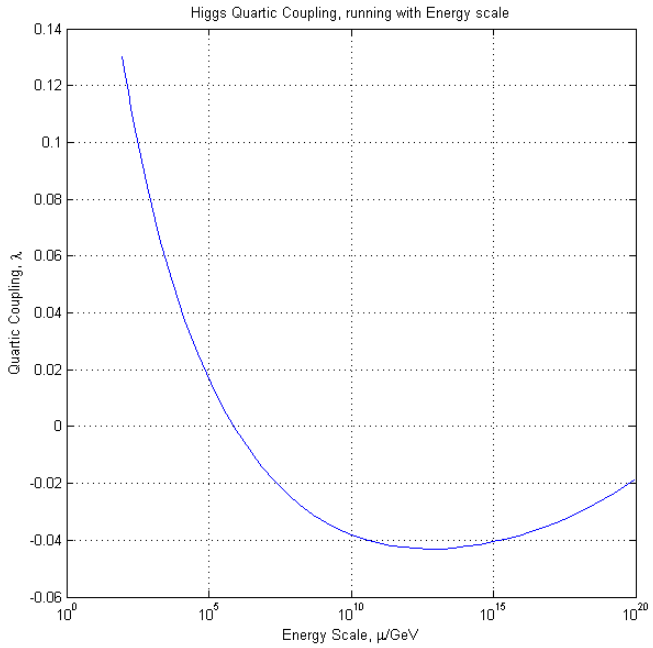

Figure 3.2: Higgs field quartic coupling running with energy in $\overline{\text{MS}}$. This appears to become negative around 10^6GeV however this is without taking into account quantum corrections to the Yukawa-coupling/top-quark mass relation.

$$\begin{aligned} V(\phi) =& \frac{1}{2}m_h^2\phi^2 + \frac{\lambda}{4}\phi^4 + \frac{H^2}{64\pi^2}\left(\ln\left(\frac{H}{\mu^2}\right) - \frac{3}{2}\right) + \frac{3G^2}{64\pi^2}\left(\ln\left(\frac{G}{\mu^2}\right) - \frac{3}{2}\right) \\ & - \frac{3T^2}{16\pi^2}\left(\ln\left(\frac{T}{\mu^2}\right) - \frac{5}{6}\right) + \frac{3W^2}{32\pi^2}\left(\ln\left(\frac{W}{\mu^2}\right) - \frac{5}{6}\right) + \frac{3Z^2}{4}\left(\ln\left(\frac{Z}{\mu^2}\right) - \frac{5}{6}\right), \end{aligned} \tag{3.2}$$

where:

$$H = m_h^2 + 3\lambda\phi^2 \tag{3.3}$$

$$T = \frac{h^2}{2}\phi^2 \tag{3.4}$$

$$G = m_h^2 + \lambda\phi^2 \tag{3.5}$$

$$W = \frac{g_1^2}{4}\phi^2 \tag{3.6}$$

$$Z = \frac{(g_1^2 + g_2^2)}{4}\phi^2 \tag{3.7}$$

and μ is the energy scale. Here, H arises from the Higgs self interaction, G from the interaction of the Higgs field with the Goldstone bosons (by Higgs field here

we mean the left over real scalar part of Φ, the other three components of which are the Goldstone bosons), T corresponds to the interaction with the top quark (note that this is negative), and W, Z arise from interaction with the W and Z bosons respectively. No term for photons appears because photons do not interact with the Higgs field.
The natural scale, μ, to choose is $\mu = \phi$, since this will ensure that the logarithms remain small for most ranges of ϕ (which is required for the loop expansion to remain perturbative). This choice is shown plotted in figure 3.3. Some caveats

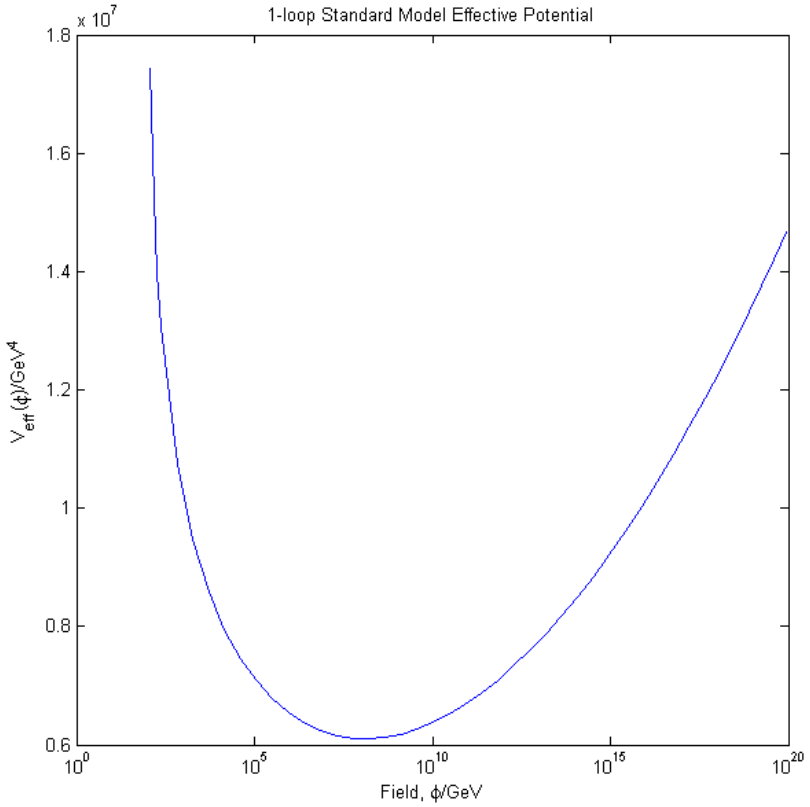

Figure 3.3: 1-loop Higgs potential, using $\mu = \phi$. Note that the apparent divergence for small ϕ is due to the logarithmic terms becoming small there. Since this means perturbation theory breaks down, this behaviour is not physically meaningful. However, we note that there is a minimum at large ϕ, around 10^8 GeV. This could cause the electroweak vacuum to become unstable.

apply when interpreting this, however:

- In setting up the initial conditions, we have ignored the fact that in the

$\overline{\text{MS}}$ scheme, relations like $m_h^2 = 2\lambda v^2$ where v is the vacuum expectation value, are only valid at tree level (this is in contrast to the off-shell scheme, or 'physical' scheme, where these relations are valid to all orders). So to obtain the initial parameters at M_z in terms of experimentally determined quantities requires computing higher order quantum corrections to these relations (this is done, for example, in [15]). Such computations are beyond the scope of this report.

- Independence of the scale, μ should be true non-perturbatively, but may not be manifest in perturbation theory. We can improve the effective potential by making use of the renormalisation group, by requiring it to satisfy the Callan-Symanzik equation. This procedure would lead to a 'renormalisation group improved' effective potential [9].

- We have only considered the top quark, however, due to the large mass of this fermion, this is still a good approximation.

- Generally speaking, we should interpret only the minima of the effective potential as being physically meaningful (see a discussion in [8] - this is related to the fact that perturbation theory has to take place in a stable minimum to be meaningful and so regions where the second derivative of the effective potential are negative cannot be trusted as perturbative calculations).

- The effective potential appears to diverge at small ϕ. However, the loop expansion requires that the logarithmic terms appearing in the potential are small (otherwise, perturbation theory fails). Since the apparent divergence occurs in a regime where this is not the case, we cannot trust the prediction for small ϕ. So, figure 3.3 says nothing about the electro-weak minimum. More sophisticated techniques are required to analyse that . The minimum we have found, however, is at large ϕ (around $10^8\,\text{GeV}$). Interpreted literally, if this minimum is at a lower value of the potential than the electroweak minimum at $v = 246.22\,\text{GeV}$, it would mean that the electroweak minimum is only meta-stable.

This running of the standard model couplings has been studied in depth and requiring the non-existence of the second minimum up to the Planck scale was used, for example, to give bounds on the allowed mass of the Higgs boson, before its discovery (see [7] for example).
However, with the detection of a particle consistent with the standard model Higgs boson [16][17], we are now in a better position to make predictions about the stability of the standard model vacuum. The current estimate of the Higgs boson mass is $m_h = 125.7 \pm 0.4\,\text{GeV}$[13].
In principle this is sufficient, however, the location of the Higgs mass complicates matters. It places the Higgs potential close (in parameter space) to the boundary between instability ($V_{eff}(\phi)$ turns down at large ϕ, so nothing can stop the field rolling to infinite ϕ), and stability (the second minimum is at a

higher potential than the electroweak minimum, which is therefore the absolutely stable global minimum). In fact this boundary is not a 'hard' boundary, but consists of a third region of parameter space where the electroweak minimum is *meta-stable* (that is, there is a second minimum, but as in figure 3.3 the potential does not turn down at large ϕ, so the second minimum is absolutely stable).

3.2 Meta-stability and Bubble-Nucleation

In the metastability scenario, the electro-weak vacuum would be a long-lived state which could collapse to the global minimum at any time, via quantum tunnelling. Not all regions of the universe are causally connected, however. The transition from the electroweak vacuum to the global minimum would occur via *bubble nucleation*, a process in which local 'bubbles' of the lower-potential Higgs-field form. Note that because the Hamiltonian-density for a scalar field is given by:

$$\mathcal{H} = \frac{\dot{\phi}^2}{2} + \frac{1}{2}(\nabla\phi)^2 + V(\phi), \tag{3.8}$$

spatial gradients in the Higgs field always increase the local energy. To understand how the bubble will behave, it is useful to consider the close analogy of a phase change in a thermodynamic system. Let forming a bubble change the Gibbs free energy by ΔG_{bubble} per unit volume. This always decreases the Gibbs free energy if the tunnelling is to a lower value of the potential. However, the bubble has a surface tension, T per unit area which tends to increase the free energy (because the bubble must sustain itself against pressure from the external region of a different phase, which costs energy). Assuming a spherical bubble, the change in Gibbs free energy for a bubble of radius r is:

$$\Delta G = \frac{4\pi r^3}{3}\Delta G_{\text{bubble}} + 4\pi r^2 T. \tag{3.9}$$

Thus:

$$\frac{\mathrm{d}\Delta G}{\mathrm{d}r} = 4\pi r^2 \Delta G_{\text{bubble}} + 8\pi r T. \tag{3.10}$$

If ΔG_{bubble} is positive (so that creating bubbles costs energy - this only happens for bubbles of a higher potential) then bubbles will tend to shrink. However, for negative ΔG_{bubble}, then there is a critical radius $R_c = -\frac{2T}{\Delta G_{\text{bubble}}} > 0$ above which the bubble expands, despite the surface tension. Similarly, bubbles of the lower potential phase in the Higgs potential tend to expand if they are large enough. Thus eventually, the entire universe will be converted to the lower potential phase[1].

[1]Note that this may not happen if the universe is expanding fast enough, so that the rate of increase of the universes volume exceeds the rate at which that volume is converted to the lower phase. This becomes relevant in an inflationary scenario.

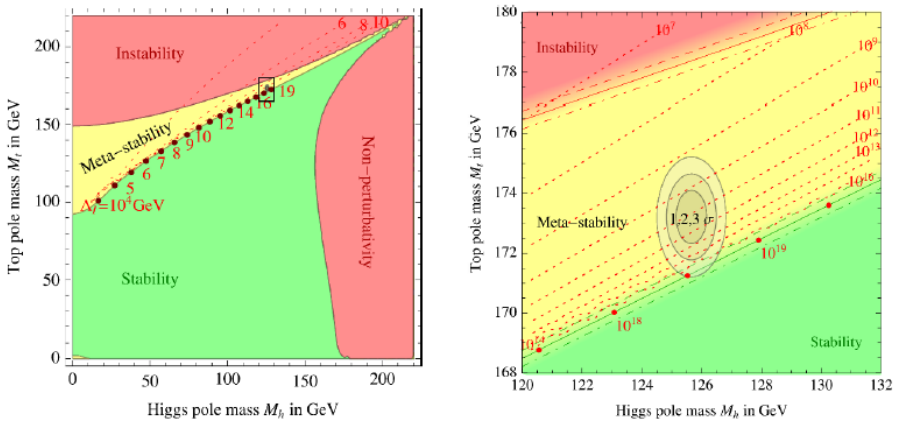

Figure 3.4: Regions of m_h - m_t parameter space and their associated electro-weak vacuum stability. Circles give 1-3 σ uncertainty for m_h and m_t, while the uncertainty in the stability region boundaries is given by the dashed line, and is principally due to the uncertainty in $\alpha_s(M_z)$ [19]. The red dotted lines indicate the scale at which the Higgs quartic coupling crosses zero, which gives the energy scale at which the global minimum occurs. This figure is by Buttazzo et al. [3].

3.3 Studies of Electro-weak vacuum stability

It turns out that two main quantities most significantly affect the stability of the electro-weak vacuum: The Higgs mass, and the top-quark mass. The mean values of $m_h = 125.7 \pm 0.4\,\text{GeV}$ and $m_t = 173.21 \pm 0.51 \pm 0.71\,\text{GeV}$ (first error statistical, second error systematic) [13], place the electroweak vacuum in the meta-stability region[18], as can be seen in figure 3.4, from Buttazzo et al. [3]. Thus, it would appear, to 2σ confidence, that the standard model electroweak vacuum is only metastable. There are several things to note about this:

- The uncertainties still allow for stability at 3σ, so there is a need for more precise measurements of the top-quark and higgs boson masses to narrow down precisely the state of the electroweak vacuum.
- The fact that the current region of the universe has not yet decayed to the lower energy state is certainly evidence in favour of the life-time being very long, at least of order the age of the universe.
- Being close to the instability region constrains the possibility of new particles at higher energies. For example, an undiscovered massive fermion might easily destabilise the vacuum if it coupled to the Higgs field, unless some undiscovered mechanism prevents this, for example by balancing it out with another boson (we will discuss this possibility in section 6).

- If the electro-weak vacuum is metastable, then collapse to the global minimum could also be precipitated by disturbing the Higgs field with sufficiently large amounts of energy. While this is unlikely in the context of the current universe, in an inflating universe, quantum fluctuations can potentially be sufficient to push the Higgs field over the potential barrier into the global minimum. Thus, if inflation occurred at a sufficiently high energy scale, it would strongly indicate the presence of new physics changing the structure of the Higgs potential at large field values.

The results from Buttazzo et al.[3] and Degrassi et al.[19] indicate that to three sigma confidence, the electroweak vacuum is metastable, developing an instability between $\phi \sim 10^9 - 10^{15}\,\text{GeV}$.
This leads to the question of whether the vacuum could spontaneously collapse to the lower minimum via quantum tunnelling. This process would proceed via the bubble nucleation discussed in section 3.2. To compute the expected life-time of the vacuum, it is necessary to compute the probability that a sufficiently large[2] bubble of the lower vacuum nucleated at some point in the past life-cone of the visible universe. This calculation was performed in [3], where it was found that the expected life-time, while very uncertain, is much longer than the present age of the universe (see figure 3.5). As can be seen, the uncertainty strongly affects the life-time, however, the current data seems to suggest a life-time much longer than the current age of the universe - consistent with the observation that our current vacuum has not yet decayed.

3.4 Stability of the Electroweak Vacuum during inflation

There are actually two cosmological issues caused by the electroweak vacuum being meta-stable:

- Is the high temperature in the early universe sufficient to push the Higgs field over the potential barrier into the global minimum? This is a potential problem even in the absence of inflation, and if the Higgs potential is not modified by new physics at higher energies, it would place a bound on the highest temperature reached. In an inflationary context, it constrains the allowed reheating temperature.

- Are the quantum fluctuations of a scalar field in an inflationary (de Sitter) background sufficient to push the Higgs field into the global minimum?

The first question can be answered by thermal field theory - the theory of quantum fields in a non-zero temperature background. At finite temperature, instead of quantum effects being accounted for by *pure* states, the best representation is in terms of a *mixed state* with a probability distribution associated to the energy of each state, drawn from the Boltzmann distribution, $\frac{1}{Z}e^{-\beta E_n}$ where $\beta = \frac{1}{k_B T}$

[2] In order to over-come the suppression due to surface tension.

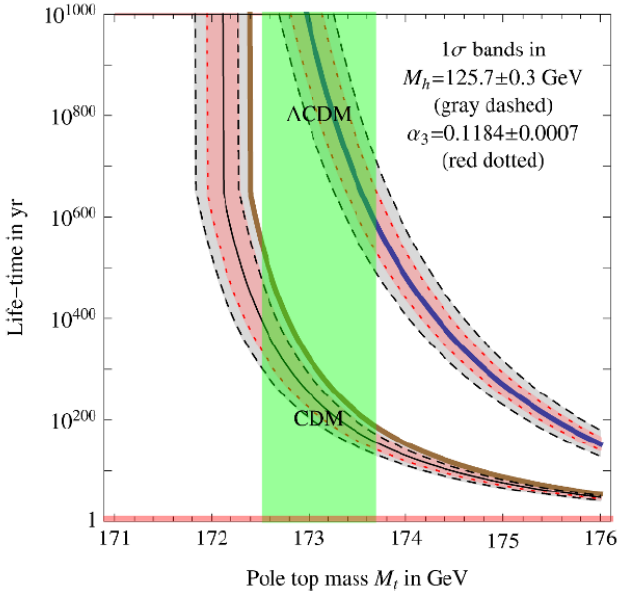

Figure 3.5: Expected life-time of the universe as a function of the top quark and Higgs masses. The uncertainty in the top mass is indicated by the green bar, while the uncertainty in the higgs mass and strong coupling are indicated by the grey and red lines respectively. The computation is performed for two separate assumptions about cosmology - a future universe dominated by cold dark matter (CDM) and cosmological constant (ΛCDM). The life-time varies considerably with the uncertainty, however, it appears that a life-time greater than 10^{100} years is favoured at the 1σ level. Figure credit: Buttazzo et al. [3]

and Z is the (statistical) partition function. Thus, one finds that expectation values are to be computed using a density matrix:

$$\langle \hat{O} \rangle_T = \mathrm{Tr}(\rho \hat{O}). \tag{3.11}$$

Where the density matrix ρ is given by:

$$\rho = \frac{1}{Z} \sum_n e^{-\beta E_n} |n\rangle \langle n| = \frac{1}{Z} \sum_n e^{-\beta \hat{H}} |n\rangle \langle n| = \frac{e^{-\beta \hat{H}}}{Z}, \tag{3.12}$$

since $|n\rangle$ are orthonormal states. It is worth noting, in fact, that:

$$Z = \sum_n e^{-\beta E_n} = \mathrm{Tr}(e^{-\beta \hat{H}}). \tag{3.13}$$

Thus:

$$\langle \hat{O} \rangle_T = \frac{\mathrm{Tr}(e^{-\beta \hat{H}} \hat{O})}{\mathrm{Tr}(e^{-\beta \hat{H}})}. \tag{3.14}$$

This bears more than a passing resemblance to the field theory expression $\frac{\langle 0|\,\hat{O}e^{iS}\,|0\rangle}{\langle 0|\,e^{iS}\,|0\rangle}$, and in fact, by using a position basis it is possible to re-write this expression in terms of path integrals[20].

Espinosa, Giudice and Riotto[7] applied the methods of thermal field theory to the issue of electroweak vacuum stability, and computed the maximum allowed temperature as a function of Higgs and top quark masses. Their argument was to compute the energy, E_c of the smallest possible nucleation bubble (see section 3.2) (ie, a bubble of the critical radius, R_c that just overcomes the free energy increasing effect of surface tension that would otherwise suppress the bubble). Since this energy gain is suppressed in probability by a Boltzmann factor, $e^{-\beta E_c}$, then the smallest allowed energy dominates the nucleation is the source is thermal. They used this result to compute the decay rate per unit volume, and thus the probability of the universe surviving, taking into account the time spent at each temperature in an expanding universe, assuming radiation dominance.

The matter is complicated by the fact that thermal corrections change the shape of the Higgs effective potential (actually in a thermal context, we should examine the Helmholtz free energy). However, taking this into account, they found that for m_h exceeding:

$$m_h > 117.4\,\text{GeV} + 4.2\,\text{GeV}\left(\frac{m_t - 170.9\,\text{GeV}}{1.8\,\text{GeV}}\right) - 1.6\,\text{GeV}\left(\frac{\alpha_s(M_z) - 0.1176}{0.0020}\right) \pm 3\,\text{GeV}, \tag{3.15}$$

then the electroweak vacuum can survive even up to Planckian temperatures. Using the central values of $m_t = 173.21 \pm 0.51 \pm 0.71$ and $\alpha_s(Mz) = 0.1185 \pm 0.0006$[13] and combining errors in quadrature, this implies we need:

$$m_h > 122.1 \pm 3.7\,\text{GeV}. \tag{3.16}$$

It is interesting to note that while the measured Higgs mass of $m_h = 125.7 \pm 0.4\,\text{GeV}$ is at the edge of this range, there is significant overlap, so it is not clear whether some temperature below the Planckian scale will destabilise the vacuum. However, it would appear that a very high temperature would be needed to achieve this.

The second issue - whether inflation itself can destabilise the vacuum via the quantum fluctuations it generates - is more complicated. To discuss this, we need to understand how these fluctuations are produced. This will be the topic of the next major section of this report. The main focus will be on the computation of two point functions in an inflationary (de Sitter) background, but once we have the necessary machinery, we will return to the question of inflation promoting decay of the electroweak vacuum.

Chapter 4

Correlation Functions in de Sitter Space-time

This section discuses the computation of correlation functions for scalar fields in a de Sitter background, with particular focus on long wave-length fluctuations and the 'stochastic approach' to inflation.

4.1 Introduction and Motivation

Since the Hubble rate, H, is slowly varying during inflation, the space-time is approximately de Sitter. As a first approximation then, it is useful to study the behaviour of quantum fields in de Sitter space-times, particularly with regards calculating observable quantities like the correlation function:

$$G(\mathbf{x}_1, \mathbf{x}_2, t_1, t_2) = \langle \phi(\mathbf{x}_1, t_1)\phi(\mathbf{x}_2, t_2)\rangle. \tag{4.1}$$

This will be simplified by the fact that de Sitter space is a space-time of maximal symmetry, much like Minkowski space-time, although the curvature does ensure the computation is much more complicated. The action for a scalar field in de Sitter space-time is, assuming a minimal coupling to gravity:

$$S = \int \mathrm{d}^4x\sqrt{|\det(g)|}\left(-\frac{1}{2}\nabla_\mu\phi\nabla^\mu\phi - V(\phi)\right). \tag{4.2}$$

Variation gives rise to the Euler-Lagrange equations:

$$\ddot{\phi}(\mathbf{x}, t) + 3H\dot{\phi}(\mathbf{x}, t) - \frac{1}{a^2}\delta^{ij}\partial_i\partial_j\phi(\mathbf{x}, t) + V'(\phi) = 0. \tag{4.3}$$

4.2 Quantum Field Theory in de Sitter Spacetime

The first element required for setting up a quantum field theory is an understanding of the behaviour of a massive, non-interacting scalar field. The following argument is based on that by Bunch and Davies [21]. In their paper, they also include a term in the Lagrangian for non-minimal coupling of the scalar field to gravity. This has the effect of creating a scalar-tensor theory of gravity, which breaks the equivalence principle, but is a useful model (for example, it can be used for an inflationary model using the Higgs field alone as the inflaton, [22]). The Lagrangian for this situation is:

$$S = \int \mathrm{d}^4x\sqrt{|\det(g)|}\left(\frac{M^2}{2}R - \frac{1}{2}\nabla_\mu\phi\nabla^\mu\phi - \frac{1}{2}m^2\phi^2 - \frac{\xi}{2}\phi^2 R\right), \tag{4.4}$$

where M is some mass scale (if $\xi = 0$, then M is the Planck scale[22]). ξ is the non-minimal coupling constant between gravity and the scalar field. The field equation for the scalar field is[1]:

$$(\nabla_\mu\nabla^\mu - m^2 - \xi R)\phi = 0. \tag{4.5}$$

The (flat[2]) de Sitter metric as it derives from the FRLW metric can be written in the form:

$$\mathrm{d}s^2 = -\mathrm{d}t^2 + a_0^2 e^{2Ht}(\mathrm{d}x^2 + \mathrm{d}y^2 + \mathrm{d}z^2). \tag{4.6}$$

Following Bunch and Davies[21], it is convenient to write this in a manner conformally related to the Minkowski metric by choosing instead the time co-ordinate:

$$\eta = -\frac{1}{Ha_0e^{Ht}}, \tag{4.7}$$

which ranges from $\eta \to -\infty$ as $t \to -\infty$ and $\eta \to 0$ as $t \to 0$. Note that this demonstrates that the FLRW derived de Sitter metric does not cover all of de Sitter spacetime - it is possible to analytically extend the η co-ordinate to the range $-\infty < \eta < \infty$. For this reason, we say that the FLRW form only covers half of de Sitter space-time[3]. Using this time co-ordinate, the metric can be written:

$$\mathrm{d}s^2 = \left(\frac{1}{H\eta}\right)^2(-\mathrm{d}\eta^2 + \mathrm{d}x^2 - \mathrm{d}y^2 - \mathrm{d}z^2). \tag{4.8}$$

Quantisation can be achieved by moving to the Fourier space representation:

$$\phi(t,\mathbf{x}) = \int \frac{\mathrm{d}^3\mathbf{k}}{(2\pi)^{\frac{3}{2}}}(\hat{a}_\mathbf{k}\phi_\mathbf{k}(t)e^{i\mathbf{k}\cdot\mathbf{x}} + \hat{a}^\dagger_\mathbf{k}\phi^*_\mathbf{k}(t)e^{-i\mathbf{k}\cdot\mathbf{x}}), \tag{4.9}$$

[1] Note that here we are using the $-+++$ metric convention, while Bunch and Davies use the $+---$ convention.

[2] After some length of time for a de Sitter phase any curvature is negligible

[3] In much the same way that Schwarzschild Co-ordinates to not cover the interior of a Black Hole's event horizon.

where:

$$\ddot{\phi}_{\mathbf{k}} + 3H\dot{\phi}_{\mathbf{k}} + \left(\frac{\mathbf{k}^2}{a^2} + m^2 + \xi R\right)\phi_{\mathbf{k}} = 0. \tag{4.10}$$

At this point, it is convenient to change variables to a, since we know this is a monotonic function of time. Thus:

$$\frac{\mathrm{d}}{\mathrm{d}t} = \frac{\mathrm{d}a}{\mathrm{d}t}\frac{\mathrm{d}}{\mathrm{d}a} = aH\frac{\mathrm{d}}{\mathrm{d}a},$$
$$\frac{\mathrm{d}^2}{\mathrm{d}t^2} = a^2H^2\frac{\mathrm{d}^2}{\mathrm{d}a^2} + aH^2\frac{\mathrm{d}}{\mathrm{d}a},$$

which gives the equation:

$$\frac{\mathrm{d}^2\phi_{\mathbf{k}}}{\mathrm{d}a^2} + \frac{4}{a}\frac{\mathrm{d}\phi_{\mathbf{k}}}{\mathrm{d}a} + \left(\frac{k^2}{a^4H^2} + \frac{m^2+\xi R}{a^2H^2}\right)\phi_{\mathbf{k}} = 0. \tag{4.11}$$

The solution to this equation can be written in terms of Bessel functions (see appendix 7.2):

$$\phi_{\mathbf{k}}(a(t)) = a^{-\frac{3}{2}}Z_p\left(\frac{k}{aH}\right) = A_1(-\eta H)^{\frac{3}{2}}H_p^{(1)}(-k\eta) + A_2(-\eta H)^{\frac{3}{2}}H_p^{(2)}(-\eta H), \tag{4.12}$$

where Z_p is an arbitrary sum of Bessel functions of type p and p is given by:

$$p = \sqrt{\frac{9}{4} - \frac{(m^2+\xi R)}{H^2}}. \tag{4.13}$$

There is an issue here, however, which is not present in Minkowski space. Curved space-times do not in fact have unique vacuum states, $\hat{a}_{\mathbf{k}}|0\rangle = 0$, so the notion of whether a state contains particles or not is ambiguous and depends on the choice of vacuum[4]. However, for inflationary purposes, there is a distinguished choice of vacuum. In the far past, as $\eta \to -\infty$, all length scales, k, are much smaller than the de Sitter horizon and indeed than the curvature scale. Consequently, they do not 'see' the curvature, so the space-time should behave like Minkowski space-time, which *does* have a unique vacuum state. This choice - the 'Bunch Davies' vacuum, is natural because it makes contact with the flat space definition of particles. The coefficients A_1 and A_2 are fixed then by adopting the boundary condition that the field should reduce to the flat space case in the limit as $\eta \to 0$. This is where using Hankel functions is the most natural way to proceed. In the limit as $\eta \to -\infty$, the Hankel functions are asymptotically[23]:

$$H_p^{(1)}(-k\eta) = \sqrt{\frac{2}{-\pi k\eta}}e^{-ik\eta - i(2p+1)\frac{\pi}{4}} + O((-k\eta)^{-\frac{3}{2}}), \tag{4.14}$$

$$H_p^{(2)}(-k\eta) = \sqrt{\frac{2}{-\pi k\eta}}e^{+ik\eta + i(2p+1)\frac{\pi}{4}} + O((-k\eta)^{-\frac{3}{2}}). \tag{4.15}$$

[4]It is for this reason, for example, that black holes can emit Hawking radiation, as a state starting as a vacuum in the far past contains particles in a thermal distribution in the far future.

In Minkowski space, the field would decompose as:

$$\phi(\mathbf{x},t)=\int\frac{\mathrm{d}^3\mathbf{k}}{(2\pi)^{\frac{3}{2}}}\left(\hat{a}_{\mathbf{k}}e^{-iE_{\mathbf{k}}t}e^{+i\mathbf{k}\cdot\mathbf{x}}+\hat{a}^{\dagger}_{\mathbf{k}}e^{iE_{\mathbf{k}}t}e^{-i\mathbf{k}\cdot\mathbf{x}}\right). \tag{4.16}$$

This immediately fixes $A_2=0$ since $H_p^{(2)}$ has the wrong sign in the exponential for the time dependent term. A_1, however, is fixed by requiring the field to satisfy the equal time commutation relations in the $\eta\to-\infty$ limit:

$$[\phi(t,\mathbf{x}),\pi(t,\mathbf{y})]=i\delta^{(3)}(\mathbf{x}-\mathbf{y}), \tag{4.17}$$

or equivalently[5]:

$$[\hat{a}_{\mathbf{k}},\hat{a}^{\dagger}_{\mathbf{k}'}]=\delta^{(3)}(\mathbf{k}-\mathbf{k}'). \tag{4.18}$$

Note that $\pi(t,\mathbf{y})=a^3\dot{\phi}(t,\mathbf{y})$ (the factor of a^3 comes from the $\sqrt{|\det(g)|}$ in the Lagrangian). Computing this commutator, we find:

$$a^3\int\frac{\mathrm{d}^3\mathbf{k}}{(2\pi)^3}(\phi_{\mathbf{k}}\dot{\phi}^*_{\mathbf{k}}-\phi^*_{\mathbf{k}}\dot{\phi}_{\mathbf{k}})e^{-i\mathbf{k}\cdot(\mathbf{x}-\mathbf{y})}=i\delta^{(3)}(\mathbf{x}-\mathbf{y}). \tag{4.19}$$

Now, use $\dot{\phi}_{\mathbf{k}}=\dot{\eta}\frac{\mathrm{d}\phi_{\mathbf{k}}}{\mathrm{d}\eta}=\frac{1}{a}\frac{\mathrm{d}\phi_{\mathbf{k}}}{\mathrm{d}\eta}=-\eta H\frac{\mathrm{d}\phi_{\mathbf{k}}}{\mathrm{d}\eta}$. It is convenient to use the asymptotic expansion of $H_p^{(1)}$ to evaluate this derivative:

$$\phi_{\mathbf{k}}=A_1(-\eta H)^{\frac{3}{2}}H_p^{(1)}(-k\eta)\sim A_1H^{\frac{3}{2}}(-\eta)\sqrt{\frac{2}{\pi k}}e^{-ik\eta}e^{-i(2p+1)\frac{\pi}{4}}+O(1), \tag{4.20}$$

$$\frac{\mathrm{d}\phi_{\mathbf{k}}}{\mathrm{d}\eta}\sim-ikA_1H^{\frac{3}{2}}(-\eta)\sqrt{\frac{2}{\pi k}}e^{-ik\eta}e^{-i(2p+1)\frac{\pi}{4}}+O(1). \tag{4.21}$$

Only the exponential part contributes to the derivative at leading order. Thus:

$$\phi_{\mathbf{k}}\dot{\phi}^*_{\mathbf{k}}=-\eta HikA_1^2H^3\eta^2\frac{2}{\pi k}+O(\eta). \tag{4.22}$$

The k factors cancel, so $\phi_{\mathbf{k}}\dot{\phi}^*_{\mathbf{k}}-\phi^*_{\mathbf{k}}\dot{\phi}_{\mathbf{k}}=-\frac{4i}{\pi}A_1^2H^4\eta^3$. Consequently:

$$-\frac{4i}{\pi}A_1^2H^4\eta^3a^3\int\frac{\mathrm{d}^3\mathbf{k}}{(2\pi)^3}e^{-i\mathbf{k}\cdot(\mathbf{x}-\mathbf{y})}=-\frac{4i}{\pi}A_1^2H^4\eta^3a^3\delta^{(3)}(\mathbf{x}-\mathbf{y})=i\delta^{(3)}(\mathbf{x}-\mathbf{y}), \tag{4.23}$$

in the limit as $\eta\to-\infty$. This therefore fixes the constant A_1 as:

$$A_1=\sqrt{-\frac{\pi}{4H^4\eta^3a^3}}=\sqrt{\frac{\pi}{4H}}, \tag{4.24}$$

[5]The lack of a factor $(2\pi)^3$ here is due to choosing a factor $\frac{1}{(2\pi)^{\frac{3}{2}}}$ in the Fourier expansion of the field, rather than $\frac{1}{(2\pi)^3}$.

so:

$$\phi_{\mathbf{k}}(\eta) = H(-\eta)^{\frac{3}{2}}\sqrt{\frac{\pi}{4}}H_p^{(1)}(-k\eta). \tag{4.25}$$

Using this, and the definition $\hat{a}_{\mathbf{k}}|0\rangle = 0$ in the Bunch Davies vacuum, $|0\rangle$, it is possible to compute the correlation function:

$$\begin{aligned}
G(\mathbf{x}_1, \mathbf{x}_2, t_1, t_2) &= \int \frac{\mathrm{d}^3\mathbf{k}}{(2\pi)^3} e^{i\mathbf{k}\cdot(\mathbf{x_1}-\mathbf{x_2})}\phi_{\mathbf{k}}(t_1)\phi^*_{\mathbf{k}}(t_2) \\
&= \frac{1}{(2\pi)^2}\int_0^\pi \mathrm{d}\theta \int_0^\infty \mathrm{d}k k^2 \sin\theta e^{ik|\mathbf{x_1}-\mathbf{x_2}|\cos\theta}\phi_{\mathbf{k}}(t_1)\phi^*_{\mathbf{k}}(t_2) \\
&= \frac{1}{(2\pi)^2}\int_0^\infty \mathrm{d}k \frac{k}{-i|\mathbf{x_1}-\mathbf{x_2}|}\left[e^{ik|\mathbf{x_1}-\mathbf{x_2}|\cos\theta}\right]_0^\pi \phi_{\mathbf{k}}(t_1)\phi^*_{\mathbf{k}}(t_2) \\
&= \frac{1}{2\pi^2}\int_0^\infty \mathrm{d}k \frac{k}{|\mathbf{x_1}-\mathbf{x_2}|}\sin(k|\mathbf{x_1}-\mathbf{x_2}|)\phi_{\mathbf{k}}(t_1)\phi^*_{\mathbf{k}}(t_2) \\
&= \frac{H^2}{8\pi|\mathbf{x_1}-\mathbf{x_2}|}(\eta_1\eta_2)^{\frac{3}{2}}\int_0^\infty \mathrm{d}k k \sin(k|\mathbf{x_1}-\mathbf{x_2}|)H_p^{(1)}(-k\eta_1)H_p^{(2)}(-k\eta_2).
\end{aligned}$$

Integrals like this can be performed using the hypergeometric function[21]. We are most interested in the Feynman propagator, for which the final answer is[24]:

$$\begin{aligned}
D_F(x_1, x_2) =& \theta(-\frac{1}{\eta_2}+\frac{1}{\eta_1})\frac{H^2(c-1)(c-2)}{16\pi\sin[(c-1)\pi]}F(c, 3-c, 2; Z(x_1, x_2)) \\
&+ \theta(-\frac{1}{\eta_1}+\frac{1}{\eta_2})\frac{H^2(c-1)(c-2)}{16\pi\sin[(c-1)\pi]}F(c, 2-c, 2; Z(x_2, x_1)),
\end{aligned} \tag{4.26}$$

where:

$$Z(x_i, y_j) = 1 + \frac{(\eta_2-\eta_1-i\varepsilon)^2 - (\mathbf{x_2}-\mathbf{x_1})^2}{4\eta_1\eta_2} \tag{4.27}$$

and:

$$c = \frac{3}{2} - p. \tag{4.28}$$

This covers the free case. If, however, we are interested in the interacting case, the situation is somewhat different. In fact, a divergence occurs for light fields. Sasaki et al[24] computed the four point correlation function for the ϕ^4 interaction, and found the connected part to be:

$$\begin{aligned}
G^c_{(4)}(x_1, x_2, x_3, x_4; \eta) =& 2\lambda\mathrm{Im}\left[\prod_{i=1}^4\left(\int\frac{\mathrm{d}^3\mathbf{k_i}}{(2\pi)^3}\right)(2\pi)^3\delta^{(3)}(\sum_{i=1}^4\mathbf{k}_i)\exp\left(i\sum_{i=1}^4\mathbf{k_i}\cdot\mathbf{x_i}\right)\right. \\
&\left.\prod_{i=1}^4(\phi_{\mathbf{k}_i}(\eta))\left(\int_{-\infty}^\eta \mathrm{d}\eta' + \int_0^\infty \mathrm{d}\eta'\right)\frac{1}{(H\eta')^4}\prod_{i=1}^4(\phi^*_{\mathbf{k}_i}(\eta'))\right].
\end{aligned} \tag{4.29}$$

The η' integral potentially diverges at $\eta' \to 0$. To analyse this, consider the limit as $\eta' \to 0$. We know already that $\phi_{\mathbf{k}} \sim \eta^{\frac{3}{2}}H_p^{(1)}(-\eta k)$. Note also that as $\eta' \to 0$,

the Hankel function $H_p^{(1)}$ is dominated[6] by η'^{-p}. Thus, $\phi_{\mathbf{k}}(\eta') \sim |\eta'|^{\frac{3}{2}-p} = |\eta'|^c$ as $\eta' \to 0$. The asymptotic behaviour of the Hankel functions for large η' is $\sim \eta e^{ik\eta'} + \eta^{\frac{3}{2}} O(\eta^{-\frac{3}{2}})$ which does not diverge, so any divergence must arise from the area around $\eta' = 0$. Power law integrals of this form:

$$\int_0^{\varepsilon} x^q \mathrm{d}x = \frac{\varepsilon^{q+1}}{q+1} - \frac{0^{q+1}}{q+1}, \tag{4.30}$$

converge so long as $q > -1$ and diverge if $q \leq -1$. In this case, there are four Hankel functions (each giving a factor η'^c) and a factor of η'^{-4} which originates from $\sqrt{|\det(g)|}$ (in the conformal co-ordinates where $\det(g) = -\frac{1}{(H\eta)^8}$). Thus, the divergence condition is $-4 + 4c \leq -1$, or $c \leq \frac{3}{4}$. Consequently, the four point function diverges if the mass obeys the inequality:

$$\frac{3}{2} - \sqrt{\frac{9}{4} - \frac{(m^2 + \xi R)}{H^2}} \leq \frac{3}{4}. \tag{4.31}$$

It is straightforward to derive the Ricci scalar in (four-dimensional) de Sitter space. The result is: $R = 12H^2$. Consequently, if:

$$m^2 \leq \left(\frac{27}{16} - 12\xi\right) H^2, \tag{4.32}$$

then the four point function diverges. Sasaki et al[24] showed that this divergence is in fact completely general, and not just present in the four point function.

The origin of the divergence is at small η, which corresponds to $t \to \infty$. Note that for positive m and ξ, $c > 0$ so the divergence is only present as a consequence of the determinant factors, $\frac{1}{(\eta H)^4}$. This indicates that physically, it should be interpreted as a result of the unbounded growth of the de Sitter space-time, and thus an unbounded volume of intermediate positions for the vertices of Feynman diagrams to be found. This identifies it as an infra-red divergence, rather than a UV divergence. This does not mean that the theory breaks down, only that the structure for m^2 in this range is not amenable to perturbation theory.

4.3 Stochastic Formalism

Infra-red divergences like that encountered in section 4.2 are closely connected to the behaviour of long wave-length modes in the scalar field. One method to approach this then, is to introduce an infra red cut-off and deal with the long wavelength modes separately. Starobinsky [25] showed that in fact the long

[6] This can be seen from the power series for $J_{-p}(x)$, whose lowest power is x^{-p}, while the lowest power of $J_p(x)$ is x^p. Since $H_p^{(1)}$ is just a linear sum of these, it is also dominated by x^{-p} as $x \to 0$

wavelength modes can be treated as c-numbers, rather than operators.
More precisely, the scalar field is split as:

$$\phi(\mathbf{x},t) = \bar{\phi}(\mathbf{x},t) + \int \frac{\mathrm{d}^3\mathbf{k}}{(2\pi)^{\frac{3}{2}}}\theta(k-\varepsilon a(t)H)\left[\hat{a}_{\mathbf{k}}\phi_{\mathbf{k}}(t)e^{-i\mathbf{k}\cdot\mathbf{x}} + \hat{a}^{\dagger}_{\mathbf{k}}\phi^{*}_{\mathbf{k}}(t)e^{i\mathbf{k}\cdot\mathbf{x}}\right]. \tag{4.33}$$

The Heaviside step function, $\theta(k-\varepsilon a(t)H)$ ensures that only those short-wavelength modes with wavenumber $k > \varepsilon a(t)H$ are quantised (long wavelength modes with $k < \varepsilon a(t)H$ are included in $\bar{\phi}$). $\bar{\phi}$ can be interpreted as the field average over a length scale[7] $\frac{1}{\varepsilon H}$. It is assumed that $\varepsilon < 1$, in which case, this length scale is larger than the de Sitter Horizon, $R = \frac{1}{H}$.
The basic idea of the stochastic formulation is that the long wave-length behaviour can be treated classically, and the quantised short wavelength modes provide an effective stochastic term to the equation of motion for $\bar{\phi}$. To do this, we also have to compute, instead of ϕ, the *average* of ϕ over a volume associated to the length scale $\frac{1}{\varepsilon H}$. Space-time is then split into these 'fundamental averaging volumes' and we say that any two points closer than $\frac{1}{\varepsilon H}$ are considered to be the 'same point' (in the sense that they have the same average). This procedure is called *coarse graining* and is used frequently in statistical mechanics.
We can see how this works by writing $\phi = \bar{\phi} + \delta\phi_{\mathrm{short}}$. The equation of motion for ϕ in a generic potential can be written:

$$\ddot{\phi} + 3H\dot{\phi} - \frac{1}{a^2}\delta^{ij}\partial_i\partial_j\phi + V'(\phi) = 0, \tag{4.34}$$

which decomposes as:

$$\begin{aligned}&\ddot{\bar{\phi}} + 3H\dot{\bar{\phi}} + \ddot{\delta\phi}_{\mathrm{short}} + 3H\dot{\delta\phi}_{\mathrm{short}} - \frac{1}{a^2}\delta^{ij}\partial_i\partial_j\bar{\phi} - \frac{1}{a^2}\delta^{ij}\partial_i\partial_j\delta\phi_{\mathrm{short}} \\ &+ V'(\bar{\phi}) + \delta\phi_{\mathrm{short}}V''(\bar{\phi}) + O(\delta\phi^2_{\mathrm{short}}) = 0.\end{aligned} \tag{4.35}$$

The short wavelength corrections $\delta\phi_{\mathrm{short}}$ can be regarded as small, so we ignore the second order terms. Note that this equation applies for each $\phi_{\mathbf{k}}$ separately in Fourier space, so for $k > \varepsilon a(t)H$ we have:

$$\ddot{\phi}_{\mathbf{k}} + 3H\dot{\phi}_{\mathbf{k}} + \frac{k^2}{a^2}\phi_{\mathbf{k}} + V''(\bar{\phi})\phi_{\mathbf{k}} = 0. \tag{4.36}$$

Note that $k^2 > \varepsilon^2 a^2 H^2$ for the short wavelength modes. Now, the scalar field may contributes little to the de Sitter expansion, in which case it is possible to choose ε to be small, but not too small, so that $\varepsilon^2 H^2 \gg V''(\phi)$. If however, the scalar field contributes significantly then it can be assumed that it satisfies the slow roll conditions (if it does not, then the space-time is not de Sitter), in which case:

$$\varepsilon^2 H^2 \sim \varepsilon^2 \frac{8\pi G_N}{3}\left(\frac{\dot{\phi}^2}{2} + V(\phi)\right), \tag{4.37}$$

[7] $\mathbf{x}$ is a co-moving co-ordinate, so the wave-number k and thus wavelength $\frac{1}{\varepsilon a(t)H}$ is also co-moving. Multiplying by $a(t)$ gives the physical averaging scale, $\frac{1}{\varepsilon H}$, which is constant in time.

where $\frac{\dot{\phi}^2}{2} \ll V(\phi)$ for slow-roll inflation, and the slow roll conditions also require $V''(\phi) \ll V(\phi)G_N$, so it follows that $V''(\phi) \ll \frac{k^2}{a^2}$. In both cases then, the field equation for the short wavelength modes can be written:

$$\ddot{\phi}_{\mathbf{k}} + 3H\dot{\phi}_{\mathbf{k}} + \frac{k^2}{a^2}\phi_{\mathbf{k}} = 0. \tag{4.38}$$

The solution for an equation like this was already discussed in section 4.2. Assuming a Bunch-Davies vacuum, it is:

$$\phi_{\mathbf{k}}(\eta) = H(-\eta)^{\frac{3}{2}}\sqrt{\frac{\pi}{4}}H^{(1)}_{\frac{3}{2}}(-k\eta) = \frac{H}{\sqrt{2k}}\left(\eta - \frac{i}{k}\right)e^{-ik\eta}. \tag{4.39}$$

Now, to proceed further, note that the last two terms in Eq. (4.35) can be neglected - the last because $\delta\phi^2_{\text{short}}$ is small, and the penultimate by the slow-roll discussion above. The spatial derivative of the long wavelength modes can also be neglected[25]. This is also easier to see in momentum space, where we can compare it to the $3H\dot{\phi}_{\mathbf{k}}$ term:

$$3H^2\frac{\partial\phi_{\mathbf{k}}}{\partial(Ht)} + \frac{k^2}{a^2}\phi_{\mathbf{k}}, \tag{4.40}$$

where we use the dimensionless time scale Ht. Observe that $k^2 < \varepsilon^2 a^2 H^2 \ll a^2H^2$ for the long wavelength part of ϕ. Thus, the $3H\dot{\phi}_{\mathbf{k}}$ term dominates over the second derivative.
Neglecting these terms, the equation for $\bar{\phi}$ is:

$$\ddot{\bar{\phi}} + 3H\dot{\bar{\phi}} + V'(\bar{\phi}) + \left[\delta\ddot{\phi}_{\text{short}} + 3H\delta\dot{\phi}_{\text{short}} - \frac{1}{a^2}\delta^{ij}\partial_i\partial_j\delta\phi_{\text{short}}\right] = 0. \tag{4.41}$$

At this point, it is useful to note that the terms with second derivatives in time can be neglected. Physically speaking, this is because the $3H\dot{\phi}$ terms act as damping terms, which erode any initial inertia of the field (more precisely, the expansion red-shifts away momenta, so acts like a damping term). A nice analogy is an object sliding down a quadratic potential well ($h = \frac{1}{2}\omega^2x^2$) under gravity, but with a high friction surface:

$$m\frac{\mathrm{d}^2x}{\mathrm{d}t^2} + \gamma\frac{\mathrm{d}x}{\mathrm{d}t} + mg\omega^2x = 0. \tag{4.42}$$

Assuming significant over-damping, ie, $\left(\frac{\gamma}{m}\right)^2 \gg g\omega^2$, then the solution is:

$$\begin{aligned} x(t) \simeq &-\left[\frac{mv_0}{\gamma} + (x_0 + \frac{2mv_0}{\gamma})\frac{g\omega^2m^2}{\gamma^2}\right]e^{-\left(\frac{\gamma}{m} - \frac{g\omega^2m}{\gamma}\right)t} \\ &+ \left[(x_0 + \frac{v_0m}{\gamma}) + \frac{g\omega^2m^2}{\gamma^2}(x_0 + \frac{2v_0m}{\gamma})\right]e^{-\frac{g\omega^2m}{\gamma}t}. \end{aligned} \tag{4.43}$$

The overdamping means that the first term decays exponentially faster than the second. Physically speaking, this corresponds to the friction eroding the initial velocity. The solution quickly decays towards an attractor solution:

$$x(t) = \left[(x_0 + \frac{v_0 m}{\gamma}) + \frac{g\omega^2 m^2}{\gamma^2}(x_0 + \frac{2v_0 m}{\gamma})\right] e^{-\frac{g\omega^2 m}{\gamma}t}. \tag{4.44}$$

However, this attractor solution is, up to initial conditions, what we would obtain by neglecting the inertia term:

$$\frac{\gamma}{m}\frac{\mathrm{d}x}{\mathrm{d}t} + g\omega^2 x = 0 \implies x(t) = x_0 e^{-\frac{g\omega^2 m}{\gamma}t}. \tag{4.45}$$

The same is true of Eq. (4.41) - the kinetic terms will rapidly die away and the solution tends towards an attractor solution, satisfying:

$$3H\dot{\bar{\phi}} + V'(\bar{\phi}) + \left[3H\dot{\delta\phi}_{\mathrm{short}} - \frac{1}{a^2}\delta^{ij}\partial_i\partial_j\delta\phi_{\mathrm{short}}\right] = 0, \tag{4.46}$$

where:

$$\delta\phi_{\mathrm{short}} = \int \frac{\mathrm{d}^3\mathbf{k}}{(2\pi)^{\frac{3}{2}}}\theta(k - \varepsilon a(t)H)(\hat{a}_{\mathbf{k}}\phi_{\mathbf{k}}(t)e^{-i\mathbf{k}\cdot\mathbf{x}} + \mathrm{h.c.}). \tag{4.47}$$

Taking time derivatives of $\delta\phi_{\mathrm{short}}$ is complicated by the time dependence of $\varepsilon a(t)H$. For slowly varying H, it is possible to assume that ε also varies in time in such a way that εH is constant, so we need only worry about the time dependence of $a(t)$. In fact, any time derivative acting on the Heaviside step function will behave the following way:

$$\begin{aligned}\frac{\partial}{\partial t}\theta(k - \varepsilon a(t)H) &= \frac{\mathrm{d}(k - \varepsilon a(t)H)}{\mathrm{d}t}\left.\frac{\mathrm{d}\theta(s)}{\mathrm{d}s}\right|_{s=k-\varepsilon a(t)H} \\ &= -\varepsilon\dot{a}H\delta(k - \varepsilon a(t)H) = -\varepsilon a(t)H^2\delta(k - \varepsilon a(t)H).\end{aligned} \tag{4.48}$$

The equation thus becomes:

$$\begin{aligned}3H\dot{\bar{\phi}} + V'(\bar{\phi}) + \int \frac{\mathrm{d}^3\mathbf{k}}{(2\pi)^{\frac{3}{2}}}\theta(k - \varepsilon a(t)H)(\hat{a}_{\mathbf{k}}\left[3H\dot{\phi}_{\mathbf{k}} + \frac{k^2}{a^2}\delta^{ij}\phi_{\mathbf{k}}\right]e^{-i\mathbf{k}\cdot\mathbf{x}} + \mathrm{h.c.}\ ) \\ - 3H\varepsilon a(t)H^2\int \frac{\mathrm{d}^3\mathbf{k}}{(2\pi)^{\frac{3}{2}}}\delta(k - \varepsilon a(t)H)\left(\hat{a}_{\mathbf{k}}\phi_{\mathbf{k}}e^{-i\mathbf{k}\cdot\mathbf{x}} + \mathrm{h.c.}\right) = 0.\end{aligned} \tag{4.49}$$

Eq. (4.38) with neglected $\ddot{\phi}$ term implies that the third term here vanishes. Consequently, we can write the equation for $\bar{\phi}$ as:

$$\dot{\bar{\phi}} = -\frac{V'(\phi)}{3H} + f(\mathbf{x}, t), \tag{4.50}$$

where:

$$f(\mathbf{x}, t) = \varepsilon a(t)H^2\int \frac{\mathrm{d}^3\mathbf{k}}{(2\pi)^{\frac{3}{2}}}\delta(k - \varepsilon a(t)H)\left(\hat{a}_{\mathbf{k}}\phi_{\mathbf{k}}e^{-i\mathbf{k}\cdot\mathbf{x}} + \mathrm{h.c.}\right). \tag{4.51}$$

The crucial step now is to interpret Eq. (4.50) as a *Langevin equation* - a stochastic differential equation where $f(\mathbf{x}, t)$ constitutes a noise term. In this sense, it is equivalent to Brownian motion. In some small time step, Δt, $\bar{\phi}$ receives a classical drift, $-\frac{V'(\bar{\phi})}{3H}$ and a large number of random 'kicks', the source of which is the random behaviour of the short wave-length quantum field. Note - although the distribution of kicks from $f(\mathbf{x}, t)$ is not necessarily a Gaussian distribution - the total effect on $\bar{\phi}$ in some time Δt is Gaussian by the Central Limit Theorem, because of the coarse graining procedure discussed at the beginning of this section. We took $\bar{\phi}$ to be the *average*[8] of the long wavelength part of ϕ over a volume defined by the physical length scale $\frac{1}{\varepsilon H}$. Consequently, f in Eq. (4.50) is the arithmetic mean of the quantum 'kicks' over this same region. But the Central Limit theorem says that the arithmetic mean of a set of independent random variables drawn from the same distribution is approximately normally distributed with the same mean and variance as the original distribution (whatever that may be). Thus, we can take $f(\mathbf{x}, t)$ to be normally distributed and it is now a true random number, rather than a quantum operator.
However, f is clearly a multivariate normal distribution since it covers many different points. In fact, an infinite number of them. To obtain the precise distribution, it is necessary to compute the 2-point correlation function of f. This is because a generic, N-point multi-variate distribution with mean μ_i and variance matrix g_{ij} has the following form:

$$p(x_1, x_2, \ldots, x_N) = \sqrt{\frac{\det(g)}{(2\pi)^N}} \exp\left(-\frac{1}{2}(x_i - \mu_i) g_{ij} (x_j - \mu_j)\right) \tag{4.52}$$

and the two-point correlation function is given by:

$$\langle x_i x_j \rangle = {g^{-1}}_{ij}. \tag{4.53}$$

[8] Specifically the arithmetic mean

In this case, there are a continuous infinite number of variables, $f(\mathbf{x}, t)$. We can compute the correlation function:

$$\begin{aligned}
\langle f(\mathbf{x}_1, t_1) f(\mathbf{x}_2, t_2)\rangle =& \int \frac{\mathrm{d}^3\mathbf{k}_1 \mathrm{d}^3\mathbf{k}_2}{(2\pi)^3} \Big[\varepsilon^2 a(t_1)a(t_2)H^4\delta(k_1 - \varepsilon a(t_1)H) \\
& \times \delta(k_2 - \varepsilon a(t_2)H)\, \langle 0|\, [\hat{a}_{\mathbf{k}_1}, \hat{a}^\dagger_{\mathbf{k}_2}]\, |0\rangle\, e^{-i\mathbf{k_1}\cdot\mathbf{x_1}} e^{i\mathbf{k_2}\cdot\mathbf{x_2}} \phi_{\mathbf{k}_1}(t_1)\phi^*_{\mathbf{k}_2}(t_2)\Big] \\
=& \int \frac{\mathrm{d}^3\mathbf{k_1}}{(2\pi)^3} \Big[\varepsilon^2 a(t_1)a(t_2)H^4\delta(k_1 - \varepsilon a(t_1)H)\delta(k_1 - \varepsilon a(t_2)H) \\
& \times e^{-i\mathbf{k_1}\cdot(\mathbf{x_1}-\mathbf{x_2})} \phi_{\mathbf{k}_1}(t_1)\phi^*_{\mathbf{k}_1}(t_2)\Big] \\
=& \frac{1}{(2\pi)^2}\int_0^\infty \Big[k_1^2 \mathrm{d}k_1 \int_0^\pi \mathrm{d}\theta \sin\theta e^{-ik_1|\mathbf{x_1}-\mathbf{x_2}|\cos\theta} \\
& \times \varepsilon^2 a(t_1)a(t_2)H^4\delta(k_1 - \varepsilon a(t_1)H)\delta(k_1 - \varepsilon a(t_2)H)\phi_{\mathbf{k}_1}(t_1)\phi^*_{\mathbf{k}_1}(t_2)\Big] \\
=& \frac{1}{4\pi^2}\int_0^\infty \Big[\mathrm{d}k_1 \frac{k_1}{i|\mathbf{x_1}-\mathbf{x_2}|}\int_0^\pi \mathrm{d}\theta \frac{\mathrm{d}}{\mathrm{d}\theta}\left[e^{-ik_1|\mathbf{x_1}-\mathbf{x_2}|\cos\theta}\right] \\
& \times \varepsilon^2 a(t_1)a(t_2)H^4\delta(k_1 - \varepsilon a(t_1)H)\delta(k_1 - \varepsilon a(t_2)H)\phi_{\mathbf{k}_1}(t_1)\phi^*_{\mathbf{k}_1}(t_2)\Big] \\
=& \frac{1}{2\pi^2}\int_0^\infty \mathrm{d}k_1 \Big[\frac{k_1\sin(k_1|\mathbf{x_1}-\mathbf{x_2}|)}{|\mathbf{x_1}-\mathbf{x_2}|}\varepsilon^2 a(t_1)a(t_2)H^4 \\
& \times \delta(k_1 - \varepsilon a(t_1)H)\delta(\varepsilon a(t_2)H - \varepsilon a(t_2)H)\phi_{\mathbf{k}_1}(t_1)\phi^*_{\mathbf{k}_1}(t_2)\Big] \\
=& \frac{1}{2\pi^2}\left[\frac{k_1\sin(k_1|\mathbf{x_1}-\mathbf{x_2}|)}{|\mathbf{x_1}-\mathbf{x_2}|}\varepsilon^2 a(t_1)a(t_2)H^4\frac{\delta(t_1-t_2)}{|\varepsilon a(t_1)H^2|}\phi_{\mathbf{k}_1}(t_1)\phi^*_{\mathbf{k}_1}(t_2)\right]_{k_1=\varepsilon a(t_1)H} \\
=& \frac{1}{2\pi^2}\varepsilon^2 a(t_1)^2 H^3\delta(t_1-t_2)|\phi_{\varepsilon a(t_1)H}(t_1)|^2\frac{\sin(\varepsilon a(t_1)H|\mathbf{x_1}-\mathbf{x_2}|)}{|\mathbf{x_1}-\mathbf{x_2}|} \\
=& \frac{H^3}{4\pi^2}a(t_1)^2\varepsilon^2\delta(t_1-t_2)\frac{H^2}{\varepsilon a(t_1)H}\left(\frac{1}{a(t_1)^2H^2}+\frac{1}{\varepsilon^2 a(t_1)^2H^2}\right) \\
& \times \frac{\sin(\varepsilon a(t_1)H|\mathbf{x_1}-\mathbf{x_2}|)}{|\mathbf{x_1}-\mathbf{x_2}|} \\
=& \frac{H^3}{4\pi^2}\delta(t_1-t_2)(1+\varepsilon^2)\frac{\sin(\varepsilon a(t_1)H|\mathbf{x_1}-\mathbf{x_2}|)}{\varepsilon a(t_1)H|\mathbf{x_1}-\mathbf{x_2}|}.
\end{aligned}$$

The first step uses $[\hat{a}_{\mathbf{k}_1}, \hat{a}^\dagger_{\mathbf{k_2}}] = \delta^{(3)}(\mathbf{k_1}-\mathbf{k_2})$. The second step moves to polar co-ordinates with the z axis chosen along the $\mathbf{x_1}-\mathbf{x_2}$ direction. The third can be shown using integration by parts, but it is faster to observe that θ integrand is proportional to $g'(\theta)e^{g(\theta)}$ and write this in terms of $\frac{\mathrm{d}}{\mathrm{d}\theta}(e^{g(\theta)})$. The fourth step then evaluates the θ integral and uses the $\delta(x-y)f(x) = \delta(x-y)f(y)$ property of delta functions. The fifth collapses the k_1 integral and uses $\delta(f(x)-f(y)) = \frac{\delta(x-y)}{|f'(x)|}$, while the sixth step involve substituting in Eq. (4.39) and the seventh

performs some algebraic re-arrangements. We now define the sinc function as:

$$\mathrm{sinc}(x) = \frac{\sin x}{x} \tag{4.54}$$

and neglect ε^2 to obtain the final result:

$$\langle f(\mathbf{x}_1, t_1) f(\mathbf{x}_2, t_2)\rangle = \frac{H^3}{4\pi^2}\delta(t_1 - t_2)\mathrm{sinc}(\varepsilon a(t_1) H|\mathbf{x_1} - \mathbf{x_2}|). \tag{4.55}$$

Solving the Langevin equation (4.50) is evidently not unique, since the random element will lead to a different result each time, but it should give rise to a probability density distribution, $\rho(\bar{\phi}(\mathbf{x}, t) = \varphi) \equiv \rho(\varphi(\mathbf{x}, t))$, for the field to take on the value φ at $(\mathbf{x}, t)$. In principle, it is possible to find this via a Monte-Carlo simulation, running the system many times to estimate the probability of the field taking on the value φ, but there is another technique to extract the exact distribution. This will form the subject of the next section.

4.4 The Fokker-Planck Equation

The Fokker-Planck equation is a partial differential equation describing the time evolution of the probability density distribution, $\rho(\varphi, t)$ for a field to take on some value, φ. The advantage of this equation is that it is easier to interpret than the equivalent Langevin equation.
The derivation we will give here is based on [26] and [27]. The derivation in [26] is slightly heuristic, although correct in its approach, since it does not take proper account of the non-commutation of the operators involved (and thus the need for a time ordered exponential, as opposed to a conventional exponential). However, we base our derivation on it because it is both elegant and simple. Consider a generic set of Langevin equations:

$$\frac{\mathrm{d}a_i}{\mathrm{d}t} = v_i(\mathbf{a}) + \xi_i(t), \tag{4.56}$$

where $\xi_i(t)$ are a set of stochastic variables (possibly correlated) and $v_i(\mathbf{a})$ are deterministic 'velocity' terms. This gives the time evolution of a number of degrees of a freedom, a_i, arranged in the vector $\mathbf{a}$. Note that we can consider second order equations (for example, as is the case for Brownian motion) by choosing one variable, a_1 to be position and another, a_2, to be velocity. In the Brownian motion example, we would have:

$$\frac{\mathrm{d}x}{\mathrm{d}t} = v \tag{4.57}$$

$$\frac{\mathrm{d}v}{\mathrm{d}t} = -\underbrace{\frac{\gamma}{m}v}_{\text{damping term}} - \underbrace{\frac{1}{m}V'(x)}_{\text{Potential term}} + \underbrace{\frac{1}{m}\xi(t)}_{\text{Random 'kicks'}}. \tag{4.58}$$

Thus, higher order equations can always be written as as set of coupled Langevin equations, just like ordinary differential equations. a_i need not be positions -

they are simply any dynamic variable used to describe the system.
It is assumed that the stochastic variables ξ_i obey the correlation properties:

$$\langle \xi_i(t_1)\xi_i(t_2)\rangle = g_{ij}\delta(t_1 - t_2) \tag{4.59}$$
$$\langle \xi_i(t)\rangle = 0. \tag{4.60}$$

Now, consider a large ensemble: an infinite number of independent copies of the system. The phase space trajectory of the vector $\mathbf{a}$ will be different for each copy, resulting in a phase space distribution, $\rho(\mathbf{a}, t)$ over the ensemble. It is a basic principle of statistical mechanics (the Liouville Theorem) that this distribution is conserved in time:

$$\frac{\mathrm{d}\rho}{\mathrm{d}t} = \frac{\partial\rho}{\partial t} + \sum_i \left[\frac{\partial\rho}{\partial q_i}\dot{q}_i + \frac{\partial\rho}{\partial p_i}\dot{p}_i\right] = 0. \tag{4.61}$$

Note that the Liouville theorem is really a special case of the continuity equation:

$$\begin{aligned}
&\frac{\partial\rho}{\partial t} + \sum_i \left[\frac{\partial(\rho\dot{q}_i)}{\partial q_i} + \frac{\partial(\rho\dot{p}_i)}{\partial p_i}\right] \\
&= \frac{\partial\rho}{\partial t} + \sum_i \left[\frac{\partial\rho}{\partial q_i}\dot{q}_i + \frac{\partial\rho}{\partial p_i}\dot{p}_i\right] + \rho\sum_i \left[\frac{\partial\dot{q}_i}{\partial q_i} + \frac{\partial\dot{p}_i}{\partial p_i}\right] \\
&= \frac{\partial\rho}{\partial t} + \sum_i \left[\frac{\partial\rho}{\partial q_i}\dot{q}_i + \frac{\partial\rho}{\partial p_i}\dot{p}_i\right] + \rho\sum_i \left[\frac{\partial^2 H}{\partial q_i\partial p_i} - \frac{\partial^2 H}{\partial p_i\partial q_i}\right] \\
&= \frac{\partial\rho}{\partial t} + \sum_i \left[\frac{\partial\rho}{\partial q_i}\dot{q}_i + \frac{\partial\rho}{\partial p_i}\dot{p}_i\right],
\end{aligned}$$

where we have used Hamilton's equations, $\dot{q}_i = \frac{\partial H}{\partial p_i}$ and $\dot{p}_i = -\frac{\partial H}{\partial q_i}$. This form will prove the most useful, in fact. First note that momenta, p_i are actually assumed to be included in the set of dynamical variables, a_i (or else they are not included because the Hamiltonian has no dependence on them). Thus, we can write the Liouville theorem in this case:

$$\frac{\partial\rho(\mathbf{a}, t)}{\partial t} + \sum_i \frac{\partial(\rho(\mathbf{a}, t)\dot{a}_i)}{\partial a_i} = 0. \tag{4.62}$$

Physically speaking, this says that probability is conserved in the sense that the total probability in some region V, $\int_V \mathrm{d}^d\mathbf{a}\rho(\mathbf{a}, t)$ can only change via a probability current $\rho\dot{a}_i$ leaving the surface ∂V. Using the Langevin equations, we can write this as:

$$\begin{aligned}
\frac{\partial\rho}{\partial t} &= -\frac{\partial}{\partial a_i}(v_i(\mathbf{a})\rho) - \frac{\partial}{\partial a_i}(\xi_i(t)\rho) \\
&= -L_0\rho - \sum_i \xi_i(t)L_{1i}\rho,
\end{aligned} \tag{4.63}$$

where the operators L_0 and L_{1i} are defined by:

$$L_0 \equiv \sum_i \left(\frac{\partial v_i(\mathbf{a})}{\partial a_i} + v_i(\mathbf{a}) \frac{\partial}{\partial a_i} \right), \tag{4.64}$$

$$L_{1i} \equiv \frac{\partial}{\partial a_i}. \tag{4.65}$$

Now, let us find $\sigma(\mathbf{a}, t)$ such that:

$$\rho = e^{-tL_0}\sigma. \tag{4.66}$$

The Liouville theorem implies:

$$-e^{-tL_0}L_0\sigma + e^{-tL_0}\frac{\partial \sigma}{\partial t} = -\sum_i \xi_i L_{1i}(e^{-tL_0}\sigma) - e^{-tL_0}L_0\sigma, \tag{4.67}$$

so, σ must satisfy:

$$\frac{\partial \sigma}{\partial t} = -e^{tL_0}\sum_i \xi_i(t) L_{1i} e^{-tL_0}\sigma \equiv \sum_i \xi_i(t) M_i(t)\sigma. \tag{4.68}$$

This is analogous to the time evolution equation for a state in the interaction picture, in quantum field theory. σ can thus be found via a Dyson series:

$$\sigma(t) = \mathrm{T}\exp\left(-\int_0^t \mathrm{d}t' \sum_i \xi_i(t') M_i(t') \right) \sigma(0), \tag{4.69}$$

where T exp denotes the time ordered exponential. Now, this evidently depends on the stochastic function ξ_i, so we take an average over ξ_i:

$$\langle \sigma(t) \rangle = \int \mathrm{d}^d\xi P(\xi) \mathrm{T}\exp\left(-\int_0^t \mathrm{d}t' \sum_i \xi_i(t') M_i(t') \right) \sigma(0), \tag{4.70}$$

where $P(\xi)$ is a multivariate Gaussian distribution. This is tricky to express since there are a continuous infinity of $\xi_i(t)$. Consider the discrete form with N variables[9], ξ_μ. We would then have:

$$P(\xi) = \sqrt{\frac{|\det(g)|}{(2\pi)^N}} \exp\left(-\frac{1}{2}\xi_\mu g_{\mu\nu}\xi_\nu \right), \tag{4.71}$$

where $g_{\mu\nu}$ is the correlation matrix for this distribution. Note that the time ordering symbol, T can be taken outside the integral as all it really does is impose a re-ordering of the matrices:

$$\langle \sigma(t) \rangle = \mathrm{T}\left(\sqrt{\frac{|\det(g)|}{(2\pi)^N}} \int \mathrm{d}^N\xi \exp\left(-\xi_\mu M_\mu - \frac{1}{2}\xi_\mu g_{\mu\nu}\xi_\nu \right) \right) \sigma(0). \tag{4.72}$$

[9] we will use Greek indices to distinguish between ξ_i, the discrete set of functions, and ξ_μ, a discrete approximation to $\xi(t)$ - note that μ includes the discrete ξ_i degrees of freedom implicitly - essentially we have made time discrete and gathered the resulting 2D array $\xi_i(t_a)$ into a single index, μ

We have to be careful, however, because M_μ is a matrix. Seemingly, we have the integral of the exponential of a matrix, which is hard to define. The most reasonable definition would be a matrix of the integral of each component, but computing the components and then integrating them is not easy to do. However, we can use the shift invariance of Gaussian integrals. Recall the simpler case of a constant k and a single dimension:

$$\begin{aligned}\int_{-\infty}^{\infty} \mathrm{d}x e^{kx-\frac{x^2}{2}} &= e^{\frac{k^2}{2}} \int_{-\infty}^{\infty} \mathrm{d}x e^{-\frac{1}{2}(x-k)^2} \\ &= e^{\frac{k^2}{2}} \int_{-\infty}^{\infty} \mathrm{d}x' e^{-\frac{1}{2}x'^2} \\ &= \sqrt{2\pi} e^{\frac{k^2}{2}}, \end{aligned} \tag{4.73}$$

where $x' = x - k$. It is not entirely obvious that the same holds if k is a matrix, because it doesn't really make sense to shift x by a matrix k and then integrate with respect to $x - k$. We can, however, put this calculation on firmer grounds for matrices by proving it using a different method. Simply expand the exponential:

$$\begin{aligned}\int_{\infty}^{\infty} \mathrm{d}x e^{kx} e^{-\frac{x^2}{2}} &= \sum_{i=0}^{\infty} \frac{k^n}{n!} \int_{-\infty}^{\infty} \mathrm{d}x x^n e^{-\frac{x^2}{2}} \\ &= \sum_{i=0}^{\infty} \frac{k^{2n}}{(2n)!} \int_{-\infty}^{\infty} x^{2n} e^{-\frac{x^2}{2}} \\ &= \sum_{i=0}^{\infty} \frac{k^{2n}}{(2n)!} \sqrt{2\pi} \frac{(2n)!}{n!} \left(\frac{1}{\sqrt{2}}\right)^{2n} \\ &= \sqrt{2\pi} \sum_{i=0}^{\infty} \frac{(\frac{k^2}{2})^n}{n!} \\ &= \sqrt{2\pi} e^{\frac{k^2}{2}}. \end{aligned}$$

In the second line we used the fact that this integral vanishes for odd n, and in the third we used the well known result for $\int_{-\infty}^{\infty} x^{2n} e^{-\frac{x^2}{2}}$. This shows that the result holds even if k is a matrix. The multi-dimensional generalisation of this result is:

$$\begin{aligned}\langle \sigma(t) \rangle &= \mathrm{T} \left(\sqrt{\frac{|\det(g)|}{(2\pi)^N}} \int \mathrm{d}^N \xi \exp\left(-\xi_\mu M_\mu - \frac{1}{2} \xi_\mu g_{\mu\nu} \xi_\nu \right) \right) \sigma(0) \\ &= \mathrm{T} \left(\sum_{n=0}^{\infty} \frac{(-1)^n M_{\mu_1} \dots M_{\mu_n}}{n!} \langle \xi_{\mu_1} \dots \xi_{\mu_n} \rangle \right) \sigma(0) \\ &= \mathrm{T} \left(\sum_{n=0}^{\infty} \frac{M_{\mu_1} \dots M_{\mu_{2n}}}{(2n)!} \langle \xi_{\mu_1} \dots \xi_{\mu_{2n}} \rangle \right) \sigma(0), \end{aligned}$$

since again the odd n terms vanish. Now, $\langle \xi_{\mu_1} \dots \xi_{\mu_{2n}} \rangle$ is given by Wick's Theorem to be a sum of products of all possible pairs $\langle \xi_\mu \xi_\nu \rangle$. For $2n$ terms, some careful combinatorics reveals that there are:

$$\#\text{ of Pairs } = \frac{(2n)!}{n!2^n} \tag{4.74}$$

such possible pairings, each a product of n factors $\sim \langle \xi_\mu \xi_\nu \rangle$. Now, it can be shown that this gives $\langle \xi_\mu \xi_\nu \rangle = {g^{-1}}_{\mu\nu}$ (see any text on Gaussian integrals or Path integral quantum field theory). Also, the time ordering, T ensures that the precise order of M_{μ_i} is irrelevant, since they will be re-ordered anyway, so in each term of the Wick decomposition, we can re-order the M_{μ_i}:

$$M_{\mu_1} \dots M_{\mu_{2n}} {g^{-1}}_{\mu_i \mu_j} \dots {g^{-1}}_{\mu_l \mu_k} \to (M_\mu {g^{-1}}_{\mu\nu} M_\nu)^n. \tag{4.75}$$

Because we sum over all μ_i, this will actually be the same thing for *each* term in the Wick expansion, so we pick up a factor of the number of possible Wick pairings:

$$\langle \sigma(t) \rangle = \mathrm{T} \left(\sum_{n=0}^{\infty} \frac{(M_\mu {g^{-1}}_{\mu\nu} M_\nu)^n}{(2n)!} \times \frac{(2n)!}{n!2^n} \right) \sigma(0) = \mathrm{T} \exp \left(\frac{1}{2} M_\mu {g^{-1}}_{\mu\nu} M_\nu \right) \sigma(0). \tag{4.76}$$

Note that we would have obtained exactly the same result by writing:

$$-\xi_\mu M_\mu - \frac{1}{2} \xi_\mu g_{\mu\nu} \xi_\nu = \frac{1}{2} M_\mu {g^{-1}}_{\mu\nu} M_\nu - \frac{1}{2} (\xi_\mu + M_\rho {g^{-1}}_{\rho\mu}) g_{\mu\nu} (\xi_\nu + M_\sigma {g^{-1}}_{\sigma\nu}) \tag{4.77}$$

and asserting shift invariance of the Gaussian integral, despite the fact that ξ_μ was shifted by a matrix.
Now all that remains is to make time continuous again. Thus, the result becomes:

$$\begin{aligned}
\langle \sigma(t) \rangle &= \mathrm{T} \exp \left(\frac{1}{2} \int_0^t \mathrm{d}t_1 \int_0^t \mathrm{d}t_2 M_i(t_1) \langle \xi_i(t_1) \xi_j(t_2) \rangle M_j(t_2) \right) \sigma(0) \\
&= \mathrm{T} \exp \left(\frac{1}{2} \int_0^t \mathrm{d}t_1 \int_0^t \mathrm{d}t_2 g_{ij} \delta(t_1 - t_2) e^{t_1 L_0} L_{1i} e^{-t_1 L_0} e^{t_2 L_0} L_{1j} e^{-t_2 L_0} \right) \sigma(0) \\
&= \mathrm{T} \exp \left(\frac{1}{2} \int_0^t \mathrm{d}t_1 g_{ij} e^{t_1 L_0} L_{1i} L_{1j} e^{-t_1 L_0} \right) \sigma(0) \\
&= \mathrm{T} \exp \left(\frac{1}{2} \int_0^t \mathrm{d}t_1 g_{ij} e^{t_1 L_0} \frac{\partial^2}{\partial a_i \partial a_j} e^{-t_1 L_0} \right) \sigma(0). \qquad (4.78) \\
& \qquad (4.79)
\end{aligned}$$

From this, it follows that[10]:

$$\frac{\partial \langle \sigma(t) \rangle}{\partial t} = \frac{g_{ij}}{2} e^{t L_0} \frac{\partial^2}{\partial a_i \partial a_j} \left(e^{-t L_0} \langle \sigma(t) \rangle \right), \tag{4.80}$$

[10]The time ordered exponential actually satisfies this equation *by definition*.

so:

$$\frac{\partial\langle\rho(\mathbf{a},t)\rangle}{\partial t} = \frac{\partial(e^{-tL_0}\langle\sigma(t)\rangle)}{\partial t}$$
$$= -L_0(e^{-tL_0}\langle\sigma(t)\rangle) + e^{-tL_0}\frac{g_{ij}}{2}e^{tL_0}\frac{\partial^2}{\partial a_i\partial a_j}\left(e^{-tL_0}\langle\sigma(t)\rangle\right). \quad (4.81)$$

Defining $P(\mathbf{a},t) \equiv \langle\rho(\mathbf{a},t)\rangle$, which is the expectation value of the phase space distribution, we have the Fokker-Planck equation:

$$\frac{\partial P(\mathbf{a},t)}{\partial t} = -\sum_i \frac{\partial}{\partial a_i}\left(v_i(\mathbf{a})P(\mathbf{a},t)\right) + \sum_{i,j}\frac{g_{ij}}{2}\frac{\partial^2 P(\mathbf{a},t)}{\partial a_i\partial a_j}, \quad (4.82)$$

where v_i is the deterministic velocity term from the Langevin equation, 4.50.

4.5 Fokker-Planck Equation in De Sitter Space

In section 4.3 we derived the Langevin equations for a scalar field in de Sitter space, which we repeat here for convenience:

$$\dot{\bar{\phi}} = -\frac{V'(\bar{\phi})}{3H} + f(\mathbf{x},t), \quad (4.83)$$

where:

$$\langle f(\mathbf{x}_1,t_1)f(\mathbf{x}_2,t_2)\rangle = \frac{H^3}{4\pi^2}\delta(t_1-t_2)\mathrm{sinc}(\varepsilon a(t_1)H|\mathbf{x_1}-\mathbf{x_2}|). \quad (4.84)$$

Consider the correlation function for f at a single point, $\mathbf{x}$. Then:

$$\langle f(\mathbf{x},t_1)f(\mathbf{x},t_2)\rangle = \frac{H^3}{4\pi^2}\delta(t_1-t_2). \quad (4.85)$$

Let us define $\rho_1(\varphi,t)$ as the expectation value of the phase space distribution for the field φ at time t. This satisfies the Fokker-Planck equation for a single dynamical variable, φ, with $g_{11} = \frac{H^3}{4\pi^2}$ and $v_1(\varphi) = -\frac{V'(\varphi)}{3H}$. Thus:

$$\frac{\partial\rho_1(\varphi,t)}{\partial t} = \frac{1}{3H}\frac{\partial}{\partial\varphi}\left(V'(\varphi)\rho_1(\varphi,t)\right) + \frac{H^3}{8\pi^2}\frac{\partial^2\rho_1(\varphi,t)}{\partial\varphi^2}. \quad (4.86)$$

This partial differential equation is essentially a diffusion equation for the probability density. Assuming we know the initial distribution, (e.g, if the field starts at φ_0 for this point, then $\rho(\varphi,t_0) = \delta(\varphi-\varphi_0)$) then we can compute the probability distribution for the fields value at any other point in the future. More generally, we can define $r = |\mathbf{x_1}-\mathbf{x_2}|$ and obtain:

$$g_{ij} = \frac{H^3}{4\pi^2}\begin{pmatrix}1 & \mathrm{sinc}(\varepsilon a(t_1)Hr)\\ \mathrm{sinc}(\varepsilon a(t_1)Hr) & 1\end{pmatrix}. \quad (4.87)$$

This time, there are two dynamical variables, φ_1, φ_2 for the field at the two space-time points, and the Fokker-Planck equation is:

$$\begin{aligned}\frac{\partial \rho_2(\varphi_1,\varphi_2,t)}{\partial t} =& \frac{1}{3H}\frac{\partial}{\partial \varphi_1}\left(V'(\varphi_1)\rho_2\right) + \frac{1}{3H}\frac{\partial}{\partial \varphi_2}\left(V'(\varphi_2)\rho_2\right) \\ &+ \frac{H^3}{8\pi^2}\frac{\partial^2 \rho_2}{\partial \varphi_1^2} + \frac{H^3}{8\pi^2}\frac{\partial^2 \rho_2}{\partial \varphi_2^2} + \mathrm{sinc}(\varepsilon a(t_1) H r)\frac{H^3}{4\pi^2}\frac{\partial^2 \rho_2}{\partial \varphi_1 \partial \varphi_2}. \quad (4.88)\end{aligned}$$

Starobinsky and Yokoyama studied the properties of Eq. (4.86) in detail in [28]. They found that the general solution was:

$$\rho_1(\varphi, t) = \exp\left(-\nu(\varphi)\right) \sum_{n=0}^{\infty} a_n \Phi_n(\varphi) e^{-\Lambda_n (t-t_0)}, \quad (4.89)$$

where $\Phi_n(\varphi)$ are eigenfunctions and Λ_n eigenvalues of the following Schroedinger-like equation:

$$-\frac{1}{2}\frac{\mathrm{d}\Phi_n}{\mathrm{d}\varphi^2} + \frac{1}{2}\left[v'(\varphi)^2 - \nu''(\varphi)\right]\Phi_n = \frac{4\pi^2 \Lambda_n}{H^3}\Phi_n \quad (4.90)$$

and $\nu(\varphi)$ is defined by:

$$\nu(\varphi) \equiv \frac{4\pi^2 V(\varphi)}{3H^4}. \quad (4.91)$$

To show that this is the general solution, first note that Eq. (4.86) is a separable partial differential equation. Applying the method of separation of variables implies:

$$\frac{1}{T}\frac{\mathrm{d}T(t)}{\mathrm{d}t} = -\Lambda \quad (4.92)$$

$$\Gamma_\varphi \tilde{\Phi}(\varphi) \equiv \frac{1}{3H}\frac{\partial}{\partial \varphi}(V'(\varphi)\tilde{\Phi}(\varphi)) + \frac{H^3}{8\pi^2}\frac{\partial^2 \tilde{\Phi}(\varphi)}{\partial \varphi^2} = -\Lambda \tilde{\Phi}(\varphi). \quad (4.93)$$

We choose $-\Lambda$ on the right hand side for later convenience (we will later show that this ensures Λ is positive). Eq. (4.92) is trivial to solve, but (4.93) requires some thought - it contains a term with a single $\frac{\partial}{\partial \varphi}$ derivative, but is otherwise very similar to the time independent Schroedinger equation. Consider making the substitution $\tilde{\Phi}(\varphi) = f(\varphi)\Phi(\varphi)$. Then Eq. (4.93) becomes:

$$\begin{aligned}&\left[\frac{V''(\varphi)}{3H}f(\varphi) + \frac{H^3}{8\pi^2}\frac{\mathrm{d}^2 f}{\mathrm{d}\varphi^2} + \frac{V'(\varphi)}{3H}\frac{\mathrm{d}f}{\mathrm{d}\varphi}\right]\Phi + \left[\frac{V'(\varphi)}{3H}f(\varphi) + \frac{H^3}{4\pi^2}\frac{\mathrm{d}f}{\mathrm{d}\varphi}\right]\frac{\mathrm{d}\Phi}{\mathrm{d}\varphi} \\ &+ \frac{H^3}{8\pi^2}f(\varphi)\frac{\mathrm{d}^2\Phi}{\mathrm{d}\varphi^2} = -\Lambda f(\varphi)\Phi(\varphi). \quad (4.94)\end{aligned}$$

The first derivative term can be made to vanish if f is chosen to satisfy:

$$\frac{\mathrm{d}f}{\mathrm{d}\varphi} = -\frac{4\pi^2 V'(\varphi)}{3H^4}f, \quad (4.95)$$

which has the solution:

$$f(\varphi) = \exp\left(-\frac{4\pi^2 V(\varphi)}{3H^4}\right) \equiv \exp\left(-\nu(\varphi)\right), \tag{4.96}$$

up to constants, which will cancel. Now, making this substitution gives:

$$\left[\frac{V''(\varphi)}{6H} - \frac{2\pi^2 V'(\varphi)^2}{9H^5}\right] f(\varphi)\Phi + \frac{H^3}{8\pi^2}\frac{\mathrm{d}^2\Phi}{\mathrm{d}\varphi^2} f(\varphi) = -\Lambda f(\varphi)\Phi. \tag{4.97}$$

Cancelling f and multiplying by $-\frac{4\pi^2}{H^3}$, we see that this gives rise to the Schroedinger equation:

$$-\frac{1}{2}\frac{\mathrm{d}^2\Phi_n}{\mathrm{d}\varphi^2} + \frac{1}{2}\left[\frac{4\pi^2}{3H^4}V''(\varphi) - \left(\frac{4\pi^2}{3H^4}\right)^2 V'(\varphi)^2\right]\Phi_n = \frac{4\pi^2\Lambda_n}{H^3}\Phi_n, \tag{4.98}$$

where we know that only discrete sets of Λ_n, Φ_n satisfy this, since the Schroedinger equation is a Sturm-Liouville equation. The general solution to equation 4.86 can thus be written as in Eq. (4.89). The coefficients a_n are chosen so as to match the initial condition at $t = t_0$, i.e., $\rho_1(\varphi, t_0)$. The orthogonality relation for the Schroedinger equation means that:

$$\int \mathrm{d}\varphi \Phi_n(\varphi)\Phi_m(\varphi) = \delta_{nm} \tag{4.99}$$

and using this, the a_n coefficients can be expressed as:

$$a_n = \int \mathrm{d}\varphi e^{\nu(\varphi)}\Phi_n(\varphi)\rho_1(\varphi, t_0). \tag{4.100}$$

A useful observation about Eq. (4.90) is that it can be written in the form:

$$\frac{1}{2}\left(-\frac{\partial}{\partial\varphi} + \nu'(\varphi)\right)\left(\frac{\partial}{\partial\varphi} + \nu'(\varphi)\right)\Phi_n = \frac{4\pi^2\Lambda_n}{H^3}\Phi_n \tag{4.101}$$

and given that $\frac{\partial}{\partial\varphi}^\dagger = -\frac{\partial}{\partial\varphi}$ (this follows from integration by parts), then this is in the form $\frac{1}{2}AA^\dagger\Phi_n = E_n\Phi_n$. Again, the orthogonality here will help because, taking $(y, z\cdot) = \int \mathrm{d}\varphi y(\varphi)z(\varphi)$ as the inner product allows us to write:

$$E_n = \left(\Phi_n, \frac{1}{2}AA^\dagger\Phi_n\right) = \frac{1}{2}\left(A^\dagger\Phi_n, A^\dagger\Phi_n\right) \geq 0, \tag{4.102}$$

by the definition of the hermitian conjugate and exploiting the positive-definiteness of this inner product. Thus, we can conclude that $\Lambda_n \geq 0$.
One final property that Starobinsky and Yokoyama pointed out was the existence of a $\Lambda_0 = 0$ eigenvalue for certain cases:

$$-\frac{1}{2}\frac{\mathrm{d}^2}{\mathrm{d}\varphi^2}e^{-\nu(\varphi)} + \frac{1}{2}[\nu'(\varphi)^2 - \nu''(\varphi)]e^{-\nu(\varphi)} = 0. \tag{4.103}$$

However, this is only a valid eigenfunction if it is normalisable:

$$N \equiv \int \mathrm{d}\varphi e^{-2\nu(\varphi)} < \infty. \tag{4.104}$$

Provided this condition holds, then there exists a static solution of the Fokker-Planck equation:

$$\rho_{eq}(\varphi) = N^{-\frac{1}{2}} e^{-\nu(\varphi)}, \tag{4.105}$$

which usefully reveals the zeroth eigenfunction. This is significant, because after a long period of time, all the components of $\rho(\varphi, t_0)$ with non-zero Λ_n decay exponentially, leaving Φ_0 as the solution. Thus, Φ_0 is said to be an 'attractor solution' - all other solutions of the partial differential equation ultimately end up as this solution. For this reason, we refer to Φ_0 as the equilibrium solution. A consequence of this is that the quantity N tell us *whether or not a given system has an equilibrium solution.* If N is finite, then Φ_0 exists, but if it diverges, then no such equilibrium solution exists. One reason this could happen is if $V(\varphi) \to -\infty$ at $\pm\infty$, in which case, N diverges because $e^{-2\nu(\varphi)} \to +\infty$ as $\varphi \to \pm\infty$. Physically, this corresponds to the fact that the classical behaviour of an object in this potential is to roll away to negative infinity. Since this motion will carry on forever, then there is no way the system can come to equilibrium.

4.6 Calculation of Arbitrary Correlation Functions

In quantum field theory, a quantity frequently of interest is the two point correlation function. The one point function, $\langle\phi(t,x)\rangle$ tells us about the behaviour of the average value of the field, but the two-point function can give information which can actually be observed, by measuring the statistical correlation between different parts of the cosmic microwave background, for example. In the stochastic approach to inflation, the two point correlation function between the auxiliary φ at times separated by t and both at the same point x is given by:

$$G(t) \equiv \langle\varphi(t,x)\varphi(0,x)\rangle = \int \mathrm{d}\varphi_1\varphi_2\varphi_1(t)\varphi_2(0)\rho_2(\varphi_1(t),\varphi_2(0)). \tag{4.106}$$

Here, ρ_2 is the joint probability density of φ_1 and φ_2 simultaneously taking on the values that they do. In this section, we will detail a way of calculating $G(t)$ described by Starobinsky and Yokoyama[28]. If φ_1 and φ_2 are correlated in some way, then evidently they are not independent. In particular, ρ_2 is given by:

$$\begin{aligned}\rho_2(\varphi_1(t_1),\varphi_2(t_2)) =&\Pi(\varphi_1(t_1)|\varphi_2(t_2))\rho_1(\varphi_2(t_2))\theta(t_1-t_2)\\ &+\Pi(\varphi_2(t_2)|\varphi_1(t_1))\rho_1(\varphi_1(t_1))\theta(t_2-t_1),\end{aligned} \tag{4.107}$$

where $\rho_1(\varphi_1(t_1))$ is the probability density for $\varphi = \varphi_1(t_1)$ at time t_2, and $\Pi(\varphi_2(t_2)|\varphi_1(t_1))$ is the conditional probability density that φ takes on the value

$\varphi_2(t_2)$ at time $t_2 > t_1$, given that $\varphi = \varphi_1(t_1)$ at t_1. The Heaviside step function[11], $\theta(t_2 - t_1)$ ensures that $t_2 > t_1$. Both of these are one-point probability distributions, so satisfy the Fokker-Planck equation. Π in particular has the initial condition:

$$\Pi(\varphi_1(t)|\varphi_2(t)) = \delta(\varphi_1 - \varphi_2). \tag{4.108}$$

This is because φ must (obviously) be single valued at t so has zero probability density of being anything except φ_2.
We must have:

$$G(t) = \int \mathrm{d}\varphi_1 \mathrm{d}\varphi_2 \varphi_1 \varphi_2 \Pi(\varphi_1(t_0 + t)|\varphi_2(t_0))\rho_1(\varphi_2, t_0) \tag{4.109}$$

$$= \int \mathrm{d}\varphi_1 \varphi_1 \Xi((\varphi_1, t), \tag{4.110}$$

where:

$$\Xi(\varphi_1, t) \equiv \int \mathrm{d}\varphi_2 \varphi_2 \rho_1(\varphi_2, t_0)\Pi(\varphi_1(t_0 + t)|\varphi_2(t_0)) \tag{4.111}$$

$$\implies \Xi(\varphi_1, 0) = \varphi_1 \rho_1(\varphi_1, t_0). \tag{4.112}$$

Consequently:

$$\begin{aligned}\frac{\partial \Xi(\varphi_1, t)}{\partial t} &= \int \mathrm{d}\varphi_2 \varphi_2 \rho_1(\varphi_2, t_0) \frac{\partial \Pi(\varphi_1(t_0 + t)|\varphi_2(t_0)))}{\partial t} \\ &= \int \mathrm{d}\varphi_2 \varphi_2 \rho_1(\varphi_2, t_0) \Gamma_{\varphi_1} \Pi(\varphi_1(t_0 + t)|\varphi_2(t_0)) \\ &= \Gamma_{\varphi_1} \Xi(\varphi_1, t),\end{aligned}$$

so, Ξ satisfies the same Fokker-Planck equation as the one-point probability distribution, for which we know the analytic solution.

4.6.1 Temporal Correlation Function: Static Case

Consider first the case where there exists a static solution, $\rho_{eq}(\varphi)$. After a long time, $\rho_1(\varphi_2, t_0)$ will settle down to it.

$$\Xi(\varphi, t) = e^{-\nu(\varphi)} \sum_n A_n \Phi_n(\varphi) e^{-\Lambda_n t}, \tag{4.113}$$

[11] $\theta(t) = 0$ if $t < 0, 1$ if $t > 0$

where A_n is determined by the initial condition, $\Xi(\varphi, 0) = \varphi\rho_{eq}(\varphi)$:

$$\begin{aligned} A_n &= \int \mathrm{d}\varphi_2 \Xi(\varphi_2, 0) e^{\nu(\varphi_2)} \Phi_n(\varphi_2) \\ &= \int \mathrm{d}\varphi_2 \varphi_2 \rho_{eq}(\varphi_2) e^{\nu(\varphi_2)} \Phi_n(\varphi_2) \\ &= N^{-1} \int \mathrm{d}\varphi_2 e^{-\nu(\varphi_2)} \varphi_2 \Phi_n(\varphi_2). \end{aligned} \tag{4.114}$$

N is as defined by Eq. (4.104). We can thus write:

$$\begin{aligned} G(t) &= \int \mathrm{d}\varphi_1 \Xi(\varphi_1, t) \varphi_1 \\ &= \int \mathrm{d}\varphi_1 \int \mathrm{d}\varphi_2 N^{-1} \sum_n e^{-\nu(\varphi_1)} e^{-\nu(\varphi_2)} \Phi_n(\varphi_2) \Phi_n(\varphi_1) \varphi_1 \varphi_2 e^{-\Lambda_n t} \\ &= N \sum_n A_n^2 e^{-\Lambda_n t}. \end{aligned} \tag{4.115}$$

This gives a very convenient way of computing the correlation function. All we need to do it numerically calculate the integral in Eq. (4.114) for each n, to give A_n and then sum up the results with the eigenvalues, Λ_n (Eq. (4.115)) to give the full correlation function.

4.6.2 Extension to Arbitrary Correlators

$G(t)$ gives only the behaviour for temporally separated fields at the same spacial position. In general, it is necessary to compute:

$$G(t_1, t_2, |x_1 - x_2|) = \langle \varphi(x_1, t_1) \varphi(x_2, t_2) \rangle. \tag{4.116}$$

First consider the points at the same time, $t_1 = t_2 = t$. The Fokker-Planck equation obeyed by the joint probability density $\rho(\varphi_1, \varphi_2)$ for this situation is Eq. (4.88):

$$\frac{\partial \rho}{\partial t} = \Gamma_{\varphi_1} \rho + \Gamma_{\varphi_2} \rho + \frac{\sin(\epsilon a(t) H |x_1 - x_2|)}{\epsilon a(t) H |x_1 - x_2|} \frac{H^3}{4\pi^2} \frac{\partial^2 \rho}{\partial \varphi_1 \varphi_2}. \tag{4.117}$$

The sinc function here is non-trivial to handle, but can be approximated, following Starobinsky and Yokoyama[28] by the Heaviside step function $\theta(1 - \epsilon a(t) H |x_1 - x_2|)$. In this approximation, it is assumed that any points closer together than the infra-red cut-off $a(t)|x_1 - x_2| < \frac{1}{\epsilon H}$ are completely correlated ($\theta = 1$) while those further apart are completely uncorrelated. For $a(t)|x_1 - x_2| < \frac{1}{\epsilon H}$ then, the equation is:

$$\frac{\partial \rho}{\partial t} = \Gamma_{\varphi_1} \rho + \Gamma_{\varphi_2} \rho + \frac{H^3}{4\pi^2} \frac{\partial^2 \rho}{\partial \varphi_1 \varphi_2}. \tag{4.118}$$

This can be solved by first integrating with respect to one of the fields:

$$\begin{aligned}\frac{\partial}{\partial t}\left(\int \mathrm{d}\varphi_2 \rho(\varphi_1,\varphi_2)\right) &= \Gamma_{\varphi_1}\left(\int \mathrm{d}\varphi_2 \rho(\varphi_1,\varphi_2)\right) + \frac{1}{3H}\int \mathrm{d}\varphi_2 \frac{\partial}{\partial \varphi_2}\left[V'(\varphi_2)\rho(\varphi_1,\varphi_2)\right] \\ &+ \frac{H^3}{8\pi^2}\int \mathrm{d}\varphi_2 \frac{\partial^2 \rho(\varphi_1,\varphi_2)}{\partial \varphi_2^2} + \frac{H^3}{4\pi^2}\int \mathrm{d}\varphi_2 \frac{\partial}{\partial \varphi_2}\left[\frac{\partial \rho(\varphi_1,\varphi_2)}{\partial \varphi_1}\right] \\ &= \Gamma_{\varphi_1}\left(\int \mathrm{d}\varphi_2 \rho(\varphi_1,\varphi_2)\right) + \frac{1}{3H}\left[V'(\varphi_2)\rho(\varphi_1,\varphi_2)\right]_{\varphi_2=-\infty}^{\varphi_2=\infty} \\ &+ \frac{H^3}{8\pi^2}\left[\frac{\partial \rho(\varphi_1,\varphi_2)}{\partial \varphi_2}\right]_{\varphi_2=-\infty}^{\varphi_2=\infty} + \frac{H^3}{4\pi^2}\left[\frac{\partial \rho(\varphi_1,\varphi_2)}{\partial \varphi_1}\right]_{\varphi_2=-\infty}^{\varphi_2=\infty}.\end{aligned}$$

If we impose vanishing boundary conditions on ρ and its derivatives at $\varphi_1, \varphi_2 \to \pm\infty$ then all that is left is:

$$\frac{\partial}{\partial t}\left(\int \mathrm{d}\varphi_2 \rho(\varphi_1,\varphi_2)\right) = \Gamma_{\varphi_1}\left(\int \mathrm{d}\varphi_2 \rho(\varphi_1,\varphi_2)\right). \tag{4.119}$$

This is the one-point Fokker-Planck equation, which was already solved to give the equilibrium distribution (assuming that such a state exists). If the integral with respect to φ_2 satisfies this, then:

$$\int \mathrm{d}\varphi_2 \rho(\varphi_1,\varphi_2) = \rho_{eq}(\varphi_1), \tag{4.120}$$

which implies:

$$\rho(\varphi_1,\varphi_2) = \rho_{eq}(\varphi_1)\delta(\varphi_1-\varphi_2). \tag{4.121}$$

This is to be expected - it says that there is zero probability of the fields differing, which is exactly what we would expect as they are completely correlated in this regime.

For a general separation, it is necessary to first find the time, t_r when the points at co-moving separation $r = |x_1 - x_2|$ were just leaving the completely correlated region, that is, $a(t)r = \frac{1}{\epsilon H}$. This occurs when $a_0 e^{Ht_r} r = \frac{1}{\epsilon H}$, or:

$$t_r = -\frac{1}{H}\ln(r a_0 \epsilon H). \tag{4.122}$$

By the solution, Eq. (4.121), to the equal time correlation function above, we know that both fields had the equilibrium distribution at time t_r. Assuming $t_1, t_2 > t_r$ (to be discussed below) the distribution at the later times t_1 and t_2 is given by the conditional probability:

$$\rho(\varphi_1,\varphi_2) = \int \mathrm{d}\varphi_r \rho_{eq}(\varphi_r)\Pi(\varphi_1(x_1,t_2)|\varphi_r(x_1,t_r))\Pi(\varphi_2(x_2,t_2)|\varphi_r(x_2,t_r)). \tag{4.123}$$

This equation is really just a statement of probability - we sum (integrate) over all possible values of φ_r the probability that $\varphi(x_1,t_2)$ takes on the value $\varphi_1(x_1,t_1)$ given $\varphi(x_1,t_r) = \varphi_r$, multiplying by the probability that $\varphi(x_2,t_2)$

takes on the value $\varphi_2(x_2,t_2)$ given $\varphi_r(x_2,t_2)$. Note that this assumes t_1 and t_2 both exceed $t_1,t_2 > t_r$ because multiplying $\Pi(\varphi_1|\varphi_r)$ and $\Pi(\varphi_2|\varphi_r)$ to obtain the joint probability is only valid if these two events are independent, which is only true if $|x_1 - x_2| > \frac{1}{\epsilon H}$ (recall that we required events further apart than this to be completely uncorrelated). Since t_r is the last time that this is true, then we need both $t_1,t_2 > t_r$ for this to apply. If this is not the case, then $|x_1 - x_2| < \frac{1}{\epsilon H}$ at either t_1,t_2 or both (whichever are less then t_r), in which case, the two points at that time lie inside the volume over which we averaged to form an infra-red cut-off. From the point of view of stochastic inflation then, they are completely correlated and behave as if they were the same point. In that case, the correlation function is just the temporal correlation function, $G(|t_1 - t_2|)$ as derived previously.
The correlation function is thus given by:

$$\begin{aligned} G(r,t_1,t_2) &\equiv \int \mathrm{d}\varphi_1 \mathrm{d}\varphi_2 \varphi_1 \varphi_2 \rho(\varphi_1,\varphi_2) \\ &= \int \mathrm{d}\varphi_1 \mathrm{d}\varphi_2 \mathrm{d}\varphi_r \varphi_1 \varphi_2 \Big[\Pi(\varphi_1(x_1,t_1)|\varphi_r(x_1,t_r)) \times \\ &\quad \times \Pi(\varphi_2(x_2,t_2)|\varphi_r(x_2,t_r)) \rho_{eq}(\varphi_r) \Big]. \end{aligned} \tag{4.124}$$

The conditional probability densities both satisfy the Fokker-Planck equation for a single point, subject to the initial condition $\Pi(\varphi_1(x_1,t_r)|\varphi_r(x_1,t_r)) = \delta(\varphi_1 - \varphi_r)$. The solution is:

$$\Pi(\varphi_1(x_1,t_1)|\varphi_r(x_1,t_r)) = e^{-\nu(\varphi_1)} \sum_n a_n \Phi_n(\varphi_1) e^{-\Lambda_n (t_1 - t_r)}, \tag{4.125}$$

where a_n are determined by the initial condition:

$$a_n = \int \mathrm{d}\tilde{\varphi} e^{\nu(\tilde{\varphi})} \delta(\tilde{\varphi} - \varphi_r) \Phi_n(\tilde{\varphi}) = e^{\nu(\varphi_r)} \Phi_n(\varphi_r). \tag{4.126}$$

Thus[12]:

$$\Pi(\varphi_1(x_1,t_1)|\varphi_r(x_1,t_r)) = e^{\nu(\varphi_r) - \nu(\varphi_1)} \sum_n \Phi_n(\varphi_r) \Phi_n(\varphi_1) e^{-\Lambda_n (t_1 - t_r)}. \tag{4.127}$$

Substituting this in, we find:

$$\begin{aligned} G(r,t_1,t_2) = \int \mathrm{d}\varphi_1 \mathrm{d}\varphi_2 \mathrm{d}\varphi_r \varphi_1 \varphi_2 \rho_{eq}(\varphi_r) e^{2\nu(\varphi_r) - \nu(\varphi_1) - \nu(\varphi_2)} \times \\ \times \sum_{n,m} \Phi_n(\varphi_r) \Phi_m(\varphi_r) \Phi_n(\varphi_1) \Phi_m(\varphi_2) e^{-\Lambda_n (t_1 - t_r) - \Lambda_m (t_2 - t_r)} \end{aligned}$$

[12]Note that this does recover the initial condition at $t_1 = t_r$ because $\sum_n \Phi_n(\varphi_r)\Phi_n(\varphi_1) = \delta(\varphi_r - \varphi_1)$. This follows from the completeness relation for the eigenstates of a hermitian operator, $\sum_n |\Phi_n\rangle \langle \Phi_n| = \mathbb{I}$, so $\langle \varphi_r | \mathbb{I} | \varphi_1 \rangle \equiv \delta(\varphi_r - \varphi_1) = \sum_n \langle \varphi_r | \Phi_n \rangle \langle \Phi_n | \varphi_1 \rangle = \sum_n \Phi_n(\varphi_r) \Phi_n^*(\varphi_1)$ (recalling that in this case, Φ_n is real).

Now, use the definition of the coefficients A_n (equation 4.114) to simplify this:

$$G(r,t_1,t_2) = N^2 \int \mathrm{d}\varphi_r \rho_{eq}(\varphi_r) e^{2\nu(\varphi_r)} \sum_{n,m} \Phi_n(\varphi_r)\Phi_m(\varphi_r) A_n A_m e^{-\Lambda_n(t_1-t_r)-\Lambda_m(t_2-t_r)}. \tag{4.128}$$

But, $\rho_{eq}(\varphi_r) = N^{-1}e^{-2\nu(\varphi_r)}$, so this gives:

$$\begin{aligned} G(r,t_1,t_2) &= N \int \mathrm{d}\varphi_r \sum_{n,m} \Phi_n(\varphi_r)\Phi_m(\varphi_r) A_n A_m e^{-\Lambda_n(t_1-t_r)-\Lambda_m(t_2-t_r)} \\ &= N \sum_n A_n^2 e^{-\Lambda_n(t_1+t_2-2t_r)}. \end{aligned}$$

Since $\int \mathrm{d}\varphi_r \Phi_n(\varphi_r)\Phi_m(\varphi_r) = \delta_{nm}$ by the basis function orthonormality. Comparing to Eq. (4.115), gives:

$$G(r,t_1,t_2) = G(t_1+t_2-2t_r). \tag{4.129}$$

Consequently, any correlation function can be expressed in terms of the temporal correlation function for a single point. Notice that this result depended on special properties of the equilibrium solution, and would have to be modified in the case of the non-existence of such an equilibrium solution.
This result also depends on the arbitrary small constant ϵ, however, this dependence can be removed[13] by requiring that $\epsilon^{-2\frac{\Lambda_n}{H}} \sim 1$[28]. If this is the case, then $e^{+2\Lambda_n t_r} = e^{-\frac{2\Lambda_n}{H}\ln(a_0 r \epsilon H)} = e^{-\frac{2\Lambda_n}{H}\ln(a_0 r H)} e^{-\frac{2\Lambda_n}{H}\ln(\epsilon)} = \epsilon^{-\frac{2\Lambda_n}{H}} e^{-\frac{2\Lambda_n}{H}\ln(a_0 r H)} \sim e^{-\frac{2\Lambda_n}{H}\ln(a_0 r H)}$. This means we can write the correlation function in the more useful form:

$$G(r,t_1,t_2) = G\left(t_1+t_2+\frac{2}{H}\ln(r a_0 H)\right). \tag{4.130}$$

4.6.3 Non-Static Case

If there is no static solution for the one-point probability distribution, then the situation is more complicated. The absence of static solutions is a consequence of the fact that

$$N = \int \mathrm{d}\varphi e^{-2\nu(\varphi)} \tag{4.131}$$

diverges. In this situation, it is not actually valid to assume that $\Gamma_\varphi \tilde{\Phi}_n = -\Lambda_n \tilde{\Phi}_n$ has solutions of the form $\tilde{\Phi}_n = e^{-\nu(\varphi)}\Phi_n(\varphi)$ because such solutions cannot be made to satisfy the boundary conditions in this case[14]. Instead, it is necessary to abandon this analytic simplification and simply try to solve:

$$\frac{H^3}{8\pi^2}\frac{\mathrm{d}^2\tilde{\Phi}_n(\varphi)}{\mathrm{d}\varphi^2} + \frac{V'(\varphi)}{3H}\frac{\mathrm{d}\tilde{\Phi}_n}{\mathrm{d}\varphi} + \frac{V''(\varphi)}{3H}\tilde{\Phi}_n = -\Lambda_n\tilde{\Phi}_n, \tag{4.132}$$

[13] Or at least made very weak.
[14] Φ_n cannot decrease fast enough to cancel out the divergence of $e^{-\nu(\varphi)}$

numerically. This equation is not, however, in Sturm-Liouville form. A Sturm-Liouville equation can be placed in the form:

$$-p(\varphi)\frac{\mathrm{d}^2\tilde{\Phi}_n}{\mathrm{d}\varphi^2} - p'(\varphi)\frac{\mathrm{d}\tilde{\Phi}_n}{\mathrm{d}\varphi} + q(\varphi)\tilde{\Phi}_n = \lambda_n w(\varphi)\tilde{\Phi}_n(\varphi). \tag{4.133}$$

Observe that multiplying throughout by $\frac{4\pi^2}{H^3}$ would make the coefficient of the first-order derivative term precisely $\nu'(\varphi)$. Analogously to solving a first order equation by means of an integrating factor then, one can place Eq. (4.132) in Sturm-Liouville form by multiplying throughout by $-\frac{4\pi^2}{H^3}e^{2\nu(\varphi)}$:

$$-\frac{1}{2}e^{2\nu(\varphi)}\frac{\mathrm{d}^2\tilde{\Phi}_n}{\mathrm{d}\varphi^2} - \frac{1}{2}2\nu'(\varphi)e^{2\nu(\varphi)}\frac{\mathrm{d}\tilde{\Phi}_n}{\mathrm{d}\varphi} - \nu''(\varphi)e^{2\nu(\varphi)}\tilde{\Phi}_n = \frac{4\pi^2\Lambda_n}{H^3}e^{2\nu(\varphi)}\tilde{\Phi}_n. \tag{4.134}$$

By inspection, this is indeed Sturm-Liouville form with the functions:

$$p(\varphi) = \frac{1}{2}e^{2\nu(\varphi)}, \tag{4.135}$$

$$q(\varphi) = -v''(\varphi)e^{2\nu(\varphi)}, \tag{4.136}$$

$$w(\varphi) = e^{2\nu(\varphi)}. \tag{4.137}$$

The factor of $\frac{1}{2}$ in $p(\varphi)$ is chosen so that the familiar $\frac{4\pi^2\Lambda_n}{H^3}$ appears as the eigenvalue on the right hand side, but more importantly because it ensures that the Sturm-Liouville orthonormality condition is just[15]:

$$\int \mathrm{d}\varphi\tilde{\Phi}_n(\varphi)\tilde{\Phi}_m(\varphi)e^{2\nu(\varphi)} = \delta_{nm} \tag{4.138}$$

In the case that the static solution exists, one can thus just define $\tilde{\Phi}_n = e^{-\nu(\varphi)}\Phi_n$, which was already shown to eliminate the first order term leaving the differential equation found before. Furthermore, that orthonormality condition now agrees with this one:

$$\int \mathrm{d}\varphi\Phi_n(\varphi)\Phi_m(\varphi) = \delta_{nm}. \tag{4.139}$$

Assuming that such eigenfunctions can be found, the full solution is:

$$\rho_1(\varphi, t_0) = \sum_n a_n\tilde{\Phi}_n(\varphi)e^{-\Lambda_n t_0}, \tag{4.140}$$

where a_n are determined from the initial distribution at $t = 0$ in by means of the following integral, this time exploiting orthonormality. The absence of a static solution is signalled by the absence of a (normalisable) eigenfunction to Eq. (4.134) with eigenvalue $\Lambda_0 = 0$. In this case, the solution is asymptotically

[15] In general, the eigenfunctions of a regular Sturm-Liouville equation satisfy $\int \mathrm{d}\varphi\Phi_n(\varphi)\Phi_m(\varphi)w(\varphi) = \delta_{nm}$

dominated by the smallest non-zero eigenvalue, Λ_1. After a long period of time then, we can write:

$$\rho_1(\varphi, t_0) \sim a_1 \tilde{\Phi}_1(\varphi) e^{-\Lambda_1 t_0}. \tag{4.141}$$

The auxiliary function $\Xi(\varphi, t)$ is then given by:

$$\Xi(\varphi, t) = \sum_n a_1 e^{-\Lambda_1 t_0} B_n \tilde{\Phi}_n(\varphi) e^{-\Lambda_n t}, \tag{4.142}$$

where we have extracted the factor $a_1 e^{-\Lambda_1 t_0}$ from the coefficient B_n for numerical convenience:

$$\begin{aligned} a_1 e^{-\Lambda_1 t_0} B_n &= \int \mathrm{d}\varphi_2 \Xi(\varphi_2, 0) e^{2\nu(\varphi_2)} \tilde{\Phi}_n(\varphi_2) \\ &= \int \mathrm{d}\varphi_2 \varphi_2 \rho_1(\varphi_2, t_0) e^{2\nu(\varphi_2)} \tilde{\Phi}_n(\varphi_2) \\ &= \int \mathrm{d}\varphi_2 \varphi_2 a_1 \tilde{\Phi}_1(\varphi_2) \tilde{\Phi}_n(\varphi_2) e^{2\nu(\varphi_2) - \Lambda_1 t_0} \\ &= a_1 e^{-\Lambda_1 t_0} \int \mathrm{d}\varphi \tilde{\Phi}_1(\varphi) \tilde{\Phi}_n(\varphi) \varphi e^{2\nu(\varphi)}. \end{aligned} \tag{4.143}$$

Thus:

$$B_n = \int \mathrm{d}\varphi \tilde{\Phi}_1(\varphi) \tilde{\Phi}_n(\varphi) \varphi e^{2\nu(\varphi)}. \tag{4.144}$$

With this computed, it is possible to compute the temporal correlation function:

$$G(t) = \int \mathrm{d}\varphi_1 \varphi_1 \Xi(\varphi_1, t) \tag{4.145}$$

$$= a_1 e^{-\Lambda_1 t_0} \int \mathrm{d}\varphi_1 \varphi_1 \sum_n B_n \tilde{\Phi}_n(\varphi_1) e^{-\Lambda_n t} \tag{4.146}$$

$$= a_1 e^{-\Lambda_1 t_0} \sum_n B_n C_n e^{-\Lambda_n t}, \tag{4.147}$$

where:

$$C_n \equiv \int \mathrm{d}\varphi_1 \varphi_1 \tilde{\Phi}_n(\varphi_1). \tag{4.148}$$

The B_n coefficient may be slightly problematic, as a_1, a coefficient from the initial condition on $\rho_1(\varphi, t)$ is needed. However, since the over-all scale set by $e^{-\Lambda_1 t_0}$ is also largely unknown, this isn't the most pressing difficulty. The issue here is that φ can roll to very large values because of the shape of the potential. The simplest example of a potential where Eq. (4.131) is infinite is when the potential is negative, for example, $V(\varphi) = -\frac{\lambda}{4}\varphi^4$. No static solution exists because the field just keeps moving to larger and larger values and never comes to rest. The entire solution decays, because the probability density distribution becomes stretched over an infinite range of φ (so eventually vanishes everywhere, even if the total integral remains 1).

For the general case, the expression is again more complicated. The derivation

of $G(r, t_1, t_2)$ in the static case relied on special properties of the static solution, Φ_0 which are not replicated here. Starting from Eq. (4.124), the conditional probability distribution now evolves as:

$$\Pi(\varphi_1(x_1, t_1)|\varphi_r(x_1, t_r)) = \sum_n a_n \tilde{\Phi}_n(\varphi_1) e^{-\Lambda_n(t_1 - t_r)}, \tag{4.149}$$

where a_n is determined using the orthogonality relation, Eq. (4.138)

$$a_n = \int \mathrm{d}\varphi_1 \delta(\varphi_1 - \varphi_r) \tilde{\Phi}_n(\varphi_1) e^{2\nu(\varphi_r)} = \tilde{\Phi}_n(\varphi_r) e^{2\nu(\varphi_r)}. \tag{4.150}$$

Thus, the general correlation function for $t_1, t_2 > t_r$ is given by:

$$\begin{aligned} G(r, t_1, t_2) &= \int \mathrm{d}\varphi_1 \mathrm{d}\varphi_2 \mathrm{d}\varphi_r \varphi_1 \varphi_2 \Pi(\varphi_1(x_1, t_1)|\varphi_r(x_1, t_r)) \Pi(\varphi_2(x_2, t_2)|\varphi_r(x_2, t_r)) a_1 e^{-\Lambda_1 t_r} \tilde{\Phi}_1(\varphi_r) \\ &= a_1 e^{-\Lambda_1 t_r} \int \mathrm{d}\varphi_1 \mathrm{d}\varphi_2 \mathrm{d}\varphi_r \varphi_1 \varphi_2 e^{4\nu(\varphi_r)} \times \\ &\times \sum_{n,m} \tilde{\Phi}_n(\varphi_r) \tilde{\Phi}_m(\varphi_r) \tilde{\Phi}_n(\varphi_1) \tilde{\Phi}_m(\varphi_2) \tilde{\Phi}_1(\varphi_r) e^{-\Lambda_n(t_1 - t_r)} e^{-\Lambda_m(t_2 - t_r)} \\ &= a_1 e^{-\Lambda_1 t_r} \sum_{n,m} B_{nm} C_n C_m e^{-\Lambda_n t_1} e^{-\Lambda_m t_2} e^{(\Lambda_n + \Lambda_m) t_r}, \end{aligned} \tag{4.151}$$

where C_n was defined in Eq. (4.148) and the set of coefficients B_{nm} are defined by:

$$B_{nm} \equiv \int \mathrm{d}\varphi_r \tilde{\Phi}_1(\varphi_r) \tilde{\Phi}_n(\varphi_r) \tilde{\Phi}_m(\varphi_r) e^{4\nu(\varphi_r)}. \tag{4.152}$$

It is prudent to check that this agrees with the single-point result in the limit as $r \to 0$. In that limit, set $t_r = t_0$ and $t_1 = t_r = t_0$, while $t_2 - t_1 = t \implies t_2 - t_r = t$. Thus,

$$G(0, t_0, t_0 + t) = a_1 e^{-\Lambda_1 t_0} \sum_{n,m} B_{nm} C_n C_m e^{-\Lambda_m t}, \tag{4.153}$$

but:

$$\sum_n B_{nm} C_n = \sum_n \int \mathrm{d}\varphi_r \tilde{\Phi}_1(\varphi_r) \tilde{\Phi}_n(\varphi_r) \tilde{\Phi}_m(\varphi_r) e^{4\nu(\varphi_r)} \int \mathrm{d}\varphi_1 \tilde{\Phi}_n(\varphi_1) \varphi_1. \tag{4.154}$$

Now, use Eq. (7.7) is appendix 7.1 to write:

$$\sum_n \tilde{\Phi}_n(\varphi_r) \tilde{\Phi}_n(\varphi_1) = e^{-2\nu(\varphi_r)} \delta(\varphi_r - \varphi_1), \tag{4.155}$$

giving:

$$\begin{aligned} \sum_n B_{nm} C_n &= \int \mathrm{d}\varphi_r \mathrm{d}\varphi_1 \tilde{\Phi}_1(\varphi_r) \tilde{\Phi}_m(\varphi_r) e^{2\nu(\varphi_r)} \varphi_1 \delta(\varphi_r - \varphi_1) \\ &= \int \mathrm{d}\varphi_r \tilde{\Phi}_1(\varphi_r) \tilde{\Phi}_m(\varphi_r) e^{2\nu(\varphi_r)} \varphi_r \equiv B_m. \end{aligned} \tag{4.156}$$

Thus,

$$G(0, t_0, t_0 + t) = a_1 e^{-\Lambda_1 t_0} \sum_m B_m C_m e^{-\Lambda_m t} \equiv G(t). \tag{4.157}$$

This confirms that we can recover the temporal correlation function from the more general one.

4.7 Inflationary Fluctuations and Electroweak Vacuum Stability

We now have the necessary machinery to analyse how inflationary fluctuations affect the stability of the Higgs vacuum. We want to know how the mean square expected field value, $\langle \bar{\phi}^2(t) \rangle$ evolves with time. To analyse this problem, consider the Fokker-Planck Eq. (4.88) for two points at equal times:

$$\frac{\partial \rho_2(\varphi_1, \varphi_2, t)}{\partial t} = \Gamma_{\varphi_1} \rho_2 + \Gamma_{\varphi_2} \rho_2 + \frac{H^3}{4\pi^2} \frac{\partial^2 \rho_2}{\partial \varphi_1 \partial \varphi_2}, \tag{4.158}$$

with Γ_φ defined as in Eq. (4.93). Note that we have approximated the sinc function as in Eq. (4.118), because points closer than $a(t)|x_1 - x_2| < \frac{1}{\varepsilon H}$ are assumed to be completely correlated (in fact, we will take the limit as $x_1 \to x_2$, where this becomes exact). Now, the two point correlation function is given by:

$$\langle \bar{\phi}(x_1, t) \bar{\phi}(x_2, t) \rangle = \int \mathrm{d}\varphi_1 \int \mathrm{d}\varphi_2 \varphi_1 \varphi_2 \rho_2(\varphi_1, \varphi_2, t). \tag{4.159}$$

Multiply by Eq. (4.158) by $\varphi_1 \varphi_2$ and integrate over φ_1, φ_2 to obtain:

$$\frac{\mathrm{d}\langle \bar{\phi}(x_1, t) \bar{\phi}(x_2, t) \rangle}{\mathrm{d}t} = \int \mathrm{d}\varphi_1 \mathrm{d}\varphi_2 \varphi_1 \varphi_2 \left[\Gamma_{\varphi_1} \rho_2 + \Gamma_{\varphi_2} \rho_2 + \frac{H^3}{4\pi^2} \frac{\partial^2 \rho_2}{\partial \varphi_1 \partial \varphi_2} \right]. \tag{4.160}$$

However:

$$\begin{aligned} \int \mathrm{d}\varphi_1 \mathrm{d}\varphi_2 \varphi_1 \varphi_2 \Gamma_{\varphi_1} \rho_2 &= \int \mathrm{d}\varphi_1 \mathrm{d}\varphi_1 \varphi_1 \varphi_2 \left[\frac{1}{3H} \frac{\partial}{\partial \varphi_1} \left(V'(\varphi_1) \rho_2 \right) + \frac{H^3}{8\pi^2} \frac{\partial^2 \rho_2}{\partial \varphi_1^2} \right] \\ &= - \int \mathrm{d}\varphi_1 \mathrm{d}\varphi_2 \varphi_2 \left[\frac{1}{3H} V'(\varphi_1) \rho_2 + \frac{H^3}{8\pi^2} \frac{\partial \rho_2}{\partial \varphi_1} \right]. \end{aligned} \tag{4.161}$$

The boundary terms vanish due to the boundary conditions on ρ_2 at $\varphi_1 \to \pm\infty$. We also find that

$$\int \mathrm{d}\varphi_1 \frac{\partial \rho_2}{\partial \varphi_1} = [\rho_2]_{\varphi_1 = -\infty}^{\varphi_1 = \infty} = 0, \tag{4.162}$$

by the same boundary conditions. Therefore:

$$\int \mathrm{d}\varphi_1 \mathrm{d}\varphi_1 \varphi_1 \varphi_2 \Gamma_{\varphi_1} \rho_2 = -\frac{1}{3H} \int \mathrm{d}\varphi_1 \mathrm{d}\varphi_2 V'(\varphi_1) \varphi_2 \rho_2 = -\frac{1}{3H} \langle V'(\bar{\phi}(x_1, t)) \bar{\phi}(x_2, t) \rangle. \tag{4.163}$$

The final term is the mixed derivative, however, this, it transpires, is considerably simpler to handle:

$$\int \mathrm{d}\varphi_1 \mathrm{d}\varphi_2 \varphi_1 \varphi_2 \frac{H^3}{4\pi^2} \frac{\partial^2 \rho_2}{\partial \varphi_1 \partial \varphi_2} = (-1)^2 \frac{H^3}{4\pi^2} \int \mathrm{d}\varphi_1 \mathrm{d}\varphi_2 \rho_2(\varphi_1, \varphi_2, t) = \frac{H^3}{4\pi^2}. \tag{4.164}$$

This follows again by integration by parts. Now, in the limit as $x_1 \to x_2$, the first and second terms on the RHS of Eq. (4.160) are identical under exchange of φ_1 and φ_2. Thus they add to give a factor of two and we obtain:

$$\frac{\mathrm{d}\langle \bar{\phi}^2(t) \rangle}{\mathrm{d}t} = -\frac{2}{3H} \langle \bar{\phi}(t) V'(\bar{\phi}(t)) \rangle + \frac{H^3}{4\pi^2}. \tag{4.165}$$

This is an extremely useful equation. For potentials like $\frac{1}{2}m^2\phi^2 + \frac{\lambda}{4!}\phi^4$, the expectation value $\langle \bar{\phi} V'(\bar{\phi}) \rangle$ is positive and the first term on the RHS acts to damp oscillations. The second term, however, tends to increase them with time. Nothing in our derivation prevents H being time dependent (except for the derivation of the Fokker-Planck equation where we took time derivatives of $a(t)\varepsilon H$, however, extra terms can be avoided by allowing the arbitrary ε parameter to be time dependent in such a way that $\varepsilon(t)H(t)$ is constant in time).

We see, therefore, that in an inflationary scenario, the expansion, characterised by H, causes the mean square of $\bar{\phi}$ to increase with time, creating larger and larger fluctuations (however, the first term will keep these from growing too much). Assuming that $\bar{\phi}$ starts near to 0, then for small t (until $\bar{\phi}$ is comparable to H) we have the solution:

$$\langle \bar{\phi}^2(t) \rangle = \frac{H^3 t}{4\pi^2} \tag{4.166}$$

This is diffusive behaviour. A standard deviation proportional to $\sqrt{t}$ is typical of Brownian motion (to which stochastic inflation is equivalent). Examining the first term - if the mass is light, so that $m \ll H$, we have $V'(\bar{\phi}) = m^2\bar{\phi} + \text{h.o.t.}$. This will not be of similar magnitude to the second term (and thus, the fluctuations will not stop growing) until $\bar{\phi} \sim H$.

Generally speaking then, inflationary fluctuations will tend to push $\bar{\phi}$ up to the scale of H. If H is large, then this may push $\bar{\phi}$ into the global minimum. So there are two questions that need to be answered - at what scale does the second minimum arise, if at all, and what is the scale of H? Our discussion in section 3 is not precise enough to answer the first question. However, this issue has been studied in detail, for example in [3] and [19], which we discussed in section 3.3. The central values of the top mass and Higgs mass seem to indicate an instability around $10^{10}\,\mathrm{GeV}$[2].

The value of the Hubble rate, H, is trickier to pin down. We have seen that H characterises the fluctuations in quantum fields during inflation. These fluctuations should in principle leave a trace in the cosmic microwave background. In particular, inflation will create fluctuations in the metric (a tensor field) as well as scalar fields like the Higgs field. These fluctuations take the form of

gravitational waves. It has been shown that the ratio, r, of tensor fluctuations to scalar fluctuations is directly determined by the inflationary energy scale, in other words, the Hubble constant $H = \sqrt{\frac{8\pi G_N V(\phi)}{3}}$. We follow the notation and definitions of [29], which gives the relationship between r and V as:

$$V(\phi)^{\frac{1}{4}} \sim \left(\frac{r}{0.01}\right)^{\frac{1}{4}} 10^{16}\,\text{GeV}. \tag{4.167}$$

To be more precise about this, the ratio r is defined by:

$$r \equiv \frac{\Delta_t^2(k)}{\Delta_s^2(k)} \tag{4.168}$$

Where $\Delta_t^2(k)$ and $\Delta_s^2(k)$ are the power spectra for tensor and scalar fluctuations respectively, derived from the two point correlation functions in momentum space. For example:

$$\langle \mathcal{R}_{\mathbf{k}} \mathcal{R}_{\mathbf{k}'} \rangle = (2\pi)^3 \delta^{(3)}(\mathbf{k} + \mathbf{k}') \frac{(2\pi^2)\Delta_s^2(k)}{k^3}, \tag{4.169}$$

where $\mathcal{R}$ characterises scalar perturbations[16]. The dependence on k here indicates that we are interested in H at the time when the scale k leaves the de Sitter horizon. Consequently, a measurement of r is all that is needed to measure H. However, to do this it is necessary to distinguish between fluctuations in the CMB related to tensor field, and those related to scalar fields. The polarisation of light from the CMB provides a way to do this.

The CMB is generated when the universe cools sufficiently that neutral atoms formed, and Thompson scattering of photons becomes insufficient to sustain photons in thermal equilibrium with matter. This is known as the time of 'last scattering'. However, in addition to fluctuations in the temperature, there are also fluctuations in the pattern of polarisation of scattered photons, since Thompson scattering tends to polarise light.

This means that the light of the CMB contains patterns of polarisation. These patterns can be decomposed into two orthogonal patterns, known as E-modes and B-modes, in analogy to electric and magnetic fields, which are derived from the gradient and curl of a vector potential, respectively. To understand where these come from, we need to use some machinery for the description of polarisation, in particular, Stokes parameters. These are described in appendix 7.3. The parameters I and V are not the most relevant to the CMB, since I describes only the intensity (when we are more interested in the pattern, not its overall scale) and V described circular polarisation. However, Thompson scattering is an electromagnetic process which respects parity, so there is no way of generating a net circular polarisation[30]. The two relevant parameters are therefore Q and U. These correspond to linear polarisation along axis rotated with respect

[16]Note that these are not just from scalar fields, but from scalar degrees of freedom in the decomposition of the metric

to each other by $\frac{\pi}{4}$. However, these axis are arbitrary. Examining figure 7.2 of appendix 7.3 one can see that a rotation of θ must transform Q and U as:

$$\begin{aligned} Q' =& Q\cos 2\theta + U\sin 2\theta \\ U' =& -Q\sin 2\theta + U\cos 2\theta. \end{aligned} \tag{4.170}$$

The factor of 2 is due to the fact that a rotation of $\frac{\pi}{4}$ should swap Q and U (up to a sign), rather than a factor of $\frac{\pi}{2}$. Note that this transformation rule is the same as a that for the second rank tensor representation of $SO(2)$, which in matrix notation transforms as:

$$\begin{pmatrix} U' & Q' \\ Q' & -U' \end{pmatrix} = \begin{pmatrix} \cos\theta & -\sin\theta \\ \sin\theta & \cos\theta \end{pmatrix} \begin{pmatrix} U & Q \\ Q & -U \end{pmatrix} \begin{pmatrix} \cos\theta & \sin\theta \\ -\sin\theta & \cos\theta \end{pmatrix}. \tag{4.171}$$

Thus, the relevant polarisation information consists of a symmetric, traceless second rank tensor field over a 2-sphere consisting of the surface of last scattering. Now, a scalar field (for example, the temperature distribution) on a 2-sphere can be decomposed into spherical harmonics. The same is true of tensor fields. This was studied by [30].In analogy to the fact that any vector field can be decomposed into a gradient and a curl part, this tensor field can be decomposed into E-modes and B-modes. The technical details require a study of the differential geometry of a 2-sphere, given in [30], the details of which are beyond the scope of this report. However, the essential physics here is that B mode polarisation fields can only be produced by tensor fluctuations (such as gravitational waves), and not scalar fluctuations (such as density or temperature fluctuation). Consequently, if the B-mode fluctuations can be extracted, they give a measure of r, and thus the energy scale of inflation.
This was done recently by BICEP2 collaboration[1], who measured $r = 0.20^{+0.07}_{-0.05}$. This result requires confirmation, however, and there is still active discussion regarding the degree to which dust in space may have impacted the results. In principle, however, this measurement (if confirmed) implies that the inflationary energy scale is around the GUT scale, which coupled with central values of the Higgs bosons and top quark masses implies that inflationary fluctuations should have pushed the universe into the new minimum with a very large probability[2].

Chapter 5

Numerical Study - The Harmonic Oscillator Method

In this section, we discuss solutions to the Fokker-Planck equation in various quadratic and quartic potentials, with particular focus on numerical methods. We present numerical results for a method of solving the Sturm-Lioville problem associated to the Fokker-Planck equation, by expressing the resulting ordinary differential equation in a harmonic oscillator basis.

5.1 Solving the Fokker-Planck Equation

The Fokker-Planck equation:

$$\frac{\partial \rho(t,\varphi)}{\partial t} = \frac{1}{3H}\frac{\partial}{\partial \varphi}(V'(\varphi)\rho(t,\varphi)) + \frac{H^3}{8\pi^2}\frac{\partial^2 \rho(t,\varphi)}{\partial \varphi^2}, \tag{5.1}$$

can in principle be solved explicitly since it is a separable equation. In section 4.5 We found the Sturm-Liouville problem associated to the Fokker-Planck equation in the equilibrium case to be:

$$\frac{1}{2}\left(-\frac{\mathrm{d}}{\mathrm{d}\varphi} + \nu'(\varphi)\right)\left(-\frac{\mathrm{d}}{\mathrm{d}\varphi} + \nu'(\varphi)\right)^{\dagger}\Phi_n = \frac{4\pi^2\Lambda_n}{H^3}\Phi_n, \tag{5.2}$$

(Recall that $\frac{\mathrm{d}}{\mathrm{d}\varphi}^{\dagger} = -\frac{\mathrm{d}}{\mathrm{d}\varphi}$, which follows from the product rule). This equation is equivalent to the Schroedinger equation for the effective potential $W(\varphi) = \frac{1}{2}(\nu'(\varphi)^2 - \nu''(\varphi))$ (its physical interpretation is different, however, since $\rho(t,\varphi)$ is a probability distribution, not a wave-function). Once the Φ_n are known, the

general solution can be written:

$$\rho(t,\varphi) = \exp\left(-\frac{4\pi^2 V(\varphi)}{3H^4}\right)\sum_{n=0}^{\infty} a_n \Phi_n e^{-\Lambda_n (t-t_0)}, \tag{5.3}$$

where the coefficients a_n can be determined by exploiting the orthonormality of the Φ_n and using the initial state of ρ:

$$a_n = \int \mathrm{d}\varphi \exp\left(\frac{4\pi^2 V(\varphi)}{3H^4}\right)\rho(t_0,\varphi)\Phi_n(\varphi). \tag{5.4}$$

While it would be possible to solve the Fokker-Planck equation simply by discretising Eq. (5.1), another approach is to solve Eq. (5.2) for the eigenfunctions Φ_n and eigenvalues Λ_n, and evaluate the coefficients using Eq. (5.4). This reduces a partial differential equation problem to an eigenvalue problem for an ordinary differential equation. There are two main numerical challenges here:

- Solving Eq. (5.2)
- Evaluating the coefficients a_n (a numerical integration problem, as it is unlikely that a closed form solution can be found).

One approach to the first problem is to express the 'matrix' left hand side of Eq. (5.2) in a different basis. A convenient basis to pick is the set of harmonic oscillator basis functions. This method is described in [31]. See also section 5.2. Using the definition $p = -i\frac{\mathrm{d}}{\mathrm{d}\varphi}$ one can write:

$$\left(\frac{p^2}{2} + W(\varphi)\right)\Phi_n = E_n \Phi_n, \tag{5.5}$$

where we consider $\hbar = 1$ and $m = 1$. Now, in a basis of harmonic oscillator function, it is easy to evaluate both φ and p:

$$\varphi = \frac{1}{\sqrt{2\omega}}(\hat{a} + \hat{a}^\dagger), \tag{5.6}$$

$$p = i\sqrt{\frac{\omega}{2}}(\hat{a}^\dagger - \hat{a}). \tag{5.7}$$

Using $\hat{a}\,|n\rangle = \sqrt{n}\,|n-1\rangle$ and $\hat{a}^\dagger\,|n\rangle = \sqrt{n+1}\,|n+1\rangle$, the matrix elements are:

$$\begin{aligned}
\varphi_{nm} &= \langle n|\,\varphi\,|m\rangle = \frac{1}{\sqrt{2\omega}}(\langle n|\sqrt{m}\,|m-1\rangle + \langle n|\sqrt{m+1}\,|m+1\rangle) \\
&= \frac{1}{\sqrt{2\omega}}(\sqrt{m}\delta_{n,m-1} + \sqrt{m+1}\delta_{n,m+1}), \\
p_{nm} &= i\sqrt{\frac{\omega}{2}}(\sqrt{m+1}\delta_{n,m+1} - \sqrt{m}\delta_{n,m-1}).
\end{aligned}$$

In matrix form, these are:

$$p = i\sqrt{\frac{\omega}{2}}\begin{pmatrix} 0 & -\sqrt{1} & 0 & 0 & \dots \\ \sqrt{1} & 0 & -\sqrt{2} & 0 & \dots \\ 0 & \sqrt{2} & 0 & \ddots & 0 \\ 0 & 0 & \ddots & \ddots & \vdots \\ \vdots & \vdots & \dots & \ddots & \ddots \end{pmatrix}, \varphi = \sqrt{\frac{1}{2\omega}}\begin{pmatrix} 0 & \sqrt{1} & 0 & 0 & \dots \\ \sqrt{1} & 0 & \sqrt{2} & 0 & \dots \\ 0 & \sqrt{2} & 0 & \ddots & 0 \\ 0 & 0 & \ddots & \ddots & \vdots \\ \vdots & \vdots & \dots & \ddots & \ddots \end{pmatrix}. \tag{5.8}$$

The size of these matrices is infinite, since there are an infinite number of harmonic oscillator basis functions. However, if we are mostly interested in the low energy states of some potential, then truncating the matrices to some large N provides a good approximation for bound states, as these will not differ too much from the low energy states of the harmonic oscillator. Choosing some large N, the Hamiltonian can thus be written as an $N \times N$ matrix and diagonalised to find the eigenfunctions and eigenvalues. The eigenfunctions will be expressed in the form of a discrete vector, however, the components of this vector will be the approximate components of the decomposition of the eigenfunction Φ_n into harmonic oscillator basis states. i.e.,

$$\Phi_n = \sum_m c_{nm}\psi_m, \tag{5.9}$$

where:

$$\psi_m(\varphi) = \frac{1}{\sqrt{2^m m!}}\left(\frac{\omega}{\pi}\right)^{\frac{1}{4}} H_m(\sqrt{\omega}\varphi)\exp\left(-\frac{\omega}{2}\varphi^2\right). \tag{5.10}$$

H_m being the m Hermite polynomial. The coefficients c_{nm} are given by the m^{th} component of the n^{th} eigenvector of Eq. (5.5). These are estimated by truncating the matrix representation of Eq. (5.5) at size $N \times N$, and numerically evaluating the eigenvalues. We chose to use the MATLAB 'Eig' function, to diagonalise the $N \times N$ matrices, choosing $N = 700$ for reasons that will be discussed below.

In fact, computing the eigenvectors and eigenfunctions of the large matrix approximation to the Hamiltonian is not the main numerical challenge of this method. The limiting factor is the ability to (numerically) evaluate the integrals like Eq. (5.4), since for large n, the harmonic oscillator functions ψ_n become highly oscillatory. Another related problem is that directly evaluating Eq. (5.10) is difficult using numbers stored under IEEE Standard 754. It will inevitably result in products of numbers which are very large or very small, even if the result is not (for example - choosing $n = 700$ would require evaluating $2^{700} \times 700!$ which is of order $10^{1.9\times10^3}$, significantly higher than can be stored by most double precision systems). One way around this problem is to use logarithms, but in this case we were able to devise a better approach, exploiting the properties of Hermite polynomials. One of these is that they obey[32]:

$$H_n(x) = 2xH_{n-1}(x) - 2(n-1)H_{n-2}(x). \tag{5.11}$$

It is then convenient to define a modified Hermite polynomial by combining the n-dependent part of Eq. (5.10) as:

$$\tilde{H}_n(x) = \frac{1}{\sqrt{2^n n!}} H_n(x). \tag{5.12}$$

These modified polynomials can easily be shown to obey the recursion relation:

$$\tilde{H}_n(x) = x\sqrt{\frac{2}{n}}\tilde{H}_{n-1}(x) - \sqrt{\frac{n-1}{n}}\tilde{H}_{n-2}(x). \tag{5.13}$$

The advantage of this is that the increasingly large coefficients of the Hermite polynomials to some degree cancel out the increasingly large factors from the $\frac{1}{\sqrt{2^n n!}}$, with each step not involving numbers too large to be handled. Eventually, however, even this approach will suffer from numerical errors. To test the range over which this approach is viable, it is useful to compute, numerically, the integral:

$$I = \int_{-\infty}^{\infty} |\psi_n(x)|^2 \mathrm{d}x. \tag{5.14}$$

For the normalised simple harmonic oscillator states, Eq. (5.10), this should always give $I = 1$, so any numerical errors will most readily show up in a deviation from this. The Hermite polynomials were generated using the recursion relation, Eq. (5.13), in MATLAB, and the MATLAB numerical integration function 'integral' used to compute I. The results for the recursive method are compared to the logarithm method in figures 5.1 and 5.2 respectively.

As can be seen, the recursive method is reliable out to $n \sim 700$ while the logarithmic approach fails much earlier. This constrains the maximum size of the matrices that can be used to give an approximation for the operators p and φ. Cutting off the matrices this way, however, can lead to inaccuracies in the computed eigenvalues and eigenfunctions. A way to test for the presence of inaccuracies is to compute the coefficients c_{nm} in Eq. (5.9) (which are just the eigenvectors of Eq. (5.5) - in other words, c_{nm} is the matrix diagonalising this 'Hamiltonian'). For a given n, we then plot them against m. Generically, this will give rise to a discrete sequence and physically speaking, so long as the energy levels of the potential under consideration are similar to those of the harmonic oscillator (whose energy scale can be set using the frequency parameter, ω), this sequence will converge to zero for large n. The physical reason for this is that any dependence on large n leads to very high gradients, associated to high momentum of the wave-function, and thus high energy, so this is only likely to occur if the scale of the harmonic oscillator is poorly chosen for the potential of interest. Examples of this are given in the next few sections. If the sequence c_{nm} for a given n is shown to converge to zero, this means that the behaviour of the eigenfunction has been accurately captured using low n harmonic oscillator states only and these is no contribution from high n states, so neglecting these is justified. This is completely analogous to truncating a Fourier transform to small frequencies for functions without large frequency components.

Figure 5.1: Integral of the modulus square of the generated harmonic oscillator basis function, with $\omega = 0.005$H, against basis label, n, when using the recursive method. The basis functions remain accurate out to about $n = 700$. Note that the failure of the numerical integration can also be caused by the highly oscillatory nature of the basis functions for large n, but as we need to compute numerical integrals using these basis functions, this graph allows us to select a range which is reliable.

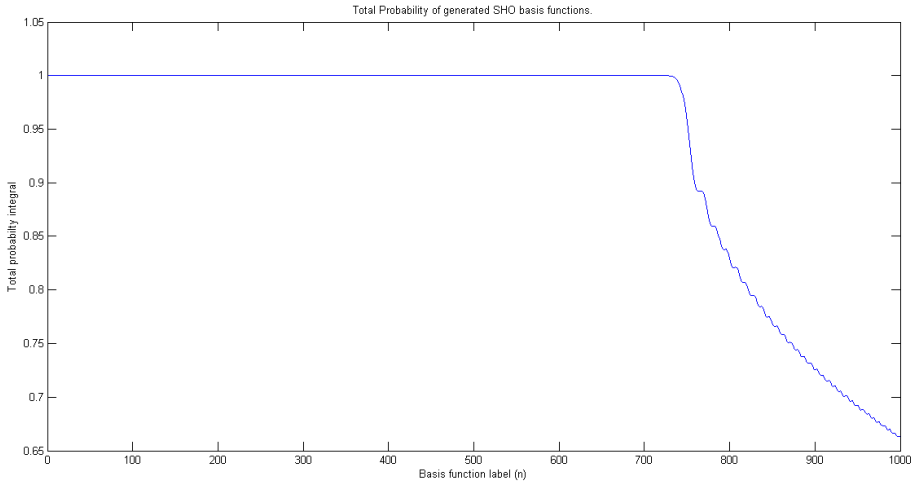

This approach will work for computing the lowest eigenfunctions of a given potential. For our purposes, this is usually all that is necessary because Eq. (5.3) indicates that the eigenfunctions with larger eigenvalues, Λ_n, decay very quickly compared to the smallest eigenvalues. We note that Eq. (5.2) is a Sturm-Liouville problem, so the eigenvalues Λ_n are ordered (and thus non-degenerate). This problem is thus readily solved by a method most reliable for the smallest eigenvalues, as this method is.

5.2 Solving the Schroedinger Equation in a Harmonic Oscillator Basis

The solution to the Schroedinger equation in a harmonic potential can be found in any text on quantum mechanics. The first part of this section will simply review these properties for convenience. The time independent Schroedinger equation for a harmonic oscillator of frequency ω and $m = 1$ is:

$$-\frac{1}{2}\frac{\mathrm{d}^2\Psi_n}{\mathrm{d}x^2} + \frac{1}{2}\omega^2 x^2 \Psi_n = E_n \Psi_n. \tag{5.15}$$

Figure 5.2: Integral of the modulus square of the generated harmonic oscillator basis function, with $\omega = 0.005\,\mathrm{H}$, against basis label, n, when using logarithms to reduce floating point number size over-flow. The method fails at around $n = 60$. The total numerical integral quickly becomes very large and the fact that this happens much sooner than the recursive method demonstrates that this is due to the computation of the basis functions, not the oscillatory nature of the integrals.

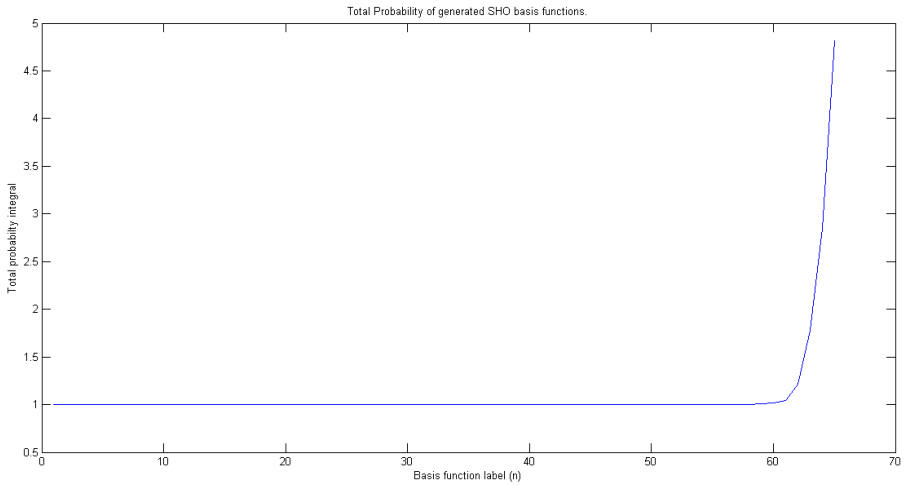

This can be solved analytically, with the eigenfunctions:

$$\Psi_n(x) = \frac{1}{\sqrt{2^n n!}} \left(\frac{\omega}{\pi}\right)^{\frac{1}{4}} e^{-\frac{\omega}{2}x^2} H_n(\sqrt{\omega}x), \tag{5.16}$$

where H_n is a Hermite polynomial. These polynomials can be defined via the recursion relation:

$$H_{n+1}(x) = 2xH_n(x) - 2nH_{n-1}(x), \tag{5.17}$$

where $H_0 = 1$ and $H_1 = 2x$ are the first pair of polynomials. The eigenvalues are given by:

$$E_n = \left(n + \frac{1}{2}\right)\omega \tag{5.18}$$

An important property of the functions $\Psi_n(x)$ is that they form a complete basis set for the vector space of square integrable functions. This means that any square integrable function, $f(x)$ can be written in the form:

$$f(x) = \sum_n c_n \Psi_n(x). \tag{5.19}$$

In addition, these states are orthogonal and normalised:

$$\int_{-\infty}^{\infty} \mathrm{d}x \Psi_n(x)\Psi_m(x) = \delta_{nm}. \tag{5.20}$$

Thus, the coefficients c_n are easily computed:

$$c_n = \int_{-\infty}^{\infty} \mathrm{d}x \Psi_n(x) f(x). \tag{5.21}$$

Another useful property of these functions is that we can express the position and momentum operators in terms of ladder operators:

$$\hat{x} = \sqrt{\frac{1}{2\omega}}(\hat{a} + \hat{a}^\dagger), \tag{5.22}$$

$$\hat{p} = i\sqrt{\frac{\omega}{2}}(\hat{a}^\dagger - \hat{a}). \tag{5.23}$$

If $|n\rangle$ represents the Hilbert space vector for which $\Psi_n(x) \equiv \langle x|n\rangle$, then the ladder operators satisfy:

$$\hat{a}^\dagger |n\rangle = \sqrt{n+1}\,|n+1\rangle\,, \tag{5.24}$$

$$\hat{a}\,|n\rangle = \sqrt{n}\,|n-1\rangle\,. \tag{5.25}$$

The factors $\sqrt{n+1}$ and $\sqrt{n}$ being chosen to ensure the states remain normalised.

5.2.1 Expressing Differential Equations in a Harmonic Oscillator basis

Now, if we choose $|n\rangle$ to be the basis for our Hilbert space for square integrable functions, it is clear that the position and momentum operators can both be written in terms of the matrix elements:

$$\langle n|\,\hat{x}\,|m\rangle = \sqrt{\frac{1}{2\omega}}(\sqrt{m}\delta_{n,m-1} + \sqrt{m+1}\delta_{n,m+1}) \tag{5.26}$$

$$\langle n|\,\hat{p}\,|m\rangle = i\sqrt{\frac{\omega}{2}}(\sqrt{m+1}\delta_{n,m+1} - \sqrt{m}\delta_{n,m-1}) \tag{5.27}$$

These can be seen in matrix form in equation 5.8. Next, it is useful to observe that a derivative with respect to x can be written:

$$\frac{\mathrm{d}}{\mathrm{d}x} = i\hat{p} \tag{5.28}$$

Thus, a generic Schroedinger equation can be written:

$$\frac{\hat{p}^2}{2}\Phi_n + V(\hat{x})\Phi_n = E_n\Phi_n \tag{5.29}$$

The advantage of using a simple harmonic oscillator basis is that we can truncate the (infinite) set Ψ_n at some large N, to give an $N \times N$ matrix approximation of the Schroedinger equation:

$$H_{N\times N}\Phi_n = E_n\Phi_n \tag{5.30}$$

Now, if the Φ_n we are interested in do not differ much from Ψ_n, which will often be the case for polynomial potentials, then for the 'infinite matrix' form of H in the harmonic basis, the eigenvectors Φ_n will have their non-zero components mostly confined to the first N rows, with the rest being approximately zero. Schematically, the eigenvalue equation will look like:

$$\begin{pmatrix} H_{N\times N} & (\text{ infinite piece }) \\ (\text{ infinite piece }) & (\text{ infinite piece }) \end{pmatrix} \begin{pmatrix} \Phi_{n,N} \\ \sim 0 \end{pmatrix} = E_n \begin{pmatrix} \Phi_{nN} \\ \sim 0 \end{pmatrix} \tag{5.31}$$

Where Φ_{nN} is an N dimensional vector. But this implies that the relation $H_{N\times N}\Phi_{nN} = E_n\Phi_{nN}$ is approximately true, so long as the majority of the non-zero components of the infinite Φ_n are found among the first N components. This will most often be the case for the lowest eigenfunctions of a given Hamiltonian. It should also be noted that using a harmonic oscillator basis for H assumes that the boundary conditions are chosen so that the wave functions vanishes at $\pm\infty$. For most equations that we wish to solve, this will be the case. Once the eigenvectors of $H_{N\times N}$ are found, it is then clear that they actually give the coefficients c_{nm} in:

$$\Phi_n(x) = \sum_m c_{nm}\Psi_m(x) \tag{5.32}$$

Because

$$|\Phi_{nN}\rangle = \begin{pmatrix} c_{n1} \\ c_{n2} \\ \vdots \\ c_{nN} \end{pmatrix} = \sum_{m=1}^{N} c_{nm}\,|\Psi_m\rangle \implies \langle x|\Phi_n\rangle \equiv \Phi_n(x) = \sum_{m=1}^{N} c_{nm}\Psi_m(x) \tag{5.33}$$

Thus, we can clearly see that the truncation gives a good approximation if the eigenfunctions have most of their non-zero c_{nm} in the first N components.
Another observation is that this method will be exact in the case of a harmonic potential, because in a harmonic oscillator basis, $H = \frac{\hat{p}^2}{2} + \frac{1}{2}\omega^2\hat{x}^2$ is by definition diagonal. Thus, the eigenvectors will be $\begin{pmatrix} 1 \\ 0 \\ 0 \\ \vdots \end{pmatrix}, \begin{pmatrix} 0 \\ 1 \\ 0 \\ \vdots \end{pmatrix} \ldots$ so $\Phi_n(x) = \Psi_n(x)$ as expected, with *no numerical error*.

5.3 Massless Theory: $V = \frac{\lambda}{4}\phi^4$

One of the simplest scalar theories that we can test is the interacting, massless field with Lagrangian:

$$\mathcal{L} = \frac{1}{2}\nabla_\mu\varphi\nabla^\mu\varphi - \frac{\lambda}{4}\varphi^4. \tag{5.34}$$

We use a normalisation of $\frac{1}{4}$ here for the interaction term, rather than the more field-theoretically convenient $\frac{1}{4!}$ for better comparison with the Higgs mechanism, in which we are ultimately interested. The potential here is:

$$V(\varphi) = \frac{\lambda}{4}\varphi^4, \tag{5.35}$$

so the solution to the Fokker-Planck equation can be written:

$$\rho(t,\varphi) = \exp\left(-\frac{\pi^2\varphi^4}{3H^4}\right)\sum_{n=0}^{\infty} a_n\Phi_n e^{-\Lambda_n(t-t_0)}. \tag{5.36}$$

Φ_n and Λ_n are determined from the solution to:

$$-\frac{1}{2}\frac{\mathrm{d}^2\Phi_n}{\mathrm{d}\varphi^2} + \frac{1}{2}\left(\left(\frac{4\pi^2\varphi^3}{3H^4}\right)^2 - \frac{4\pi^2\varphi^2}{H^4}\right)\Phi_n = \frac{4\pi^2\Lambda_n}{H^3}\Phi_n. \tag{5.37}$$

However, the field φ is not dimensionless. To process this numerically, and following Starobinsky and Yokoyama [28], it is convenient to define the dimensionless field:

$$\tilde{\varphi} = \left(\frac{8\pi^2\lambda}{3}\right)^{\frac{1}{4}}\frac{\varphi}{H}. \tag{5.38}$$

Note that in general, if the field is re-defined as $\tilde{\varphi} = Q\varphi$ then the probability densities must scale in the opposite direction: $\tilde{\rho}(t,\tilde{\varphi}) = Q^{-1}\rho(t,\varphi(\tilde{\varphi}))$. This scaling is actually carried by the wave-function Φ_n and coefficient a_n, so these too must-rescale. In fact, from the definition of a_n it is easy to see that it must scale exactly the same way as Φ_n:

$$\tilde{a}_n = \int \mathrm{d}\tilde{\varphi}\tilde{\rho}(t,\tilde{\varphi})e^{\tilde{\nu}(\tilde{\varphi})}\tilde{\Phi}_n(\tilde{\varphi}). \tag{5.39}$$

Thus if $\tilde{\Phi}_n(\tilde{\varphi}) = k\Phi_n(\varphi(\tilde{\varphi}))$ then $\tilde{a}_n = ka_n$. In this case then, to obtain the correct probability density, obeying $\tilde{\rho} = Q^{-1}\rho$ then it is necessary that $\tilde{\Phi}_n = Q^{-\frac{1}{2}}\Phi_n$[1]. Substituting this re-scaling into Eq. (5.37) gives rise to:

$$-\frac{1}{2}\frac{\mathrm{d}^2\tilde{\Phi}_n}{\mathrm{d}\tilde{\varphi}^2} + (\frac{1}{8}\tilde{\varphi}^6 - \frac{3}{4}\tilde{\varphi}^2)\tilde{\Phi}_n = \frac{\Lambda_n}{2H}\left(\frac{24\pi^2}{\lambda}\right)^{\frac{1}{2}}\tilde{\Phi}_n. \tag{5.40}$$

The left hand side is in a dimensionless form that is much easier to deal with computationally. $\tilde{\varphi} \sim 1$ roughly corresponds to a field of the energy scale of H (but not exactly, depending on the interaction strength, λ). Doing this eliminates the unknown constant λ, and so the dependence of the eigenvalues

[1] This should be no surprise, since the solutions are those of the Schroedinger equation and should thus have dimensions of the square root of the probability density. Another way to look at this is to remember that Φ_n obeys $\int \mathrm{d}\varphi\Phi_n(\varphi)^*\Phi_m(\varphi) = \delta_{nm}$, so if we re-scale φ by Q, Φ_n has to re-scale by $Q^{-\frac{1}{2}}$ in order to maintain the normalisation when integrating over $\tilde{\varphi}$ instead.

Λ_n on λ is known explicitly if the eigenvalues of this Sturm-Liouville problem can be determined. In particular, they are:

$$\Lambda_n = 2H \left(\frac{\lambda}{24\pi^2} \right)^{\frac{1}{2}} E_n, \tag{5.41}$$

where the constants E_n must be determined numerically, but do not depend on λ. Numerically solving this problem using the method described in section 5.1 is plausible. We computed the eigenvectors of Eq. (5.40), and these were checked by plotting the sequences c_{nm} as discussed in the last section. For the example of $\omega = \mathrm{H}$, see figures 5.3 and 5.4.

5.3.1 Correlation Functions

In section 4.6 it we found an expression for the generic correlation function. For our case, this is easy to compute:

$$G(t) = N \sum_n A_n^2 e^{-\Lambda_n t}, \tag{5.42}$$

where:

$$A_n = N^{-1} \int \mathrm{d}\varphi_2 e^{-\nu(\varphi_2)} \varphi_2 \Phi_n(\varphi_2). \tag{5.43}$$

Using the harmonic oscillator basis, the eigenvalues Λ_n and their associated eigenfunctions, $\Phi_n(\varphi)$ were computed. The eigenfunctions, Φ_n were evaluated numerically by means of the coefficient sequences, c_{nm} (see figures 5.3 and 5.4 for example) and the harmonic oscillator expansion:

$$\Phi_n(\varphi) = \sum_m c_{nm} \psi_m(\varphi). \tag{5.44}$$

The sequence c_{nm} thus entirely characterises Φ_n. Only Φ_n out to $n \sim 80$ were considered, since beyond this the eigenfunctions depend on ψ_m higher than $m = 700$, which was the highest harmonic oscillator basis function computed (see figure 5.4). For the purposes of computing A_n, however, this was more than enough, as figure 5.6 demonstrates. These coefficients were computed using the standard MATLAB numerical integration routine. Consequently, the correlation function for a massless ϕ^4 theory in de Sitter Space was computed. First a note on units: re-scaling φ as per Eq. (5.38) also changes $g(t) = \langle \varphi(t) \varphi(t) \rangle$, so that the non-dimensionless correlation function acquires a factor of:

$$H^2 \sqrt{\frac{3}{8\pi^2 \lambda}}. \tag{5.45}$$

It is also convenient for numerical computations to use a dimensionless time. Starobinsky and Yokoyama use[28]:

$$\tau = Ht \sqrt{\frac{\lambda}{24\pi^2}}, \tag{5.46}$$

Figure 5.3: Coefficient sequences, c_{nm}, for $n = 5$ and $n = 50$ (note that like the simple harmonic oscillator, it is convenient to start at n = 0), for a harmonic oscillator basis using $\omega = \mathrm{H}$.

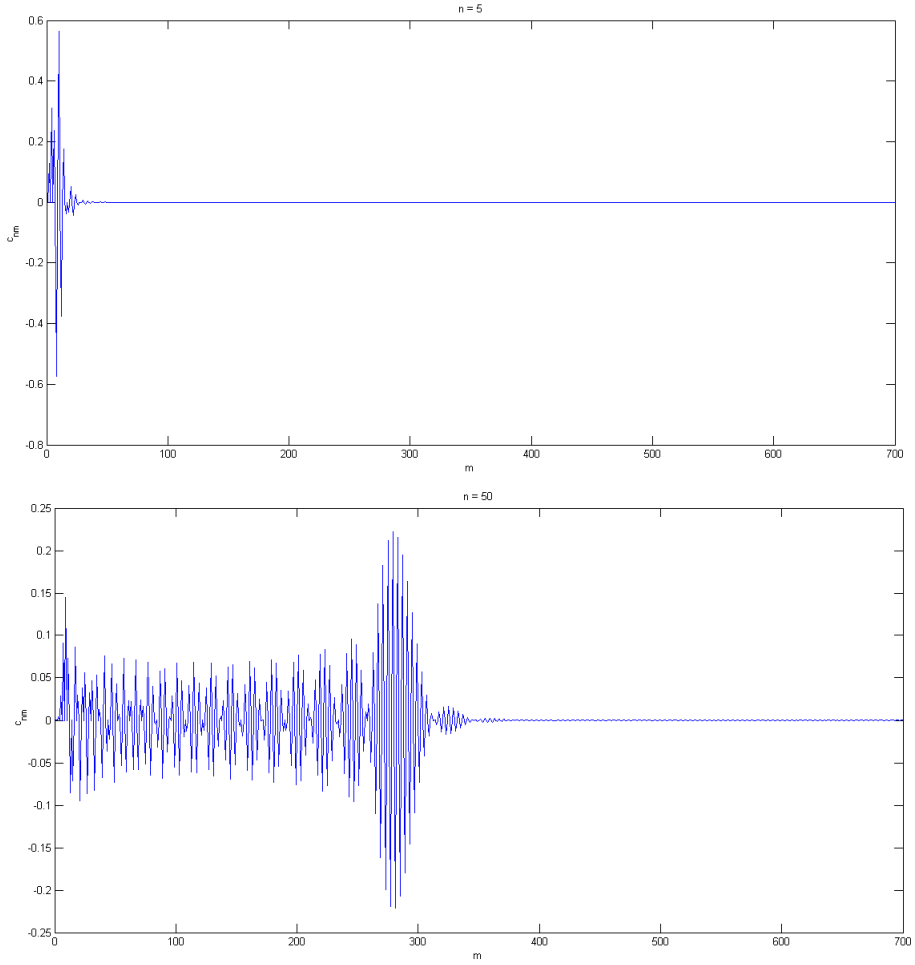

Figure 5.4: Coefficient sequences, c_{nm} for $n = 80$ and $n = 100$. These indicate, for example, that the computed eigenfunctions and eigenvalues are accurate out to around $n \sim 80$. The $n = 100$ case, however, does not appear to converge within this range so is unlikely to be an accurate representation of the eigenfunction.

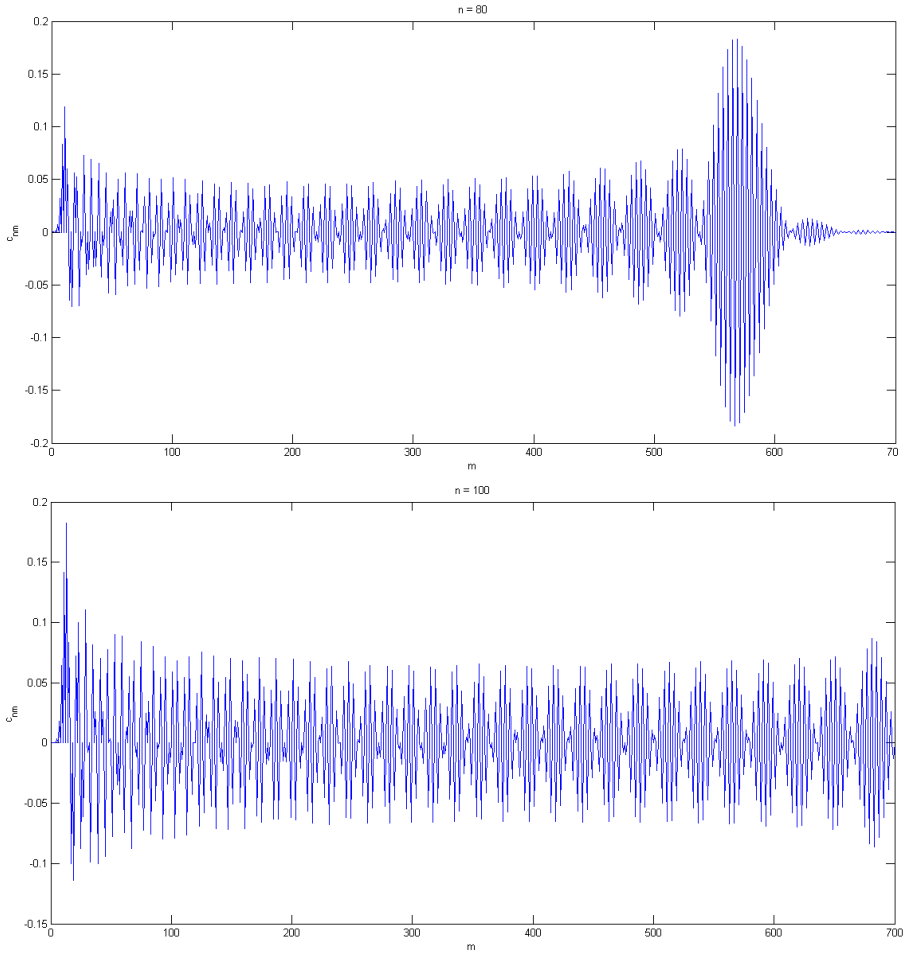

Label, n	**Raw Eigenvalue,** E_n	**Label,** n	**Raw Eigenvalue,** E_n
0	2.9363e-10	**10**	25.307
1	0.6843	**11**	29.1999
2	2.2269	**12**	33.2739
3	4.1298	**13**	37.5213
4	6.379	**14**	41.9353
5	8.9289	**15**	46.5098
6	11.7472	**16**	51.2393
7	14.8107	**17**	56.119
8	18.1012	**18**	61.1444
9	21.604	**19**	66.3113

Figure 5.5: First twenty raw eigenvalues, E_n for equation 5.40, where the physical eigenvalues Λ_n are computed via equation 5.41. Note that Λ_0 is *analytically* known to be zero, which is consistent with the very low value found numerically.

which is equivalent to choosing $\sqrt{(\frac{24\pi^2}{H^2\lambda})}$ as a unit of time. Taking these dimensions into account, the correlation function can be computed - see figure 5.7.

$$G(t) = H^2\sqrt{\frac{3}{8\pi^2\lambda}}N\sum_n A_n^2 e^{-2E_n\frac{t}{\sqrt{\frac{24\pi^2}{H^2\lambda}}}}. \tag{5.47}$$

In quantum field theory, however, we are usually more interested in the equal-time correlator at different points. This is also more of interest when studying the CMB since we are looking at fluctuations a sphere all created at the same point in time. Recall Eq. (4.130) which said that for potentials possessing an equilibrium solution, we have:

$$G(r, t_1, t_2) = G\left(t_1 + t_2 + \frac{2}{H}\ln(ra_0H)\right). \tag{5.48}$$

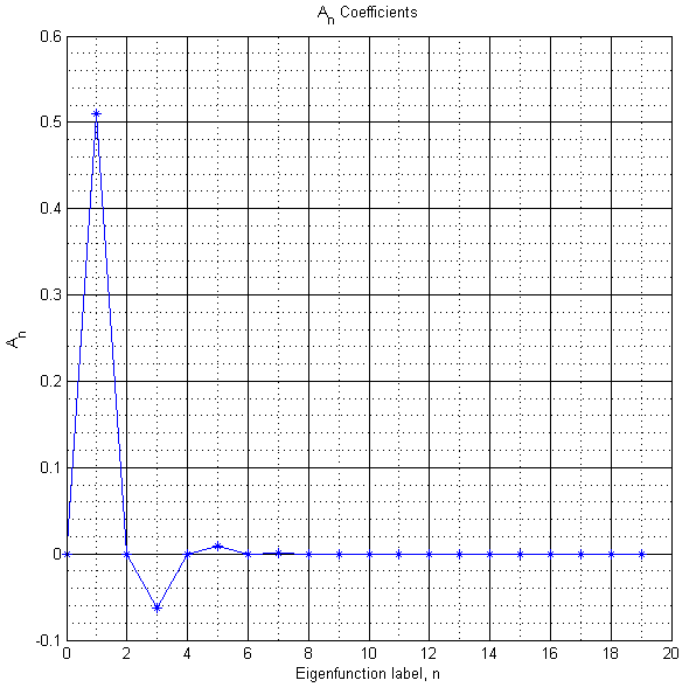

Figure 5.6: Correlation function coefficients as a function of quartic oscillator basis label. The correlation function is dominated by the smallest non-zero eigenvalue, Λ_1. This function decays rapidly with n, so the approach provides a very good numerical approximation.

Where $r = |\mathbf{x}_1 - \mathbf{x_2}|$. For equal times, we can consider $t_1 = t_2 = t$. Thus:

$$\begin{aligned}
G(r,t,t) =& H^2\sqrt{\frac{3}{8\pi^2\lambda}}N\sum_n A_n^2 \exp\left(-2\frac{E_n}{\sqrt{\frac{24\pi^2}{H^2\lambda}}}\left[2t+\frac{2}{H}\ln(ra_0H)\right]\right)\\
=& H^2\sqrt{\frac{3}{8\pi^2\lambda}}N\sum_n A_n^2 \exp\left(-\frac{4E_nt}{\sqrt{\frac{24\pi^2}{H^2\lambda}}}\right)(R_0H)^{-\frac{4E_n}{H\sqrt{\frac{24\pi^2}{H^2\lambda}}}}\\
=& H^2\sqrt{\frac{3}{8\pi^2\lambda}}N\sum_n A_n^2 \left[R_0He^{Ht}\right]^{-\frac{4E_n}{H\sqrt{\frac{24\pi^2}{H^2\lambda}}}}\\
=& H^2\sqrt{\frac{3}{8\pi^2\lambda}}N\sum_n A_n^2 \left[RH\right]^{-2E_n\sqrt{\frac{\lambda}{6\pi^2}}},
\end{aligned} \tag{5.49}$$

where $R_0 = a_0|\mathbf{x_1} - \mathbf{x_2}|$ and $R = a(t)|\mathbf{x_1} - \mathbf{x_2}|$. This result was first pointed out by Starobinsky and Yokoyama[28]. It has the interesting property that it depends on the *physical distance*, R, not the co-moving distance. In otherwords, despite any expansion, the physical distance to a nearby point with some given degree of correlation *does not change in time*. In an inflating universe, this means that the physical size of a 'bubble' of highly correlated space remains fixed (because this is given by the correlation length associated to this correlation function, the physical length of which does not change). The significance of this is that the number of 'Hubble-Volumes' (regions of high correlation) in an inflating universe rapidly proliferates, since the physical volume of the universe increases but that of the Hubble volumes does not.
This can lead to interesting effects - if the exit from inflation is random, then unless the rate of exit per hubble volume exceeds the rate at which Hubble volumes are created, inflation will persist forever in at least some regions of the universe. This is the so called 'eternal inflation' scenario. Most of the Hubble volumes would exit, so the fraction that have exited always decreases, but the physical number of still-inflating Hubble volumes *increases*.
Additionally, we might consider what happens at weak coupling, as $\lambda \to 0$. To do this, we should evaluate N. It is important to bear in mind, however, than the N appearing in Eq. (5.47) is that associated to the dimensionless field, $\tilde{\varphi}$, so does not depend on λ:

$$\begin{aligned} N =& \int_{-\infty}^{\infty} \mathrm{d}\tilde{\varphi} e^{-2\tilde{\nu}(\tilde{\varphi})} \\ =& 2\int_0^{\infty} \mathrm{d}\tilde{\varphi} \exp\left(-\frac{\tilde{\varphi}^4}{8}\right) \\ =& 2^{-\frac{1}{2}} \int_0^{\infty} \mathrm{d}z z^{\frac{1}{4}-1} e^{-z} \\ =& \frac{1}{\sqrt{2}}\Gamma\left(\frac{1}{4}\right). \end{aligned} \tag{5.50}$$

In the third line, we have made the substitution $z = \frac{\tilde{\varphi}^4}{8}$, in order to express the result in terms of Gamma functions. We see then that the dependence on λ in $G(r,t,t)$ end up with a $\lambda^{-\frac{1}{2}}$ factor in front, while the exponential terms approach 1, since all powers tend to zero. Thus, in the $\lambda \to 0$ limit we have:

$$G(r,t,t) = H^2 \sqrt{\frac{3}{16\pi^2\lambda}} \Gamma\left(\frac{1}{4}\right) \sum_n A_n^2. \tag{5.51}$$

This appears to diverge everywhere, implying that the universe becomes highly correlated at very long distances, for weak coupling.
We can also compute the correlation length. To do this, define R_{corr} as the physical distance at which the correlation drops to $\frac{1}{e}$ of its initial value. Numerically, the easiest way to do this is to find the correlation length of the dimensionless correlation function:

$$G(\tau) = N \sum_n A_n^2 e^{-2E_n\tau}, \tag{5.52}$$

since the quantities N, A_n, E_n do not depend on λ. This is ultimately a problem of finding the zero of $G(\tau) - G(0)/e$. This can be done using a variety of techniques, such as the Newton-Raphson method. The result is $\tau_{\text{corr}} = 0.719296$. Note that this is close to $\frac{1}{2E_1}$, which would be the correlation time for pure exponential decay: this is because the A_1 coefficient dominates the expansion of $G(\tau)$ into exponentials. The correlation time is therefore $t_{\text{corr}} = \frac{\tau_{\text{corr}}}{H}\sqrt{\frac{24\pi^2}{\lambda}}$. This can be converted to an equal time correlation length using Eq. (5.48), which asserts:

$$t_{\text{corr}} = 2t + \frac{2}{H}\ln(r_{\text{corr}} a_0 H). \tag{5.53}$$

Multiplying by H, exponentiating, and defining the physical distance as $R \equiv ra(t)$ gives:

$$\begin{aligned} e^{Ht_{\text{corr}}} =& a_0^2 e^{2Ht} r_{\text{corr}}^2 H^2 \\ \implies R_{\text{corr}} =& \frac{1}{H}\exp\left(\frac{\tau_{\text{corr}}}{2}\sqrt{\frac{24\pi^2}{\lambda}}\right). \end{aligned} \tag{5.54}$$

This confirms our prior result, namely that the correlation length diverges as $\lambda \to 0$. For an example of a non-zero λ, we could naïvely take the value of the Higgs quartic coupling at the M_z scale, $\lambda = 0.13$ to obtain $R_{\text{corr}} \simeq \frac{4.65\times 10^6}{H}$. This is 6 orders of magnitude larger than the Hubble Horizon scale of $\frac{1}{H}$. However, here we should take into account that H during inflation is very much larger than the present H. This means that $\frac{1}{H}$ is much smaller. In natural units, the present Hubble rate is of order $H_0 \simeq 1.4 \times 10^{-42}$ GeV, while the BICEP2 results imply that H during inflation is around the GUT scale, 10^{15} GeV. Therefore, we find:

$$R_{\text{corr}} \simeq 10^{-51}\frac{1}{H_0}. \tag{5.55}$$

This is significantly smaller than we might have expected, given that the Higgs field is correlated across the CMB. However, this ignores that λ is likely much smaller (perhaps exponentially close to zero) at large field values, and also that the actual Higgs potential has degenerate minima. For exactly the same reason that a potential with multiple wells in a solid-state lattice forms band structures of very close eigenvalues, we would expect that the lowest non-zero eigenvalue of a degenerate-vacuum potential is exponentially close to the analytically known zero eigenvalue. This is indeed what Starobinsky and Yokoyama found in their paper[28].

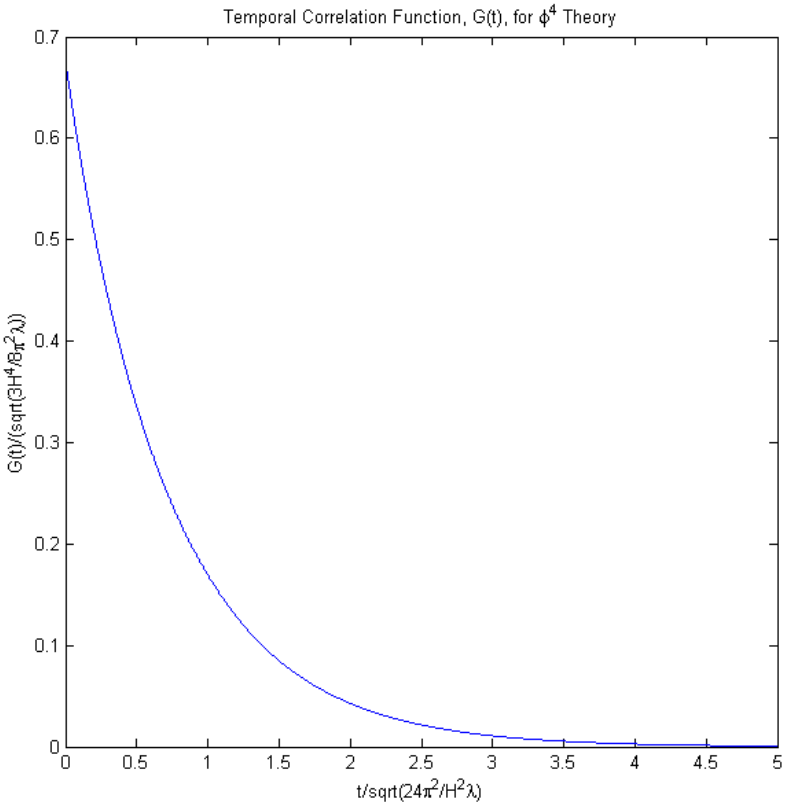

Figure 5.7: Correlation function for the massless ϕ^4 theory. Note that this theory appears to break down at $\lambda = 0$ where the units diverge. This can be traced to the non-existence of an equilibrium state for the massless non-interacting theory ($V(\phi) = 0$) where Eq. (4.104) diverges.

5.4 Massive Theory: $V(\phi) = \frac{1}{2}m^2\phi^2 + \frac{\lambda}{4}\phi^4$

Next, we investigate the behaviour of a massive ϕ^4 theory in de Sitter spacetime, with potential:

$$\begin{aligned} V(\varphi) &= \frac{1}{2}m^2\varphi^2 + \frac{\lambda}{4}\varphi^4 \\ &= \frac{\lambda}{4}\left(\varphi^2 + \frac{m^2}{\lambda}\right)^2 - \frac{m^4}{4\lambda}. \end{aligned} \tag{5.56}$$

Ignoring constant, and defining $\tilde{\varphi}$ as in Eq. (5.38) gives:

$$\tilde{\nu}(\tilde{\varphi}) = \frac{4\pi^2}{3H^4}V(\varphi(\tilde{\varphi})) = \frac{1}{8}\left(\tilde{\varphi}^2 + \gamma\right)^2, \tag{5.57}$$

where the qualitative departure of the theory from the massless case is governed by the dimensionless constant γ:

$$\gamma = \frac{m^2}{H^2}\sqrt{\frac{8\pi^2}{3\lambda}}. \tag{5.58}$$

If γ is negative, then the theory has a double well potential and allows spontaneous symmetry breaking.
The equation we wish to solve is therefore:

$$-\frac{1}{2}\frac{\mathrm{d}^2\Phi_n}{\mathrm{d}\tilde{\varphi}^2} + \frac{1}{2}\left[\frac{1}{4}(\tilde{\varphi}^2+\gamma)^2\tilde{\varphi}^2 - \frac{1}{2}(3\tilde{\varphi}^2+\gamma)\right]\Phi_n = E_n\Phi_n, \tag{5.59}$$

where as before, $E_n = \frac{\Lambda_n}{H}\sqrt{\frac{6\pi^2}{\lambda}}$. To study this problem, we need to consider the two qualitatively different cases:

- $m^2 > 0$, where the potential is still qualitatively similar to $\lambda\varphi^4$
- $m^2 < 0$, where the potential develops double wells.

Applying the harmonic oscillator method to the $m^2 < 0$ case for $\gamma = -4$, we find the lowest eigenfunction, Φ_0. This is given in figure 5.8. There are several reasons to immediately conclude that the method has failed here:

- Φ_0 is proportional to the equilibrium solution, which is a probability density. However, this computation predicts negative probability densities!
- Φ_0 is the lowest eigenfunction of a Sturm-Liouville problem. It is a property of Sturm-Liouville problems that the n^{th} eigenfunction, Φ_n has precisely n zeros, however, this function Φ_0 appears to have a single zero, when it should have none.
- Φ_0 should respect parity under $\phi \to -\phi$ (as either an odd or even function) since the potential does. However, the computed Φ_0 is clearly asymmetric.

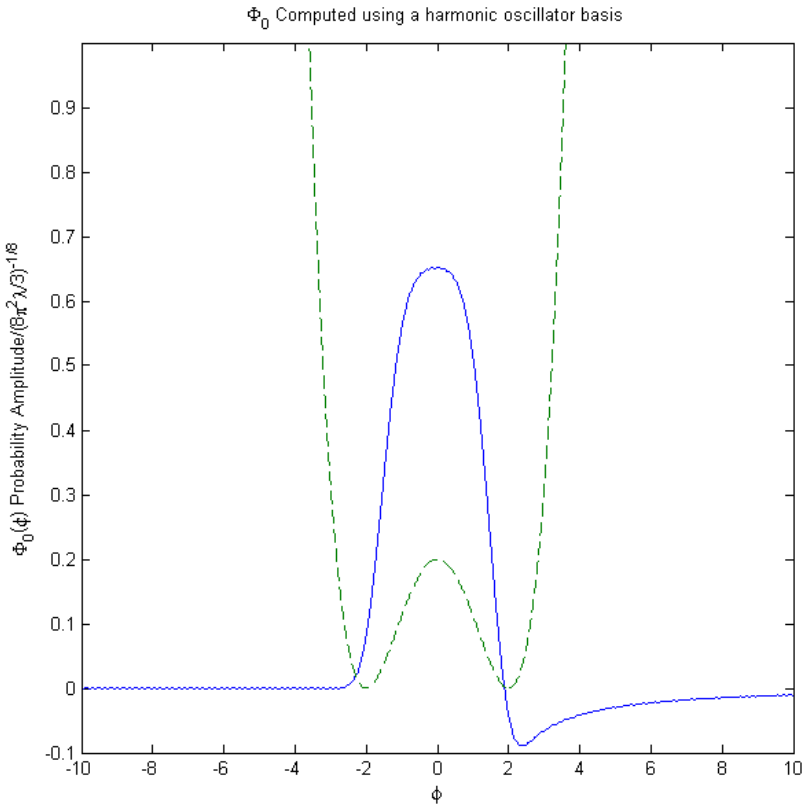

Figure 5.8: Lowest eigenfunction for $\gamma = -4$, computed using the harmonic oscillator basis. The double well potential is plotted as a dashed line to an arbitrary scale for visual convenience.

- We would expect the equilibrium distribution not to favour one minima over the other, but this distribution clearly does not do this.

It transpires, therefore, that the simple harmonic oscillator basis is not sufficient for the $m^2 < 0$ case. Part of the reason is that for $m^2 < 0$, the potential has a double well, and this means that the lowest energy eigenstate also has two peaks (however, by the fact that it originates from a Sturm-Liouville equation, we know that it cannot cross zero since for any Sturm-Liouville equation, eigenfunction Φ_n has precisely n zeros). Although a simple harmonic oscillator basis can be used to construct this, it requires very large n harmonic oscillator basis functions, which are not feasible.
However, the method also appears to fail in the $m^2 > 0$ case. The failure is in fact similar to figure 5.8 and is shown in figure 5.9. To examine why this failure

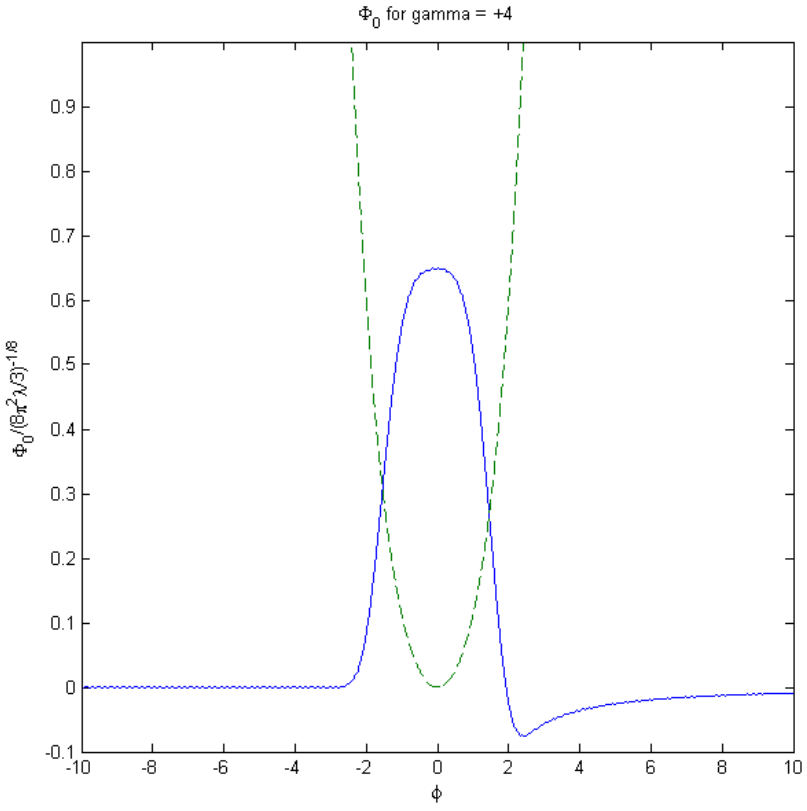

Figure 5.9: Φ_0 computed for $\gamma = +4$. Despite the positive mass, this also fails. The potential is given to an arbitrary scale.

occurs, it is useful to consider a second approach. There is a method which is

feasible for this sort of problem, namely the Numerov method [33]. The basic idea of this approach is to discretise an equation of the form:

$$-\frac{1}{2}\frac{\mathrm{d}^2\Psi}{\mathrm{d}x^2} + V(x)\Psi = E\Psi, \tag{5.60}$$

with boundary conditions $\Psi(A) = a$, $\Psi(B) = b$, into N discrete points. I.e. $\Psi_i = \Psi(A + i\frac{(B-A)}{N})$. By Taylor expansion:

$$\begin{aligned}\Psi_{i+1} =& y_i + h\Psi_i' + \frac{h^2}{2}\Psi_i'' + \frac{h^3}{6}\Psi_i''' + \frac{h^4}{24}\Psi_i'''' + \frac{h^5}{120}\Psi_i''''' + O(h^6)\\ \Psi_{i-1} =& \Psi_i - h\Psi_i' + \frac{h^2}{2}\Psi_i'' - \frac{h^3}{6}\Psi_i''' + \frac{h^4}{24}\Psi_i'''' - \frac{h^5}{120}\Psi_i''''' + O(h^6),\end{aligned} \tag{5.61}$$

where $h = \frac{B-A}{N}$, leading to the well known second-order accurate approximation of the second derivative:

$$\Psi_i'' \simeq \frac{\Psi_{i+1} + \Psi_{i-1} - 2\Psi_i}{h^2} + \frac{h^2}{12}\Psi_i'''' + O(h^4). \tag{5.62}$$

However, this is then improved by exploiting the fact that the fourth-derivative, y_i'''' can be approximated in terms of the second derivative:

$$\Psi''''(x) = \frac{\mathrm{d}^2}{\mathrm{d}x^2}\left((2V(x) - 2E)\Psi(x)\right) \tag{5.63}$$

$$\implies y_i'''' \simeq \frac{2(V_{i+1} - E)\Psi_{i+1} + 2(V_{i-1} - E)\Psi_{i-1} - 4(V_i - E)\Psi_i}{h^2} + O(h^2). \tag{5.64}$$

This gives rise to the fourth order approximation:

$$\Psi_i'' \simeq \frac{\Psi_{i+1} + \Psi_{i-1} - 2\Psi_i}{h^2} + \frac{2(V_{i+1} - E)\Psi_{i+1} + 2(V_{i-1} - E)\Psi_{i-1} - 4(V_i - E)\Psi_i}{12} + O(h^4). \tag{5.65}$$

Thus, a fourth order accurate approximation for this equation is:

$$\frac{\Psi_{i+1} + \Psi_{i-1} - 2\Psi_i}{h^2} + \frac{(V_{i+1} - E)\Psi_{i+1} + (V_{i-1} - E)\Psi_{i-1} - 14(V_i - E)\Psi_i}{6} + O(h^4) = 0. \tag{5.66}$$

Given initial conditions at two close-by points, $y(A)$ and $y(A+h)$ this is enough to solve the equation. For the widely separated y_0 and y_N, one can also re-write this as:

$$\left[\frac{1}{h^2} + \frac{V_{i+1}}{6}\right]\Psi_{i+1} + \left[\frac{-2}{h^2} - \frac{7}{3}V_i\right]\Psi_i + \left[\frac{1}{h^2} + \frac{V_{i-1}}{6}\right]\Psi_{i-1} = E\left[\frac{1}{6}\Psi_{i+1} - \frac{7}{3}\Psi_i + \frac{1}{6}\Psi_{i-1}\right]. \tag{5.67}$$

This is the component form of a *generalised eigenvalue problem*:

$$A\Psi = EB\Psi, \tag{5.68}$$

where A and B are matrices. If B is invertible (which in this case is guaranteed by Gershgorin's Circle Theorem[2]), then this just reduces to the conventional eigenvalue problem, $B^{-1}A\Psi = E\Psi$. The precise form of A and B will depend on the boundary conditions.
Applying this technique, one can compute the lowest eigenvalue of Eq. (5.59) for various values of γ. For example, the lowest energy eigenstate (to which the equilibrium solution is proportional) is shown in figure 5.10

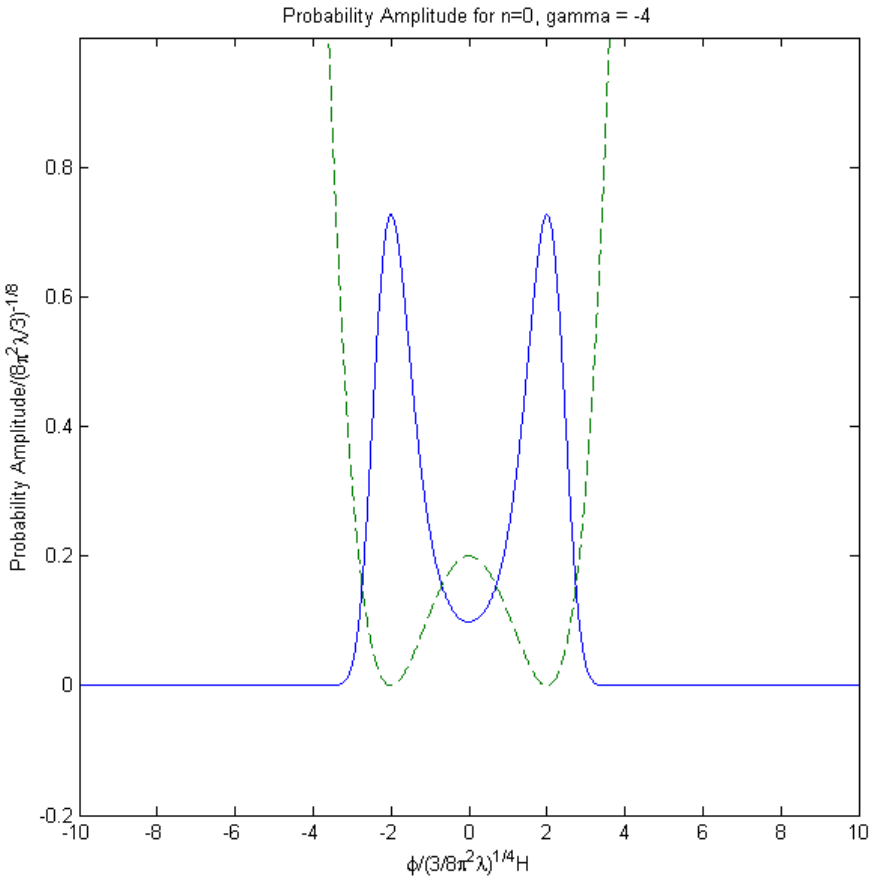

Figure 5.10: The lowest energy eigenstate ($n = 0$) for $\gamma = -4$, computed using the Numerov method. The potential is given by the dashed line, to a scale chosen for visual convenience. Notice that the solution clusters evenly around the two minima.

[2]This states that each eigenvalue of a matrix B lies within one of the disks D_i of radius $R_i = \sum_{j \neq i} |B_{ij}|$ centred on B_{ii}. Thus here, the sum of the off diagonals of B is $\frac{1}{3}$, so the eigenvalues of B must lie within $\frac{1}{3}$ of $-\frac{7}{3}$. Consequently, there are no zero eigenvalues, so B is invertible.

5.4.1 Massive Non-interacting Case: $V = \frac{1}{2}m^2\phi^2$

In the case of $\lambda = 0$, the potential for the scalar field is simply $V(\phi) = \frac{1}{2}m^2\phi^2$. For this scenario, an exact solution to the Fokker-Planck exists, however, we will mention it here to complete the discussion, and because this case is frequently considered in models of inflation. Starobinsky and Yokoyama[28] showed that we can go directly from the Fokker-Planck equation to an ordinary differential equation for the correlation function, $G(t)$, however, we will take their more generic approach here of computing:

$$G(t) = N\sum_n A_n^2 e^{-\Lambda_n t}, \tag{5.69}$$

where:

$$\begin{aligned} N =& \int_{-\infty}^{\infty} \exp\left(-\frac{8\pi^2}{3H^4} \times \frac{1}{2}m^2\varphi^2\right) \mathrm{d}\varphi \\ =& \sqrt{\frac{2\pi \times 3H^4}{8\pi^2 m^2}} = \frac{H^2}{2m}\sqrt{\frac{3}{\pi}}, \end{aligned} \tag{5.70}$$

and:

$$A_n = N^{-1}\int_{-\infty}^{\infty} \mathrm{d}\varphi \exp\left(-\frac{2\pi^2 m^2}{3H^4}\varphi^2\right)\varphi\Phi_n(\varphi). \tag{5.71}$$

Here, $\Phi_n(\varphi)$ and Λ_n satisfy:

$$-\frac{1}{2}\frac{\mathrm{d}^2\Phi_n(\varphi)}{\mathrm{d}\varphi^2} + \frac{1}{2}\left[\left(\frac{4\pi^2}{3H^4}\right)^2 m^4\varphi^2 - \frac{4\pi^2 m^2}{3H^4}\right]\Phi_n(\varphi) = \frac{4\pi^2\Lambda_n}{H^3}\Phi_n(\varphi). \tag{5.72}$$

This can be re-written as:

$$-\frac{1}{2}\frac{\mathrm{d}^2\Phi_n(\varphi)}{\mathrm{d}\varphi^2} + \frac{1}{2}\omega^2\varphi^2\Phi_n(\varphi) = E_n\Phi_n(\varphi), \tag{5.73}$$

where:

$$\begin{aligned} \omega =& \frac{4\pi^2 m^2}{3H^4} \\ E_n =& \frac{4\pi^2\Lambda_n}{H^3} + \frac{2\pi^2 m^2}{3H^4}. \end{aligned} \tag{5.74}$$

Eq. (5.73) is just the Schroedinger equation for the harmonic oscillator, whose eigenfunctions are $\Phi_n(\varphi) = \Psi_n(\varphi)$ (see section 5.2) and eigenvalues $E_n = \omega(n + \frac{1}{2})$. Hence:

$$\Lambda_n = \frac{m^2 n}{3H}. \tag{5.75}$$

This means that $\Phi_0(\varphi)$ obeys:

$$\Phi_0(\varphi) = N^{-\frac{1}{2}}\exp\left(-\frac{2\pi^2 m^2}{3H^4}\varphi^2\right). \tag{5.76}$$

Now, to analytically determine A_n, first note that $H_1(\sqrt{\omega}\varphi) = 2\sqrt{\omega}\varphi$, thus $\Psi_1(\varphi) = \frac{\sqrt{2}}{\pi^{\frac{1}{4}}}\omega^{\frac{3}{4}}e^{-\frac{\omega}{2}\varphi^2}\varphi$. It follows that we can re-write A_n as:

$$A_n = \frac{N^{-1}\pi^{\frac{1}{4}}}{\sqrt{2}}\omega^{-\frac{3}{4}}\int_{-\infty}^{\infty}\mathrm{d}\varphi\Psi_1(\varphi)\Psi_n(\varphi) = \frac{N^{-1}\pi^{\frac{1}{4}}}{\sqrt{2}}\omega^{-\frac{3}{4}}\delta_{n,1}. \tag{5.77}$$

Consequently, only the first non-zero eigenvalue contributes to the correlation function. Plugging in the values of ω and N we find:

$$A_1 = \frac{1}{\sqrt{6}}\left(\frac{3}{\pi}\right)^{\frac{3}{4}}\sqrt{\frac{H^2}{2m}} \tag{5.78}$$

$$NA_1^2 = \frac{3H^4}{8\pi^2m^2}. \tag{5.79}$$

Therefore:

$$G(t) = \frac{3H^4}{8\pi^2m^2}\exp\left(-\frac{m^2t}{3H}\right), \tag{5.80}$$

is the correlation function in this case. We finish this section by noting that the harmonic oscillator approach will yield the exact result in this case. The proof of this is given in section 5.2.

Chapter 6

Conclusions

In this report we have reviewed series of techniques for studying the behaviour of Higgs field during inflation. In section 2, we discussed Coleman and Weinberg's derivation of the effective action and effective potential and computed the one-loop corrections in the case of $\lambda\phi^4$ theory and Yukawa theory.
In section 3 we reviewed the literature regarding the stability of the Higgs vacuum. We computed the running couplings in the case of the standard model, to 1-loop, discounting the higher order loop corrections to the relationship between observables at the electroweak scale and $\overline{\text{MS}}$ couplings. There were two main ways this computation could be improved:

- Extending the accuracy by computing the Standard Model beta functions to higher loop order. These have, for example, been computed to three loops [34][35].
- Taking proper account of the relationship between the $\overline{\text{MS}}$ parameters and physical observables. This requires computing the loop corrections to the tree level relationships, for example between the Yukawa couplings and fermion pole masses.

We discussed the precise calculations of this kind performed in [3] and [2]. This implied that the electroweak vacuum is meta-stable, with stability seemingly ruled out a 2σ, given the measured Higgs boson and top quark masses. This seems to imply that the Higgs effective potential has a second minimum at large field values, around 10^{10} GeV. This opens the possibility of the vacuum decaying, however, referring to the calculation by [3], it appears that the expected life-time of the universe is greater than 10^{100} years at the 1σ level in the uncertainty of the known standard model couplings.
In section 4, we first studied quantum field theory in de-Sitter space-time, since this is the approximate space-time during inflation. We explained why this leads to an infra-red 'super-expansionary divergence', which was caused by the unbounded increase of the space-time volume. The conclusion was that the long wave-length structure of quantum field theory in de-Sitter space is beyond any

order of perturbation theory to compute. However, Starobinsky and Yokoyama solved this[28] by proposing that the long wave-length field could be separated from the short wavelength part and treated classically. In particular, it satisfied a stochastic Langevin equation, where the short-wavelength quantum behaviour acted as a stochastic 'Brownian motion' term. To approach this, we reviewed the derivation of the Fokker-Planck equation, describing the time evolution of the probability distribution for the evolution of the long-wavelength field. The derivation we gave improves upon the elegant derivation in [26] by taking proper account of the non-commutation of the differential operators involved.
Having derived the Fokker-Planck equation, we proceeded to the main topic of the second half of the report - its solution. Starobinsky and Yokoyama[28] derived an expression for the long wavelength correlation function of a scalar field in de-Sitter space, and proved its de-Sitter invariance, for the case of a certain class of potentials. Their results apply to potentials satisfying:

$$N = \int_{-\infty}^{\infty} \mathrm{d}\varphi \exp\left(-\frac{8\pi^2 V(\varphi)}{3H^4}\right) < \infty. \tag{6.1}$$

However, in the event of an unstable Higgs potential, where λ becomes negative for high energies, potentials not satisfying this condition are possible. For physical purposes, if the potential diverges to $-\infty$, it would lead to a local breakdown of the de-Sitter space approximation, creating a bubble of Anti-de-Sitter space, which rapidly collapses (see [7] for example, where they use this effect to compute the survival probability of the electroweak vacuum during inflation). However, it is interesting to study what the Fokker-Planck equation predicts in this scenario, and we derived an equivalent expression for the correlation function in the case where N diverges.
Towards the end of section 4, we used the Fokker-Planck equation to derive the ordinary differential equation satisfied by the variance, $\langle\phi^2(t)\rangle$ of a scalar field during inflation. We then used this to explain qualitatively how inflation causes fluctuations in light scalar fields of order $\phi \sim H$. There is scope to build on this qualitative explanation by solving this equation and performing a more quantitative analysis.
Section 5 dealt with numerical solutions of the Fokker-Planck equation. We described how a method detailed in [31] and also used by Bender, Boettcher and Meisinger [36] to study PT-symmetric Hamiltonians, can be adapted to solve the Schroedinger equation that results by applying separation of variables to the Fokker-Planck equation. This method consisted of expressing the 'Hamiltonian' in a harmonic oscillator eigenfunction basis, where it has a particularly simple form. The eigenvalues and eigenfunctions could then be computed numerically. We presented the results of this method applied to a variety of potentials and found:

- The method works well for the quartic potential without a mass term. We were able to compute the eigenvalues and also the correlation function.
- The method does not perform well when a mass term is added. This is particularly noticeable in the case of a double well potential ($m^2 < 0$) where

the eigenfunctions are significantly different from those of the harmonic oscillator (compare figures 5.8 computed using the method and 5.10 using Runge -Kutta, both applied to the same potential, for example). This suggests the method is most efficient for potentials which qualitatively resemble the harmonic oscillator, such as the ϕ^4 potential.

- The method produces exact results for the $V = \frac{1}{2}m^2\phi^2$ potential, for which an analytic solution was found by Starobinsky and Yokoyama[28].

In summary, it seems that the method may be a useful way to extract correlation functions for quartic potentials. Although this may seem very limited, in the context of vacuum stability, we are principally interested in the behaviour of the field at large field values, where the quartic term dominates. It may however be possible to improve the method's performance. The most straightforward way to achieve this would be to compute more harmonic oscillator basis functions. The downside is that this increases the size of the matrix whose eigenvalues need to be computed - a memory and computationally intensive task. However, our numerical results for the quartic potential indicated that the size of matrices required is generally smaller for the harmonic oscillator approach than with equivalent discretisation method (Runge-Kutta or Numerov methods, for example). The difficulty in extending it, however, as discussed in section 5.1, is the ability to reliably compute the harmonic oscillator functions Ψ_n for large n. This runs into numerical difficulties, however, one approach that might improve the method would be to investigate symbolic approaches to the computing the basis functions. Since the functions are known exactly, this should eliminate a major source of numerical error.

The recent results on the measurement of the Higgs mass, combined with those from the BICEP2 collaboration, puts particle physics in an interesting position. Should the BICEP2 result be confirmed, it would appear to indicate a conflict between inflation and the Standard Model. Assuming inflation to be correct, this constitutes strong indirect evidence of physics beyond the standard model which modifies the Higgs potential. An example would be super-symmetry. Since super-symmetry requires both bosons and fermions with similar masses (above the super-symmetry breaking scale, that is), then the contributions of new particles would be expected to change the Higgs potential very little. This is because, as we demonstrated in section 2, bosons and fermions tend to give opposite contributions to the effective potential. Consequently, any new particles would change the effective potential at high energies, while producing minimal change at lower energies.

This doesn't have to be the case, however, super-symmetry appears to offer a way of fixing this problem without drastically affecting low-energy physics. If the LHC discovers new physics, then this calculation will change. However, whatever is discovered, it is clear that more precise measurements of the Higgs and top quark masses, coupled with new measurements of the CMB B-modes, are needed if we are to better understand the position of the Standard Model.

Chapter 7

Appendices

7.1 Sturm Liouville Equations

A Sturm-Liouville equation is one that can be placed in the form:

$$-\frac{\mathrm{d}}{\mathrm{d}\varphi}\left(p(\varphi)\frac{\mathrm{d}y}{\mathrm{d}x}\right)+q(\varphi)y=\lambda w(\varphi)y, \tag{7.1}$$

where $w(\varphi)>0$. Such an equation is said to be *regular* if it satisfies the following conditions:

- $p(\varphi), w(\varphi)>0$ everywhere in some interval $[a,b]$.
- $p(\varphi), p'(\varphi), q(\varphi)$ and $w(\varphi)$ are continuous on $[a,b]$.
- The boundary functions at a and b are of the form: $\alpha_1 y(a)+\alpha_2 y'(a)=0, \beta_1 y(b)+\beta_2 y'(b)=0$ where $\alpha_1^2+\alpha_2^2>0$ and $\beta_1^2+\beta_2^2>0$.

For regular Sturm-Liouville problems, the eigenvalues Λ_n that allow the boundary conditions to be satisfied are *real* and *ordered* (ie, $\Lambda_0<\Lambda_1<\Lambda_2<\ldots$, which also means they are non-degenerate). The associated eigenfunctions, $\Phi_n(\varphi)$ obey the orthogonality relationship:

$$\int \mathrm{d}\varphi \Phi_n^*(\varphi)\Phi_m(\varphi)w(\varphi)=\delta_{nm}. \tag{7.2}$$

Crucially, they also form an orthonormal basis of a Hilbert space (known formally as $L^2([a,b],w(\varphi)\mathrm{d}\varphi)$, w is known as a the 'weight function'). Another (non-normalisable) basis for this space is the position basis, $\{|\varphi\rangle\}$, however, this basis is not normalised (although it is orthogonal). Consequently, while:

$$\sum_n |\Phi_n\rangle\langle\Phi_n| = \mathbb{I}, \tag{7.3}$$

is the completeness relation for the solutions Φ_n, $|\varphi\rangle$ obey:

$$\int \mathrm{d}\varphi w(\varphi) \left|\varphi\right\rangle \left\langle\varphi\right| = \mathbb{I}. \tag{7.4}$$

Defining $\Phi_n(\varphi) = \langle\varphi|\Phi_n\rangle$, it is easy to see this this gives rise to the orthogonality relationship above, $\langle\Phi_n|\Phi_m\rangle = \delta_{nm}$.
The inner product $\langle\varphi|\varphi'\rangle$ can also be determined, starting from the assumption that it is orthogonal, with some function $f(\varphi)$ taking into account the non-normalisation:

$$\begin{aligned}
\langle\varphi|\varphi'\rangle &= f(\varphi)\delta(\varphi-\varphi') \\
&= \langle\varphi|\,\mathbb{I}\,|\varphi'\rangle \\
&= \int \mathrm{d}\tilde{\varphi} w(\tilde{\varphi}) \langle\varphi|\tilde{\varphi}\rangle\langle\tilde{\varphi}|\varphi'\rangle \\
&= \int \mathrm{d}\tilde{\varphi} w(\tilde{\varphi}) f(\varphi)\delta(\varphi-\tilde{\varphi}) f(\tilde{\varphi})\delta(\varphi-\varphi') \\
&= w(\varphi) f(\varphi)(f(\varphi)\delta(\varphi-\varphi')).
\end{aligned} \tag{7.5}$$

This is only consistent then, if:

$$\langle\varphi|\varphi'\rangle = \frac{1}{w(\varphi)}\delta(\varphi-\varphi'), \tag{7.6}$$

which is valid as $w > 0$. Given the resolution of the identity for Φ_n then, we have:

$$\sum_n \Phi_n^*(\varphi)\Phi_n(\varphi') = \sum_n \left\langle\varphi\right|\left|\Phi_n\right\rangle\left\langle\Phi_n\right|\left|\varphi'\right\rangle = \frac{1}{w(\varphi)}\delta(\varphi-\varphi'). \tag{7.7}$$

7.2 Equation of Motion in de Sitter Space

The momentum space scalar field obeys:

$$\frac{\mathrm{d}^2\phi_{\mathbf{k}}}{\mathrm{d}a^2} + \frac{4}{a}\frac{\mathrm{d}\phi_{\mathbf{k}}}{\mathrm{d}a} + \left(\frac{k^2}{a^4H^2} + \frac{m^2+\xi R}{a^2H^2}\right)\phi_{\mathbf{k}} = 0. \tag{7.8}$$

This equation can be solved using Bessel functions. A simple technique for solving this kind of equation is to consider equations of the form[23]:

$$\frac{\mathrm{d}^2y}{\mathrm{d}x^2} + \frac{1-2\alpha}{x}\frac{\mathrm{d}y}{\mathrm{d}x} + \left[(\beta\gamma x^{\gamma-1})^2 + \frac{\alpha^2-p^2\gamma^2}{x^2}\right] y = 0. \tag{7.9}$$

By making the substitution $y = x^\alpha u$ and $z = \beta x^\gamma$ one finds that:

$$\begin{aligned}
\frac{\mathrm{d}^2}{\mathrm{d}x^2}(x^\alpha u) &= \alpha(\alpha-1)x^{\alpha-2}u + 2\alpha x^{\alpha-1}\frac{\mathrm{d}u}{\mathrm{d}x} + x^\alpha\frac{\mathrm{d}^2u}{\mathrm{d}x^2} \\
\frac{\mathrm{d}}{\mathrm{d}x}(x^\alpha u) &= \alpha x^{\alpha-1}u + x^\alpha\frac{\mathrm{d}u}{\mathrm{d}x} \\
\frac{\mathrm{d}}{\mathrm{d}x} &= \frac{\mathrm{d}z}{\mathrm{d}x}\frac{\mathrm{d}}{\mathrm{d}z} = \gamma\beta x^{\gamma-1}\frac{\mathrm{d}}{\mathrm{d}z} \\
\frac{\mathrm{d}^2}{\mathrm{d}x^2} &= (\gamma\beta x^{\gamma-1})^2\frac{\mathrm{d}^2}{\mathrm{d}z^2} + \gamma\beta(\gamma-1)x^{\gamma-2}\frac{\mathrm{d}}{\mathrm{d}z}.
\end{aligned}$$

And after some cancellations the equation becomes:

$$\begin{aligned}
&\gamma^2 x^{\alpha-2}z^2\frac{\mathrm{d}^2u}{\mathrm{d}z^2} + \gamma^2 z x^{\alpha-2}\frac{\mathrm{d}u}{\mathrm{d}z} + \gamma^2(z^2-p^2)x^{\alpha-2}u = 0 \\
\implies\ & z^2\frac{\mathrm{d}^2u}{\mathrm{d}z^2} + z\frac{\mathrm{d}u}{\mathrm{d}z} + (z^2-p^2)u = 0. \qquad (7.10)
\end{aligned}$$

This is Bessel's equation, the general solution to which can be written:

$$u(z) = Z_p(z) = A_1 H_p^{(1)}(z) + A_2 H_p^{(2)}(z). \qquad (7.11)$$

Where $H_p^{(1)}(x) = J_p(x) + iN_p(x)$, $H_p^{(2)}(x) = J_p(x) - iN_p(x)$ are the Hankel functions, defined in terms of $J_p(x)$ and $N_p(x)$, the Bessel functions of the first kind. Note that we could equally write this as a sum of J_p and N_p, but the complex nature of $\phi_{\mathbf{k}}$ means the Hankel functions are a more natural choice (in much the same way that complex exponentials are a more natural choice than sin and cos for expanding the field in momentum space).
Comparing equation 7.8 and 7.9, we see that the coefficients α, β, γ, p are given by:

$$\alpha = -\frac{3}{2}, \qquad (7.12)$$

$$\beta = \frac{k}{H}, \qquad (7.13)$$

$$\gamma = -1, \qquad (7.14)$$

$$p = \sqrt{\frac{9}{4} - \frac{(m^2+\xi R)}{H^2}}. \qquad (7.15)$$

Thus, the general solution is:

$$\phi_{\mathbf{k}}(t) = a(t)^{-\frac{3}{2}} Z_p\left(\frac{k}{a(t)H}\right). \qquad (7.16)$$

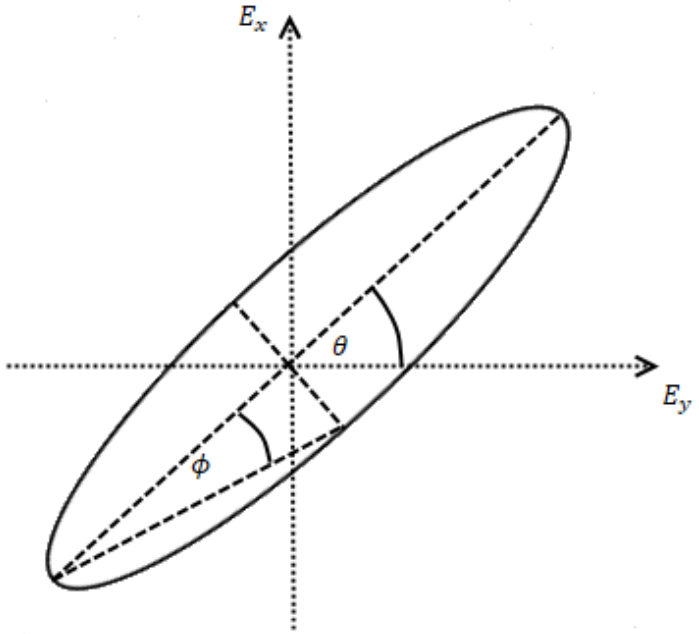

Figure 7.1: Elliptically polarised electromagnetic radiation propagating in the z directio. θ is determined by the ratio $\tan\theta = \frac{E_{x0}}{E_{y0}}$ and ϕ by the difference in phase, $\phi = \phi_1 - \phi_2$. Note that ϕ ranges from $-\frac{\pi}{4} \leq \phi \leq \frac{\pi}{4}$ because any difference in phase outside this range can be incorporated into a sign change for E_{x0} and or E_{y0}. $\phi = 0$ corresponds to linear polarisation, while $\phi = \pm\frac{\pi}{4}$ correspond to left and right circular polarisation respectively.

7.3 Stokes Parameters for Polarised Light

The most general polarised light is elliptical polarisation. For the generic electric field written as a Jones vector:

$$|E\rangle = \begin{pmatrix} E_{x0}e^{i\phi_1} \\ E_{y0}e^{i\phi_2} \end{pmatrix} e^{i(kx-\omega t)}, \tag{7.17}$$

the polarisation can be characterised by two angles, θ and ϕ, as plotted in 7.1.

There is an alternative way to encapsulate this information, however, in the form of *Stokes parameters*. Instead of presenting the information on an ellipse, it is plotted onto a sphere. This allows us to take into account the polarisation of light with a mixture of frequencies, since this will in general consist of a combination of some unpolarised light with intensity $I_{\rm up}$ and some with net polarisation, intensity $I_{\rm p}$. Defining the degree of polarisation as:

$$p = \frac{I_{\rm p}}{I_{\rm p} + I_{\rm up}}, \tag{7.18}$$

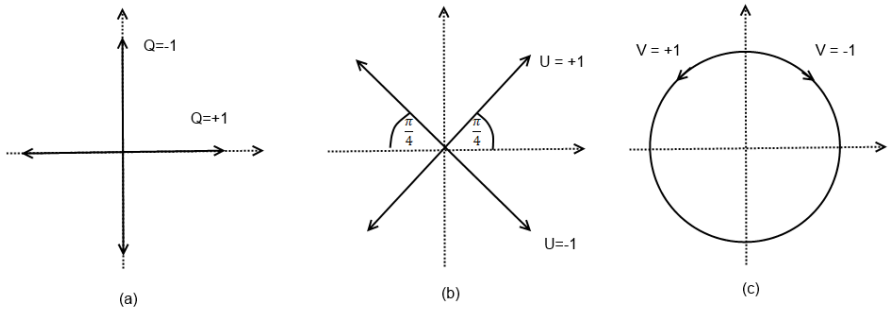

Figure 7.2: Polarisations for different stokes parameters. Note that Q and U both correspond to forms of linear polarisation, only in different axis. However, since these axis are essentially arbitrary, Q and U can be rotated into each other.

then any given combination can be plotted as a radial vector, with the net polarisation given by θ and ϕ (interpreted as polar co-ordinates for the sphere) and the radius of the vector the degree of polarisation, p (see figure **??**). The stokes parameters are then given by the Cartesian co-ordinates of these points:

$$\begin{aligned} I =& I_{\text{total}} \\ Q =& pI \cos 2\phi \cos 2\theta \\ U =& pI \cos 2\phi \sin 2\theta \\ V =& pI \sin 2\phi \end{aligned} \tag{7.19}$$

Note these are defined differently to the usual polar co-ordinates, with the polar angle, 2ϕ measured from the equator rather than the north pole (positive chosen to be a northern latitude), and a factor of 2 accounting for the fact that $-\frac{\pi}{4} \leq \phi \leq \frac{\pi}{4}$ and $0 \leq \pi \leq \pi$, half the usual ranges required to cover a sphere. These definitions allow us to interpret the Cartesian co-ordinates:

- I is the intensity of the light.
- Q is associated to the portion of light linearly polarised in the E_x axis or E_y axis, since $\cos 2\phi$ is extremised when $\phi \to 0$ (linear polarisation) and $\cos 2\theta$ is extremised when $\theta = 0$ (E_x) or $\theta = \frac{\pi}{2}$ (E_y).
- U is associated with the portion linearly polarised (since it contains $\cos 2\phi$, as with Q) about the axis $E_y = \pm E_x$ (since $\sin 2\theta$ is extremised when $\theta = \frac{\pi}{4}$ ($E_y = E_x$) or $\theta = \frac{3\pi}{4}$ ($E_y = -E_x$).
- V is associated to circularly polarised light, since it is zero for linear polarisation and extremised when $\phi = \pm\frac{\pi}{4}$.

These are plotted in figure 7.2.

Bibliography

[1] (BICEP2 Collaboration), P. A. R. Ade *et al.*, Phys. Rev. Lett. **112**, 241101 (2014).

[2] M. Fairbairn and R. Hogan, Phys. Rev. Lett. **112**, 201801 (2014).

[3] D. Buttazzo *et al.*, Journal of High Energy Physics **2013** (2013).

[4] S. Coleman and E. Weinberg, Phys. Rev. D **7**, 1888 (1973).

[5] D. J. Fixsen, The Astrophysical Journal **707**, 916 (2009).

[6] The Planck Collaboration & ESA.

[7] J. R. Espinosa, G. F. Giudice, and A. Riotto, Journal of Cosmology and Astroparticle Physics **2008**, 002 (2008).

[8] S. Weinberg, *The Quantum Theory of Fields, Vol II* (Cambridge University Press, 2005).

[9] E. J. Weinberg, *Radiative Corrections as the Origin of Spontaneous Symmetry Breaking*, PhD thesis, Harvard University Cambridge, Massachusetts, 1973.

[10] R. Jackiw, Phys. Rev. D **9**, 1686 (1974).

[11] M. E. Peskin and D. V. Schroeder, *An Introduction to Quantum Field Theory* (Westview Press, 1995).

[12] H. Arason *et al.*, Phys. Rev. D **46**, 3945 (1992).

[13] (Particle Data Group), K. A. Olive *et al.*, Chin. Phys. C **38** (2014).

[14] C. Ford, I. Jack, and D. Jones, Nuclear Physics B **387**, 373 (1992).

[15] R. Hempfling and B. A. Kniehl, Phys. Rev. D **51**, 1386 (1995).

[16] (ATLAS Collaboration), Physics Letters B **710**, 49 (2012).

[17] (ATLAS Collaboration), Phys. Rev. Lett. **108**, 111803 (2012).

[18] V. Branchina and E. Messina, Phys. Rev. Lett. **111**, 241801 (2013).

[19] G. Degrassi *et al.*, Journal of High Energy Physics **2012** (2012).

[20] M. Laine, Basics of thermal field theory: A tutorial on perturbative computations, 2013.

[21] T. S. Bunch and P. C. W. Davies, Proceedings of the Royal Society of London. A. Mathematical and Physical Sciences **360**, 117 (1978), http://rspa.royalsocietypublishing.org/content/360/1700/117.full.pdf+html.

[22] F. Bezrukov and M. Shaposhnikov, Physics Letters B **659**, 703 (2008).

[23] M. L. Boas, *Mathematical Methods in the Physical Sciences*, 3rd ed. (John Wiley & Sons Inc., 2006).

[24] M. Sasaki, H. Suzuki, K. Yamamoto, and J. Yokoyama, Classical and Quantum Gravity **10**, L55 (1993).

[25] A. Starobinsky, Physics Letters B **117**, 175 (1982).

[26] L. Sjögren, Lecture notes on stochastic processes, chapter 7, 2014.

[27] R. K. Pathria and P. D. Beale, *Statistical Mechanics*, 3rd ed. (Elsevier, 2011).

[28] A. A. Starobinsky and J. Yokoyama, Phys. Rev. D **50**, 6357 (1994).

[29] D. Baumann, Tasi lectures on inflation, 2012.

[30] M. Kamionkowski, A. Kosowsky, and A. Stebbins, Phys. Rev. D **55**, 7368 (1997).

[31] H. J. Korsch and M. Glck, European Journal of Physics **23**, 413 (2002).

[32] E. W. Weisstein, "Hermite Polynomial." From MathWorld–A Wolfram Web Resource.

[33] V. Fack and G. V. Berghe, Journal of Physics A: Mathematical and General **20**, 4153 (1987).

[34] L. N. Mihaila, J. Salomon, and M. Steinhauser, Phys. Rev. Lett. **108**, 151602 (2012).

[35] K. Chetyrkin and M. Zoller, Journal of High Energy Physics **2012** (2012).

[36] C. M. Bender, S. Boettcher, and P. N. Meisinger, Journal of Mathematical Physics **40** (1999).